2010-01-01

Dynamic Modeling Of Human Gait And Motor

Chad Everett Joshua Macdonald
University of Texas at El Paso, cemacdonald@miners.utep.edu

DYNAMIC MODELING OF HUMAN GAIT AND MOTOR ADAPTATION: TOWARDS THE SIMULATION OF ANKLE IMPAIRMENTS

CHAD EVERETT JOSHUA MACDONALD

Department of Electrical and Computer Engineering

APPROVED:

Thompson Sarkodie-Gyan, Ph.D., Chair

Scott Starks, Ph.D.

Richard Brower, M.D.

Jody Riskowski, Ph.D.

Patricia D. Witherspoon, Ph.D.
Dean of the Graduate School

Dedication

This dissertation is dedicated to the memory of

Edith Irene Obrigewitsch

March 24, 1926 - December 15, 2007

I miss you and wish you could have been here
to share in this accomplishment with me

DYNAMIC MODELING OF HUMAN GAIT AND MOTOR ADAPTATION: TOWARDS THE SIMULATION OF ANKLE IMPAIRMENTS

by

CHAD EVERETT JOSHUA MACDONALD, M.SC.

DISSERTATION

Presented to the Faculty of the Graduate School of

The University of Texas at El Paso

in Partial Fulfillment

of the Requirements

for the Degree of

DOCTOR OF PHILOSOPHY

Department of Electrical and Computer Engineering

THE UNIVERSITY OF TEXAS AT EL PASO

December 2009

Acknowledgments

I would like to acknowledge the guidance and support of my academic advisors both past a present. First, Dr. Thompson Sarkodie-Gyan for taking me into his lab when I needed an advisor. His guidance and support have been invaluable while pursuing my doctoral work. Second, Dr. Zahra Moussavi, for introducing me to the world of Biomedical Engineering, for her guidance during my Masters and for giving me that final push to go on to pursue a Ph.D. And third, Dr. Witold Kinsner for providing the engineering and research foundation upon which my graduate career is built. You have made me the engineer I am today.

I would also like to acknowledge the support of the past and present members of the Laboratory for Industrial Metrology and Automation and the Laboratory for Human Motion Analysis and Neurorehabilitation at UTEP. There are too many to mention everyone, but I would like to specifically thank Huiying Yu, Murad Alaqtash and Abdallah Hassan who were involved in the collection of experimental data for this work.

Any research in Biomedical Engineering would not be possible without collaborations with medical personnel. I would like to thank Dr. Eric Spier for his expert opinions and guidance on aspects of this research. Also, thank you to Eric Spier and Jimmy Moody for providing the patients for the case studies in this work. Finally, thank you to Miguel Guerra for providing the ankle-foot-orthosis used in the adaptation experiments.

I also thank the members of my dissertation committee for their assistance in preparing this work and for their valuable feedback regarding my research.

Finally, I want to thank my family and friends for supporting me throughout my entire academic career and particularly during time in El Paso. In particular, I want to thank Ashley for being there for me over the last two years. And especially for her patience and understanding when I had to spend those many, many hours working on campus.

Abstract

The simulation of gait, impairments and the outcomes of rehabilitation strategies is an important area of research. The ability to study the efficacy of treatment options before applying them to patients has the potential to improve the efficiency of the rehabilitation process. Any such simulations must incorporate some model of the motor learning process to properly anticipate the responses of patients. This dissertation presents initial work on the modeling of gait and the study of motor adaptation with a view towards simulating the motor adaptation process during gait.

Specifically, an inverse dynamic model of gait incorporating sagittal plane limb and torso dynamics and three degree of freedom pelvis rotation is developed and applied to determine joint moments for motor adaptation experiments. The specific experimental conditions involve studying gait changes resulting from changes in treadmill walking speed, from walking on two treads moving at different speeds and various forms of ankle contractures simulated using an ankle-foot-orthosis.

The experimental results show after-effects that suggest the formation of an internal model of the altered gait dynamics to compensate for gait errors. Kinematic performance metrics show the expected adaptations to the simulated gait impairments. In particular evidence is found to demonstrate vaulting and steppage gait adaptations in response to ankle impairments. The inverse dynamics analysis shows clear stance phase adaptations to ankle contractures while showing a limited response during swing phase. The primary adaptations evidenced by the inverse dynamics analysis are changes in pelvis joint moments leading to vaulting gait compensation when an ankle locked in an a plantarflexed position.

The results of the adaptation experiments are compared to an inverse dynamics analysis of a patient exhibiting drop foot resulting from a mid-brain stroke. The patient also exhibits pelvis moments resulting a vaulting gait pattern as was seen in the plantarflexion experiment.

Table of Contents

List of Tables

List of Figures

Chapter 1: Introduction

1.1 Motivation

The motivation for studying motor adaptation in conjunction with gait modeling is three-fold. First, by gaining an improved understanding of how the human brain learns to control locomotion, the potential for applying such understanding to the rehabilitation of motor impairments and the treatment of developmental motor diseases may be improved. Second, understanding the human motor learning system may lead to advancements in non-medical research fields such as robotics and artificial intelligence. Finally, further understanding of the interaction of motor learning and gait can be used to eventually produce computer simulations of gait adaptation and to apply these simulations to study rehabilitation. Ideally, such models would be useful for testing the efficacy of potential treatment or rehabilitation options before applying them to patients. The potential for running such what-if type scenarios in a simulated environment should lead to improved rehabilitation outcomes for the patients.

1.2 Goals and Specific Aims

The fundamental goal of this research is to study aspects of motor adaptation during gait to provide insight that will be used to develop future models of the adaptation process for simulating human locomotion and rehabilitation. To this end, the specific aims of the research are:

- To characterize the adaptations of healthy subjects when walking at different speeds
- To simulate various ankle contracture impairments on healthy subjects and examine their adaptive responses to such imposed simulated impairments
- To impose asymmetric gait on subjects via a dual-belt treadmill to examine adaptation to gait asymmetry
- Develop a computationally efficient inverse dynamic model of gait that allows for the study of pelvic rotations

- Use an inverse dynamics approach to study the changes in joint moments resulting from the motor adaptation processing
- Compare the joint torque profiles of healthy subjects with simulated contractures with those of patients with long term ankle impairments

1.3 Scope

The scope of this dissertation includes the design and implementation of an inverse dynamic model of gait and the application of that model to studying motor adaptation during gait. The focus is on characterizing the kinematic and dynamic correlates of the motor adaptation process for the specific experimental conditions studied. The work is intended to provide a starting point for developing future simulations of the motor adaptation process.

1.4 Contributions

The contributions of this research are in the area of motor adaptation correlates in joint torque profiles. While the study of motor adaptation in general and during gait specifically have been covered in the literature, the application of inverse dynamics to this area is a novel approach. Most research into gait adaptation focuses on kinematic performance metrics and not on the commands controlling the motion. A thorough understanding of how the control signals (joint torques) change as a result of adaptation to novel gait tasks is fundamental to the eventual creation of a gait adaptation simulation for use in rehabilitation scenarios.

Additionally, much research into gait adaptation focuses on adaptation to transient force fields imposed on the subject. This research seeks to make contributions towards the understanding of adaptation as applied to more long term persistent changes to gait task dynamics, such as contractures limiting the range of motion of the ankle.

1.6 Organization of Dissertation

This dissertation manuscript is divided into seven sections. This chapter outlined the motivations, goals and contributions of the research. Chapter 2 of this presents background on past research in the fields of motor adaptation and gait modeling techniques. Chapter 3 outlines the procedures used during the experimental stages of this research. Chapter 4 presents the design and implementation of an inverse dynamic model of gait to be used to analyze the motor adaptation experiment data. Chapter 5 presents the results of the experimental aspects of this research and Chapter 6 includes a discussion of these results. Chapter 7 then provides concluding remarks and recommendations for future research.

Chapter 2: Background and Significance

2.1 Modeling of Gait Dynamics

The modeling of a nonlinear multisegment system such as the human body is a complex task. Many approaches have been made to simulate healthy human locomotion. Models have ranged from simpler sagittal plane models [OnWi80] [Taga95a] [HLAA04] [ReJH07] to more complex spatial models [HaYa02] [GiWi97]. Many researchers have simplified the modeling process by lumping the head, arms and trunk (HAT) into a single segment [OnWi80] [Taga95a] [GiWi97] [HLAA04] [ReJH07] and fewer more complex models have simulated the entire body [HaYa02]. The simplification of models by using HAT segments and sagittal plane dynamics are particularly useful for initial investigations of specific aspects of the gait modeling process. Once the concepts have been demonstrated in the simplified sagittal plane environment, the work is extended to a spatial three-dimensional model. When considering whether to use a sagittal plane model or a three-dimensional model, it is important to weigh the trade-off between the motion limitations of the simpler model and the higher complexity of the three-dimensional model. In [EnWi95], it was noted that a significant amount of work was performed in the non-sagittal planes during healthy gait, particularly with the hip. Therefore, if a simpler model is to be used, particularly for simulating pathology, care must be taken to limit analysis to tasks that do not exhibit strong pathologies in the frontal or coronal planes.

One of the earlier dynamic models used for simulating healthy and pathological gait was [OnWi80]. In this work a sagittal plane model was constructed with a HAT segment and the model was driven using torque profiles derived from real-world experimental data. Healthy gait was finally simulated by trial-and-error tuning of the torque profiles and without any a priori constraints on the motion of any of the model segments. One limitation of this model was that the foot of the stance leg

was fixed to the ground, which necessitated the development of two separate models for the different stages of the gait simulation. Another limitation is the fact that the tops of the thigh segments connect directly to the HAT segment, thus ignoring the behavior of the pelvis. Of interest is the method employed to simplify the derivation of dynamic equations during the double-support phase by using a spring-damper system as a soft constraint [HeJM75] between the thigh segment of one leg and the connection between the other thigh segment and the pelvis.

In [Taga95a], the limitation of ignoring the pelvis in sagittal plane models was addressed. A pelvis segment was included with the tops of the thigh segments connecting to the lower pelvis and the trunk segment connecting to the top of the pelvis.

In [GiWi97], the authors created a three-dimensional model of the lower limbs along with a pelvis and HAT segment. The goal of this work was similar to that of [OnWi80], which was to create a dynamic model driven by joint torques derived from experimental data. A useful feature of this model was the addition of torsional spring-damper systems to each joint to enforce the natural range of motion of each joint.

The precise method employed by the CNS in generating the complex coordinated movements required for locomotion is not currently known. Current dynamic simulations employ various different approaches to generating the joint torques required to generate human-like gait patterns. Many researchers employ the use of neural oscillators and central pattern generators to represent the spinal circuits that are theorized to control coordinated rhythmic movements of the lower-limbs [Mack02] [Taga95a]. In this approach, higher-level controllers modulate the performance of these lower-level control circuits.

Other researchers [OnWi80] [GiWi97] employ a strategy of generating net joint torques at each joint and using these torque profiles as inputs to their dynamic models. The advantage of this approach

is that the control torques can be derived directly from experimental data with minor modifications. The limitation of this approach is that the performance of individual muscles cannot be controlled directly. A further step in this direction is to use multiple torque sources at each joint to represent agonist-antagonist muscles and also to possibly include the effects of biarticular muscles as was done in the balance simulations in [Jaco97].

Another approach to modeling torque sources in dynamic gait simulations is to model the physiological force generation of muscles [Taga95a] [HaYa02] [Zank02] [BLMB04]. While this approach is desirable in that it would more accurately simulate the generation of joint torques, the addition of muscle models leads to an increase in system complexity. For example, to model a specific muscle, the muscle length, velocity of contraction and joint configuration all add additional calculations to the joint calculations. In fact, the moment arm of a muscle about a specific joint changes throughout the entire range of motion of the joint [Zank02].

When designing the control architecture for a dynamic gait model, the trade-off between complexity and accuracy must be considered. When initially developing a particular model and investigating certain aspects of the control of gait, it is beneficial to begin development with simpler control architectures and add complexity in future developments.

2.2 Motor Adaptation

The human motor system is very robust and adaptable to changes in motor task dynamics or to the properties of the body itself. This is particularly evident when one considers that as the human body grows the control strategies of the central nervous system (CNS) must adapt to changes in limb length and mass. Improvements in the understanding and modeling of this motor adaptation process would provide potential clinical benefits for rehabilitation

Changes in task dynamics can be generated from many possible sources including everyday use of novel tools and sports equipment. Adaptations are also required when humans learn to perform novel tasks. The improvements in skill over many iterations of a specific task are the result of the motor system learning the task. In addition to everyday task adaptations, the changes that occur following stroke or other neurological impairments can be viewed as novel changes in task dynamics that must be learned by the motor control system. These changes could include damaged/weakened muscle control, impaired proprioception, loss of vestibular control, diminished force generation capabilities of muscles or spastic muscle activities impairing movement. In order to accurately model the reaction of the CNS to such impairments, a greater understanding of motor adaptation in healthy subjects is required.

2.1.1 Internal Models of Adaptation

Past research in the area of motor adaptation has revealed evidence that the CNS creates an internal model of the dynamics of the motor task being learned. The bulk of this research has focused on studying learning during upper limb reaching [ShMu94] [KaWo98] [BhSh99] [Muss99] [CoGM97] [DoFS03] [DoSh02] [ShMo00] [ScDM01] [ThSh00] [BhSh99]. These studies have robotic manipulators with which subjects interact. Specifically, subjects grasp the handle of the robot and perform reaching movements. The robot then generates a novel force field to perturb the subject movements. The nature of the force field varies between experiments depending on the aspect of the motor adaptation being studied.

In [ShMu94], after subjects adapted to a velocity-dependent force field, the force field was removed and the presence of after-effects of the adaptation process demonstrated that the CNS was forming a model of the predicted task dynamics and generating compensatory joint torques. The after-effects were the result of the incorrect generation of joint torques to compensate for the now-missing external force field.

Other studies have focused on determining the properties of the internal model developed by the CNS. In [ShMo00], the generalization of learning from one arm orientation to another was studied. Adaptation to unknown random force fields was studied in [ScDM01] to understand the increments made to the internal model between reaching movements. In [ThSh00] and [Muss99], the motor primitives and modular features of the adaptation process were studied. In [CDGS02], the generalization of learning from one arm to the other was studied and it was shown that learning can transfer from the dominant arm to the non-dominant arm, but the inverse is not the case.

Whatever the nature of the adaptation process, the current evidence supports the view that the CNS generates an internal model of task dynamics that is updated to correct for movement errors and adapt to changes in a given task. The result of the formation of the internal model is the generation of compensatory torques to counteract predicted task dynamics.

2.1.2 Adaptation During Gait

Recent research has focused on the extension of the study of motor adaptation from upper limb reaching to the more complex task of human locomotion. Several studies have found that the CNS uses similar processes to control the leg during gait and the arm during reaching [EmRe03] [EmRe05] [EBSB07]. In this work a robotic device was designed to exert novel force fields on the ankle of subjects during treadmill walking. This experimental setup mirrored that used previously for the upper limb during reaching. The experimental results suggest that the CNS generates an internal model to compensate for changes in gait dynamics in a similar manner as that for upper limb reaching. In addition to the above studies on adult subjects, these conclusions are supported by research on motor adaptation of infants during stepping [LaWY03] [PaLY03].

Several recent studies have examined the adaptive locomotor changes resulting from sustained modifications of walking conditions. In [LaAD06], the Lokomat system [CLBS99] was used to apply

novel resistance to hip and knee movements during walking. Similar adaptation and after-effect results were exhibited and the formation of an internal model was evident in sustained modifications of the pre-swing activity in the biceps femoris and medial hamstring muscles. Additionally, this work showed evidence of feedback strategies for gait correction in direct response to gait perturbations. These feedback modifications were not present in the after-effect trials and therefore were not part of the internal model formed by the CNS.

In [ChBa07], adaptation to walking on a dual-belt treadmill was studied. The subjects were asked to walk on the treadmill with the treads moving at different speeds and in different directions. Analysis of the after-effects showed that the adaptation for the right and left leg are stored independently and do not transfer for different directions. The independent training of the left and right legs may be of particular interest in designing therapeutic interventions to treat gait asymmetries.

Adaptation to changes in the mechanical properties of the lower limb was studied in [NoPr06]. Specifically, subjects walked on a treadmill with no modifications and then had a 2 kg weight attached to the shank of one leg and then had the weight removed to study after-effects. The results showed that the CNS was able to adapt to modifications in the mechanical properties of the lower limb. The after-effects demonstrated the result of the modification of the CNS internal model of the limb.

The general adaptability of the CNS during gait was discussed in [WiMD91]. Specifically, it was reported that adaptations during gait occur to improve performance with respect to generalized performance metrics. Some specific performance metrics of interest are the maintenance of a vertical trunk, the gentleness of heel contact and the maintenance of trunk support during gait. Also, minimum toe clearance and peak knee flexion during swing are performance metrics of particular interest.

While recent studies performed to understand adaptation during gait have focused on the kinematic results of the adaptation (changes in joint angle trajectories, stride length/time changes) fewer

studies have focused on understanding the changes in joint torques that occur as the result of adaptation. If the modeling of human gait is to be combined with the modeling of adaptation, an understanding of how the control signals (joint torques, muscle activities) change during the adaptation process will be vital.

Chapter 3: Experiment Design

3.1 Experimental Setup

All of the experiments for this research were performed in the Laboratory for Human Motion Analysis and Neurorehabilitation at the University of Texas at El Paso. This lab is equipped with state of the art systems for the analysis of human gait. Specifically, the lab contains a motion capture system for recording human movement, an instrumented treadmill for measuring ground reaction forces and EMG system for recording muscle activation levels. All three systems have been integrated and synchronized to begin recording at the same time.

3.1.1 Motion Capture System

The lab uses a 3D visual motion capture system supplied by Simi Motion Reality Systems (Munich, Germany). This system consists of eight gray-scale high speed CCD cameras and the associated software for recording and analyzing the acquired data. The system has been calibrated such that when a reflective marker above the treadmill is visible in at least two of the eight cameras the spatial location of that marker can be calculated. The calibration is also defined so that the world reference coordinate frame has a vertical Z-axis directed upwards and with the Y-axis parallel to the walking direction of the treadmill. The X-axis is oriented orthogonally from the other two axes using a right handed system. Note that this coordinate frame is oriented differently than the inverse dynamic model reference frame in Matlab. In particular, the Simi Z-axis corresponds to the inverse dynamic model Y-axis and the Y-axis in Simi represents the model X-axis.

For each camera, the two dimensional positions of the labeled markers is interpolated using a cubic spline approach to fill any gaps in the raw data resulting from occluded markers. The maximum

interpolated gap was set to 10 samples (0.143 seconds at 70 samples/sec). The interpolated data was then filtered using a second-order Butterworth filter with a cut-off frequency of 6Hz [Wint05].

The specific placement of the reflective markers on the subjects was based on the standard marker configuration defined used by the Simi software [Simi07]. Fig. 3.1 shows the marker placement diagram from the Simi Inverse Dynamics manual. The figure caption describes the specific markers used in this work. Four markers on each leg (labeled as 2, 5, 8 and 11 in Fig. 3.1) are placed on the subject for the static trial and removed for the dynamics motion trial. The static trial is used to define the locations of joint centers and the segment lengths using the full marker set.

3.1.2 Instrumented Treadmill

In order to study gait for a large number of consecutive strides, the lab is equipped with a dual-belt instrumented treadmill supplied by Bertec Corporation (Columbus, OH). This treadmill contains force plates for measuring the ground reaction forces separately for each foot. In particular, the force plate in each treadmill (left and right) measures the X, Y and Z components of the force and the moment with respect to the treadmill reference frame. This reference frame is defined such that the Z-axis is directed vertically downward and the Y-axis is directed towards the front of the treadmill in the walking direction. The X-axis is orthogonal to the YZ-plane and defined using a right-handed system. Note that, with respect to the world frame defined in Simi, the treadmill frame is rotated by π radians about the Y-axis.

The six signals from each treadmill (3 forces, 3 moments) are used to determine the center of pressure (COP) at which the ground reaction forces are applied. The COP is calculated as shown in (3.1) below, where X_P and Y_P are the coordinates on the surface of the treadmill at which the force is applied, h is the height of the treadmill surface from the treadmill coordinate frame (h = 0.015 m) and F_X, F_Y, F_Z, M_X and M_Y represent force and moment components measured from the treadmill [Bert07].

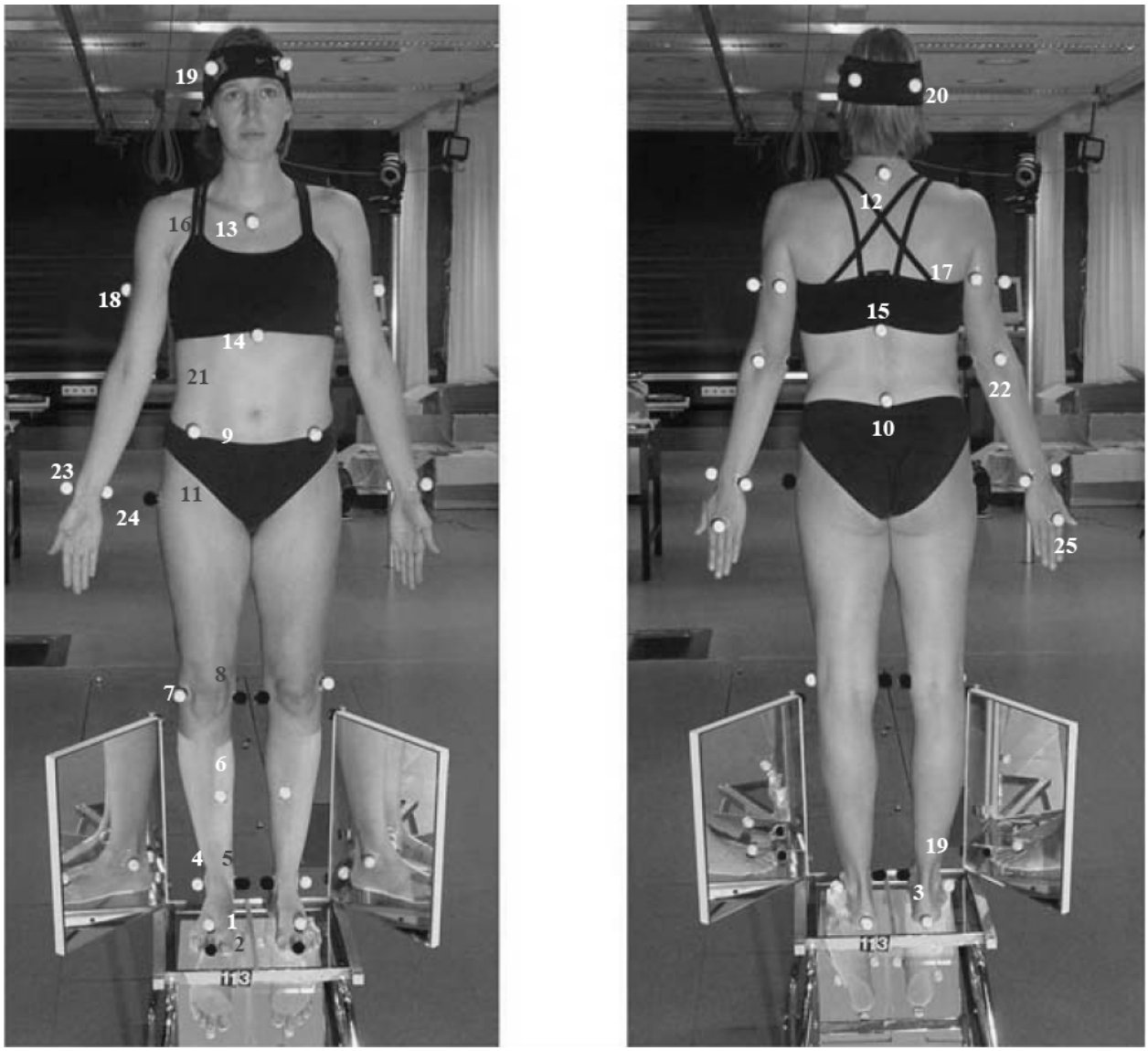

Figure 3.1: Simi marker placement [Simi]. Markers used: 1 – forefoot (over 2nd metatarsal), 2 – foot tip (tip of second toe), 3 – heel (posterior surface of calcaneus), 4 – outside ankle (maleolus lateralis), 5 – inside ankle (maleolus medialis), 6 – shank (midpoint of anterior shin), 7 – outside knee (condylis lateralis), 8 – inside knee (condylus medialis), 9 – spina iliaca anterior superior, 10 – L4 vertebra, 11 – greater trochanter, 12 – C7 vertebra, 13 – sternum (top of breast bone), 14 – xyphoid process (bottom of breast bone), 15 – Th8 vertebra. Markers 1 to 9 are for both the left and right sides. The dark markers (2, 5, 8 and 11) are present only for the static trial.

The system is calibrated such that the surface of the treadmill is level with the XY-plane, thus the COP in the Z direction is 0.

$$COP_T = \frac{-h \cdot F_Y - M_X}{F_Z} \tag{3.1}$$

Equation 3.1 gives the location of the COP in the treadmill reference frame. Since the current work is modeling the leg and foot in the sagittal plane (see Chapter 4), the COP along the Y-axis of the world frame is required. Since the Y-axes of the treadmill and world reference frames are parallel, the world frame Y-axis COP is found using the offset of the treadmill in the world frame. This is calculated in (3.2), where COP_T is the Y-axis COP from (3.1), Y_M is the Y-axis location of a marker placed on a known location on the treadmill and Y_O is the Y offset of the marker from the treadmill origin.

$$COP_W = COP_T + Y_M + Y_O \tag{3.2}$$

The signals from the treadmill are filtered using a second-order Butterworth filter with a cut-off frequency of 20 Hz. This frequency was selected to eliminate the noise in the measured ground reaction force data. Since the treadmill being used is located on the third floor of the building, the sensitive instrumentation in the treadmill picks up vibrations in the building itself. The frequency of 20 Hz effectively smoothed the force data without completely removing the high frequency components of the ground reaction forces during initial contact.

3.1.3 EMG Acquisition

In order to gain insight into the subject's control of their motion, electromyographic data (EMG) is recorded during the experiments. Subject muscle activation levels are recorded using a 16 channel Myomonitor III EMG system from Delsys Inc. (Boston, MA) and on loan from the Stanley E. Fulton Laboratory in the Kinesiology Department at UTEP.

The recording of EMG provides activation patterns that can be compared with the joint torque profiles generated by the inverse dynamics analysis. Specifically, any changes in muscle activation resulting from adaptation will be compared with the joint torque changes to see if there are any evident correlations. EMG signals were recorded for each of the following eight muscles on both the left and right legs.

- Soleus (ankle plantarflexor)
- Tibialis Anterior (ankle dorsiflexor)
- Lateral Gastrocnemius (ankle plantarflexor, knee flexor)
- Vastus Lateralis (knee extensor and stabilizer)
- Rectus Femoris (knee extensor, hip flexor)
- Biceps Femoris (knee flexor, hip extensor)
- Gluteus Medius (hip abductor)
- Erector Spinae (spine extension, torso stabilization)

The raw EMG signals are processed to obtain muscle activation envelopes. Specifically, this processing involves the following:

- Bandpass filter (20-250 Hz passband) to remove high frequency noise and low frequency motion artifacts. Motion artifacts have most of their energy located in the 0-20 Hz range and the useful energy of the EMG signal is mostly contained below 250Hz.

- The above filtering also removes any DC component from the EMG signal. EMG is by definition a zero-mean signal and any DC component in the recorded signal is an unwanted artifact.
- Full-wave rectification of the signal by taking the absolute value.
- Low pass filtering the rectified signal with a cut-off of 10Hz to generate an EMG envelope with a magnitude proportional to the muscle activation level.

The processed EMG signals are then used to determine the timing and relative activation levels of each muscle during the gait cycle. Note that the amplitudes of different muscles cannot be compared since the magnitude is dependent on several factors including electrode placement and skin resistance. However, the EMG levels measured during the adaptation experiments were collected with same electrode placement and therefore the comparison of signal amplitude for the adaptation experiment stages discussed below is possible.

3.2 Experiment #1 – Changes in Walking Speed

The goal of this experiment was to characterize the changes in joint torque profiles resulting from changes in treadmill walking speed. Specifically, the subjects were asked to walk at three different speeds (self-selected natural speed and +/-20%). When subjects are forced to walk at faster or slower speeds on a treadmill, their stride timing and stride length are affected. As a result, they must adapt to the change in speed which will result in changes to their joint torque trajectories.

3.2.1 Experiment Subjects

Three male subjects were studied for this experiment. The previously recorded data was obtained from the gait knowledge base in the Laboratory for Human Motion Analysis and Neurorehabilitation. All three subjects were healthy with no known neuromotor deficits. The

experimental protocol was reviewed and approved by the Institutional Review Board (IRB) at the University of Texas at El Paso and all subjects signed an informed consent form prior to participation. Table 3.1 shows the statistical data for the subjects.

Table 3.1: Experiment #1 subject statistics.

Subject	Age (years)	Height (m)	Weight (kg)
1	24	1.71	59.0
2	21	1.71	69.6
3	34	1.80	74.0
Average	26.3 ± 6.8	1.74 ± 0.05	67.5 ± 7.7

3.2.2 Experiment Procedure

After initial preparation (attachment of EMG electrodes and reflective markers) subjects were asked to walk on the treadmill to find their self-selected natural walking speed. The speed of the treadmill was increased until the subjects felt that it was moving faster than their natural walking speed. The speed was then decreased gradually until the subjects reported that it was going slower than their normal walking speed. The average of these maximum and minimum values was selected as their natural walking speed. The subjects were then given the opportunity to become comfortable walking on the treadmill for several minutes.

After the speed determination, the reflective markers and EMG were attached to the patients. One the EMG signal quality was verified, the subjects were asked to perform the static trial. In this trial, subjects stood on the treadmill with feet shoulder width apart and arms out to the side at shoulder level. A short recording of the subjects was made while in this position. The marker locations from this trial are used to calculate the limb lengths and joint centers required for the dynamic analysis. The static trial

was followed by three walking trials of three minutes each. The first trial was at the subject's natural walking speed, the second at 20% below their natural speed and the third at 20% above their natural speed. A rest period was given between the trials to prevent subject fatigue. Before recording each trial, the subjects were given 1-2 minutes to walk on the treadmill to become accustomed to the new speed setting. For safety reasons, whenever the treadmill was being started or stopped, the subjects were instructed to keep their hands on the safety bars to prevent falls.

3.2.3 Expected Results

When the speed of the treadmill is changed the subjects will exhibit changes in their gait patterns as the result of adaptation to the speed change. For an increase in speed, specific kinematic changes that are expected include a decreased stride time and an increased stride length. Additionally, the changes in stride length should result in increases in the peak flexion and extension of the hip. Also, an increase in ankle plantarflexion may possibly be seen during push-off along with an increase in peak knee flexion. For a decrease in treadmill speed, similar changes in the opposite direction should be expected.

An inverse kinematic analysis of gait at a faster treadmill speed should correlate with higher ankle plantarflexion moments at push-off and higher ankle dorsiflexion moments at heel strike. Additionally, the hip flexion moment should increase during swing phase to propel the leg forward at a faster speed. Also, the GRF peak levels should also exhibit increases resulting from a faster treadmill speed. Again, the changes for a slower gait speed are expected to be similar but in the opposite direction.

3.3 Experiment #2 – Adaptation to Changes in Gait Dynamics

The goal of the second group of experiments was to impose gait task modifications on healthy subjects and to analyze any changes in performance and joint torques resulting from the adaptation process. In total, five different task modifications were applied as outlined in section 3.3.2.

3.3.1 Experiment Subjects

Four healthy subjects with no known neuromotor impairments participated in these experiments. The adaptation experiment protocol was approved by the IRB at UTEP and all subjects signed an informed consent before the experiment began. In order to permit an analysis across adaptation experiments, the same four subjects were asked to perform all five of the gait task modifications. The subject statistics are presented in Table 3.2. Note that the body fat percentage statistic is included for the subjects in this set of experiments and not for the other experimental work. This is because the body fat estimating scale in the Laboratory for Human Motion Analysis and Neurorehabilitation was acquired after the other experimental data (Experiments #1) was collected.

The general criteria used to guide the subject selection were influenced by the size and design of the AFO as well as to keep subjects in a range similar to the intended patient population and the subjects from Experiment #1. The specific inclusion criteria were:

- 25-35 years old
- Self-reported average to above average balance
- Average foot size (9-10)
- Average calf-circumference (35-40 cm)

Table 3.2: Experiment #2 subject statistics.

Subject	Age (years)	Height (m)	Weight (kg)	Body Fat (%)
1	30	1.75	87.3	26.8
2	30	1.81	73.3	12.9
3	28	1.70	85.7	22.4
4	36	1.71	71.6	22.7
Average	31.0 ± 3.5	1.72 ± 0.02	79.5 ± 8.2	21.2 ± 5.9

3.3.2 Experiment Procedure

There were a total of five gait task modifications used in this experiment. Four of the gait modifications simulated ankle contracture impairments by limiting the range of motion of the ankle using an ankle-foot-orthosis (AFO). The fifth task modification was to have the subjects walk on the treadmill with the two belts moving at different speeds to simulate a limping gait.

The specific ranges of motion selected for the four AFO trials were:

- Lock ankle in 15° plantarflexed position
- Lock ankle in 15° dorsiflexed position
- Allow up to 30° plantarflexion and 0° dorsiflexion
- Allow up to 30° dorsiflexion and 0° plantarflexion

The first and third options above are intended to simulate aspects of contractures that cause drop foot by emulating limited dorsiflexion capability. The second and forth options simulate the inverse case of limited plantar flexion capability. This particular condition is not as common as drop foot and may be the result of spasticity and hypertonic conditions in the ankle dorsiflexors. The exact values used for the above cases were strongly influenced by the design of the AFO as will be described later.

As with Experiment #1, the natural walking speed was determined, the EMG and reflective markers were attached and the subject's static trials were recorded. Since the AFO altered the properties of the right leg, each subject performed two static trials (one with the AFO, one without). The subjects performed two one-minute “null” trials (one with AFO, one without AFO) to establish baseline performances before the adaptation trials. For the null trials and all of the AFO adaptation trials, the treadmill speed was set to 15% higher than the subjects natural walking speed. The reason for this is that a faster walking speed will make the task more difficult and cause greater influences from the uncertainty introduced by the task modifications.

For each of the AFO trials, the subjects walked on the treadmill for 2-3 minutes with no data collection at 15% faster than their natural walking speed to return to their baseline performance. Following this, the AFO range of motion was set to the required value and the subjects walked for one minute (adaptation trial). After one minute, the subjects were asked to stop walking while the AFO modification was removed. Subjects then walked for another one minute trial without the limited range of motion (after-effect trial). The time between the adaptation and after-effect trials was approximately 30-60 seconds.

The procedure for the final task modification where the treadmills move at two different speeds follows a similar sequence as the AFO trials. The subjects performed a single one-minute null trial walking at 1.0 m/s. This was followed by one-minute adaptation and after-effect trials. The speeds used for the treads were selected to simulate a limping gait with shortened right leg stance phase (right tread moving faster). The specific speeds used were 0.65 m/s for the left tread and 1.35 m/s for the right tread.

Ankle-Foot-Orthosis Design

The AFO used in these experiments was designed with the consultation of Dr. Eric Spier of Highlands Rehabilitation Hospital and Miguel Guerra of Total Orthotic & Prosthetic Solutions, both in El Paso, TX. The design incorporates a joint that can be locked using a series of replaceable keys. The keys are able to lock the joint in a selection of dorsiflexed and plantarflexed positions. Also, the joint can be set such that ankle rotation is allowed in one direction and not the other. The joint was manufactured by Mr. Guerra at Total Orthotic and Prosthetic Solutions.

The AFO device is shown in Figure 3.2. The upper portion attaches around the calf of the subject and is fastened with Velcro straps. The lower portion attaches to the foot and is also fastened with Velcro straps. Both of these components were manufactures using a molded plastic.

A close-up of the lockable ankle is shown in Figure 3.3. Each side of the AFO contains a hinge joint that can be locked using replaceable keys. The keys are placed in a recess and fastened with a machine screw. The key limited number of keys that are available with the joint dictated the exact ranges of motion that were selected for the experiments as discussed earlier.

3.3.3 Expected Results

Each of the AFO experiments is intended to simulate a different type of contracture of the ankle and as such, typical gait changes associated with ankle contracture impairments are expected. All of the AFO tests are meant to simulate rigid ankle contractures that resist stretching. However, it must be noted that the attachment of the AFO to the subjects is not completely rigid (elastic straps, foot may slide inside AFO) and that this may result in differences between the experimental adaptations and the typical expected contracture adaptations. For all of the adaptation experiments, based on previous research into the rates on adaptation, subjects are expected to reach a steady-state gait pattern with 20-25 strides and this steady-state pattern will incorporate combinations of specific kinematic adaptations.

Figure 3.2: Ankle-foot-orthosis (AFO). Upper and lower portions attach to subject using Velcro straps. The custom joint connecting the foot and leg components can be locked to limit ankle range of motion.

Locking the ankle in a plantarflexed position simulates drop foot during the swing phase of gait. Drop foot, therefore typical drop foot swing phase adaptations (steppage gait) are expected. This may potentially include combinations of increased knee flexion on the impaired leg, increased thigh flexion on the impaired leg and vaulting (rise up on toes) of the non-impaired leg and the frontal plane rotation of the pelvis to lift the hip of the impaired leg. During the stance phase, a plantarflexed locked ankle should prevent the forward rotation of the limb over the supporting foot. This should result in the toe-off time occurring earlier in the gait cycle and an associated asymmetry in the stance-swing ratios of the two limbs (decreased stance and increased swing on the impaired leg). There are significant changes

Figure 3.3: AFO joint with locking key inserted. Each side of the joint contains a recess for insertion of locking keys. The keys are fastened in place using a machine screw. The variety of keys allow for limiting the ankle range of motion in different ways.

expected during initial contact. As with drop foot gait, initial contact may occur with the forefoot rather than the heel. This would be expected earlier in the adaptation process, with late swing increases of hip flexion possibly occurring later in the adaptation to allow the heel to make initial contact. An inverse dynamics analysis should reveal changes in joint torques that correlate with each of these kinematic changes.

Locking the foot with the toes pulled upwards simulates the much rarer case of a dorsiflexion contracture. There should be fewer gait modifications during the swing phase for this experiment since there is no need for vaulting or steppage gait to prevent toe dragging. The transition from heel strike to flat foot will be significantly affected. Initially subjects should be expecting the foot to be in a more neutral orientation. This will result in an unexpected fast transition to foot flat and a sudden drop in the affected side of the body (increased knee and hip flexion). The increased forward shank rotation

resulting from the dorsiflexed foot should should result in a shorter stance phase since the non-impaired leg must be moved forward sooner to prevent the subject from falling forward. Similar to the previous AFO case, an inverse dynamics analysis should reveal changes in joint torques that correlate with each of these kinematic changes.

Limiting the range of motion of the ankle to only dorsiflexion and no plantarflexion should result in similar, though less significant changes as in the locked dorsiflexion experiment. The inability to plantarflex will result in the inability to properly push-off with the toes, thus resulting in an early toe-off and shortened stance time.

By not allowing the ankle to dorsiflex while allowing plantarflexion should affect the gait pattern in a similar manner to the locked plantarflexion experiment, though to a less significant degree. The subjects will not be able lift their toes past a neutral alignment, so there may still exhibit some steppage gait and vaulting to prevent toe dragging and will also have to compensate slightly with increased hip flexion to prevent initial contact with the toes. However, in this case, the toe-off adaptations seen during the locked plantarflexion case should be seen, since the subjects will be able to fully plantarflex their ankle to push-off with their toes.

Having the subjects walk on the treads at two different speeds should result in the most significant changes to their gait patterns. The obvious changes will be a decrease in the stance phase on the faster tread side. This will also be associated with a decrease in the swing time on the slower tread side. The faster tread side should exhibit similar changes in kinematics and dynamics to the changes seen in the increased speed trials of Experiment #1. Similarly, the slower tread side should exhibit similar changes to a decrease in walking speed. This particular task will be the most unnatural change during the adaptation experiments and therefore allow for more adaptation potential. This means that

the internal model formation demonstrated by the after-effect trials should show more dramatic gait deviations during the initial strides.

3.4 Experiment #3 – Patient Pilot Studies

The final set of experiments was designed to study the gait patterns of impaired patients. The intent of this work was to record the gait patterns of patients as case studies for comparison with the healthy subject adaptation data. Specifically, the question was whether it would be possible to infer any information about the patient impairments based on such comparisons. Prior to the analysis of the gait data, the researchers were blinded to the specific impairment details of the patients.

3.4.1 Experiment Subjects

Two patients with conditions causing ankle impairments were recruited for this study. The patients were supplied by Mentis Rehabilitation in El Paso, TX. The experimental protocol was approved for use with patients by the IRB at UTEP and both subjects signed informed consents before the experiment. The height, weight and age details for these patients are given in Table 3.3 below.

Table 3.3: Experiment #3 patient statistics.

Subject	Age (years)	Height (m)	Weight (kg)	Body Fat (%)
1	43	1.70	81.2	28.1
2	34	1.81	88.8	27.1
Average	38.5± 6.4	1.76 ± 0.08	85.0 ± 5.4	27.6 ± 0.7

Patient #1 Medical History

- Detailed medical history not available
- Motion on left side affected by stroke
- Able to walk without AFO or assistance
- Exhibits drop foot
- Predominantly circumduction compensation

Patient #2 Medical History

- Right mid-brain stroke in 2003
- Movement impaired on left side
- Various rehabilitation courses since
- Deep Brain Stimulation connected to brain stem
- Able to walk without AFO or other assistance
- exhibits drop foot
- Mostly vaulting compensation
- Some circumduction compensation

3.4.2 Experiment Procedure

The procedure used for the collection of patient data was similar to that used for the subjects in Experiment #1. However, the patients only performed a single three minute trial walking at their self-selected natural walking speed. Also, the subjects were brought up to speed at a more gradual rate and were given more time to become accustomed to walking on the treadmill. In addition to the safety bars

on the treadmill, research assistants were positioned next to the treadmill to catch the subject in the event of a fall.

3.4.3 Expected Results

While the specific details of the patient impairments were kept from the researchers during the data analysis stages, it was apparent during the experiment that both subjects exhibited drop foot symptoms. In this particular case, the blinding of the subject data may not have been affective since the researcher performing the analysis also participated in conducting the experiments. The drop foot exhibited by the patients implies that they will exhibit similarities to the locked plantar-flexion gait patterns, at least during the swing phase. Their decreased ability to generate dorsiflexion moments would also hinder the forward progression of the impaired limb over the support foot. Also, the subjects more than likely have decreased strength on their impaired side resulting in the inability to support their weight. Both of these factors should result in a decreased stance phase on the affected side.

Chapter 4: Inverse Dynamic Model of Gait

4.1 Model Design

The goal of the modeling in this work was to develop an inverse dynamic model that maintained much of the simplicity of sagittal plane gait models while also allowing for pelvis motion in the frontal and coronal planes. This extra pelvis motion was added to the model in anticipation of future requirements for studying more complex gait patterns in patient populations.

The overall model is divided into four subsystems including the legs, the pelvis and the head-arm-trunk (HAT) segment. The pelvis is modeled as a single triangular plate with the other three subsystems attached at the vertices. While the pelvis is permitted to have three rotational degrees of freedom, the segments of the HAT and leg systems are constrained to move only in the sagittal plane. The plane of motion for each of these constrained subsystems is defined by the medial-lateral location of the point of contact with the pelvis. Therefore, the base of each sagittal plane system (hip joints for the legs, lumbar spine joint for the HAT) is permitted to move in the frontal plane with the rest of each subsystem remaining parallel to the sagittal plane.

The HAT segment is modeled as a single segment attached to the top of the pelvis. Due to its constrained motion in the sagittal plane and the attachment to the pelvis, the HAT has a single degree of freedom (DOF) at the lumbar spine joint. Each of the legs is modeled as three segments (thigh, shank and foot) with three single DOF joints (hip, knee and ankle). Combined with the three rotational DOF of the pelvis, the model contains ten rotational DOF. In addition to these motions, the pelvis center of mass (COM) has two translational DOF in the sagittal plane, resulting in a total of 12 DOF for the overall system. Since the legs are constrained to the sagittal plane and the associated ground reaction forces are also sagittal in nature, the pelvis COM is constrained to not move in the medial-lateral

direction, thus limiting it to two translational DOF. The basic configuration of the model is shown in Figure 4.1 below:

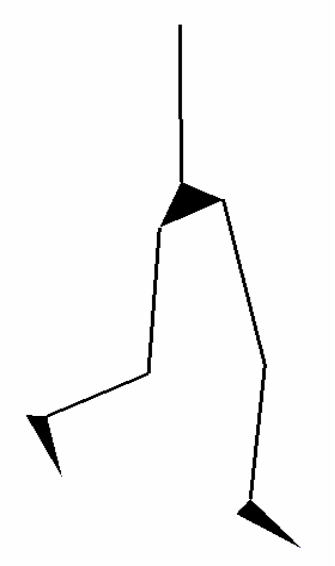

Figure 4.1: Inverse dynamic model configuration. The pelvis is modeled as a triangular plate with three rotational DOF. The legs and torso are attached to the pelvis at the triangle vertices and are constrained to be parallel to the sagittal plane.

For the inverse dynamics analysis, resultant driving torques are determined for each of the rotational degrees of freedom. The hip, knee, ankle and lumbar spine joint torques represent the typical sagittal plane motion. The three pelvis rotational DOF are located at the pelvis COM and help support the HAT segment and also control the pelvic drop and tilt that result in separate sagittal plane motions of the two hip joints.

The model inputs include joint center and segment orientation data. These inputs are derived directly form the motion data exported from the Simi motion capture software. The specific joint centers used include:

- Hips
- Knees

- Ankles
- Lumbar spine

The segment orientations include:

- Feet
- Shanks
- Thighs
- Torso

4.2 System Equations of Motion

The equations of motion for the inverse dynamic model were derived using a the Newton-Euler approach. The first stage of this process involves determining the interaction forces between the segments using the measured GRF values and the COM accelerations for each segment. The process for deriving the segment COM acceleration trajectories is outlined in Section 4.3 below.

Deriving the joint moments for the legs starts at the distal segment of the leg (the foot). The measured COM acceleration and GRF values are used to determine the foot-shank interaction force at the ankle as in (4.1), where F_G is the 2D ground reaction, F_A is the ankle reaction force, M_F is the mass of the foot , g is the acceleration due to gravity and $\ddot{X}_F$ is the 2D linear acceleration of the foot COM.

$$F_A = M_F \ddot{X}_F - F_G + M_F g \tag{4.1}$$

The ankle reaction force, F_A, represents the force exerted on the ankle by the shank. Therefore, the force exerted by the ankle on the shank is $-F_A$. Applying this force to the shank gives the knee

reaction force acting on the shank as in (4.2) where M_S is the mass of the shank, F_K is the knee reaction force and $\ddot{X}_S$ is the shank COM acceleration.

$$F_K = M_S \ddot{X}_S + F_A + M_S g \tag{4.2}$$

Ina similar manner, the hip interaction force acting on the thigh is given in (4.3), where M_T is the mass of the thigh, F_H is the hip reaction force and $\ddot{X}_T$ is the thigh COM acceleration.

$$F_H = M_T \ddot{X}_T + F_K + M_T g \tag{4.3}$$

The same process is repeated for each leg and for the torso. However, for the torso, the simplified equation for finding the lumbar spine interaction force, F_L , has no distal reaction force and is shown in (4.4) where M_H is the HAT mass and $\ddot{X}_H$ is the HAT COM acceleration.

$$F_L = M_H \ddot{X}_H + M_H g \tag{4.4}$$

Each of the reaction forces from the legs and torso are then applied to the pelvis as in (4.5), where F_{HR} and F_{HL} are the right and left hip interaction forces, M_P is the mass of the pelvis, $\ddot{X}_P$ is the acceleration of the pelvis COM and F_P is an additional force acting on the pelvis COM.

$$F_P = M_P \ddot{X}_P + M_P g + F_{HR} + F_{HL} + F_L \tag{4.5}$$

Theoretically, the residual force, F_P,should be zero, since the motion of the pelvis COM should be based only on the interaction forces with the attached segments. However, due to measurement error in the data, simplifications made during the model development and errors introduced by the differentiation of the position motion data contribute to making this force non-zero.

Once the interaction forces have been calculated, the joint moment calculation follows a similar procedure as the interaction force calculation. The ankle joint moment (or torque), T_A, is calculated as shown in (4.6), where R_{FG} and R_{FA} are the vectors from the foot COM to the point of application of the GRF (COP) and the ankle reaction force respectively. Additionally, I_F is the moment of inertia of the foot and $\ddot{\Theta}_F$ is the angular acceleration of the foot.

$$T_A = I_F \ddot{\Theta}_F - R_{FG} \times F_G - R_{FA} \times F_A \tag{4.6}$$

The magnitude of R_{FG} and R_{FA} are defined based on the position data exported from the subject's static trial in Simi, while their orientation are calculated from the segment orientations exported from the motion trial.

As with the ankle reaction force, the negative of the ankle moment acts on the shank. This relationship is used in (4.7) to calculate the knee moment, T_K, in the same manner used in (4.6).

$$T_K = I_S \ddot{\Theta}_S + T_A - R_{SA} \times F_A - R_{SK} \times F_K \tag{4.7}$$

In (4.7), I_S is the moment of inertia for the shank, $\ddot{\Theta}_S$ is the angular acceleration of the shank, and R_{SK} is the vector from the shank COM to the knee and R_{SA} is the vector to the ankle from the shank COM. Similarly, the hip moment, T_H, and lumbar moment, T_L, are calculated as in (4.8) and (4.9) respectively.

$$T_H = I_T \ddot{\Theta}_T + T_K - R_{TH} \times F_H - R_{TK} \times F_K \quad (4.8)$$

$$T_L = I_H \ddot{\Theta}_H - R_{HL} \times F_L \quad (4.9)$$

In (4.8), R_{TH} is the location of the hip with respect to the thigh COM, R_{TK} is the vector from the thigh COM to the knee, I_T is the thigh moment of inertia and $\ddot{\Theta}_T$ is the angular acceleration of the thigh. In (4.9), I_H is the HAT moment of inertia, $\ddot{\Theta}_H$ is the HAT angular acceleration and R_{HL} is the vector from the HAT COM to lumbar spine joint.

Finally, the resultant moments and forces applied to the pelvis are used to calculate the 3D moment acting about the pelvis COM. This moment is the sum of the moments generated by the CNS to control the movement along with residual torques similar in nature to the residual forces acting on the pelvis.

$$T_P = I_P \ddot{\Theta}_P + T_{RH} + T_{LH} + T_L + R_{PRH} \times F_{RH} + R_{PLH} \times F_{LH} + R_{PL} \times F_L \quad (4.10)$$

where, I_T is the moment of inertia for the pelvis, $\ddot{\Theta}_P$ is the angular acceleration of the pelvis, T_{RH} and T_{LH} are the respective moments from the right and left hips, T_L is the lumbar spine moment and R_{PRH}, R_{PLH} and R_{PL} are the vectors from the pelvis COM to the right hip, left hip and lumbar spine respectively.

The moments from the hips and lumbar spine in (4.10) represent the 2D moments from the attached segments transformed to moments acting about the Euler angle rotations. The transformation

involves the pre-multiplication of the applied torques by the rotation matrix defining the orientation of the pelvis. The derivation of the rotation matrix will be outlined in Section 4.3.

4.3 Processing of Model Inputs

There are 11 kinematic inputs to the dynamic model that must be extracted from the motion capture data. The values for the joint angle inputs for each leg and for the HAT segment are derived from the segment orientation data exported from Simi, which are measured with respect to the Simi world reference frame. The angles for the lumbar spine and both hips are taken directly from the X-axis (sagittal plane) orientation data for the segment attached to the joint.

The knee and ankle angular positions were calculated from the segment orientations of the thigh, shank and foot. Each is determined by finding the difference between the proximal and distal segments attached to the joint as given in (4.11) for the knee and (4.12) for the ankle. The angular velocity and acceleration values for these joints were determined in a similar manner.

$$\Theta_{KNEE} = \Theta_{SHANK} - \Theta_{THIGH} \tag{4.11}$$

$$\Theta_{ANKLE} = \Theta_{FOOT} - \Theta_{SHANK} \tag{4.12}$$

The final kinematic inputs represent the pelvis COM and orientation values, which can be derived from the joint centers of the hip joint and the lumbar spine joint. The dimensions of the pelvis were determined from the joint center locations during the static trial. The definition of the triangular plate by the attached joint centers can be seen in Figure 4.1.

The Euler angles for the pelvis were found by first determining a rotation matrix from unit vectors, *u*, *v* and *w*. The orientation of the *u* vector was defined by normalizing the vector pointing from

the lumbar joint to the midpoint between the hip joints. The *w* vector was found by normalizing the vector pointing from the left hip joint center to the right hip joint center. The final unit vector, *v*, was defined as the the cross product of the other unit vectors. A rotation matrix describing the orientation of the pelvis was then constructed from the unit unit vectors as shown in (4.13). This is the rotation matrix used to convert the moments from the hips and torso to the pelvis system.

$$R_P = \begin{bmatrix} u_X & v_X & w_X \\ u_Y & v_Y & w_Y \\ u_Z & v_Z & w_Z \end{bmatrix} \tag{4.13}$$

When determining the Euler angles for a given rotation matrix, one must be careful to define order of the rotations. Since each successive rotation is about the newly rotated reference frame, different rotation sequences will result in different Euler angle values. For example, an X-Y-Z rotation order does not yield the same Euler angle values as a Z-Y-X sequence. For the current work, an X-Y-Z sequence was used. Following this rotation sequence, results in the rotation matrix in (4.14), where *c* and *s* represent the cosine and sine of the indicated Euler angle. The elements of this matrix correspond to the values of the rotation matrix in (4.13).

$$R_P = \begin{bmatrix} c_Y c_Z & s_X s_Y c_Z - c_X s_Z & c_X s_Y c_Z + s_X s_Z \\ c_Y s_Z & c_X s_Y s_Z + c_X c_Z & c_X s_Y s_Z - s_X c_Z \\ -s_Y & s_X c_Y & c_X c_Y \end{bmatrix} \tag{4.14}$$

From these two equations, the following Euler angle equations can be derived as shown in (4.15). The velocities and accelerations of these Euler angles were then determined using numerical differentiation.

$$\Theta_Y = asin(-R_P(3,1))$$

$$\Theta_X = atan2\left(\frac{R_P(3,2)}{\cos(\Theta_Y)}, \frac{R_P(3,3)}{\cos(\Theta_Y)}\right) \tag{4.15}$$

$$\Theta_Z = atan2\left(\frac{R_P(2,1)}{\cos(\Theta_Y)}, \frac{R_P(1,1)}{\cos(\Theta_Y)}\right)$$

The Simi software provides estimates of the COM locations of each body segment. During the static trial, the COM locations were used in conjunction with the joint center data to determine the COM location for each of the leg segments in the simulation and for the pelvis. For the thigh and shank segments, the distance of the COM from the proximal endpoint was defined as the distance between the proximal joint center and the COM locations. For the foot segments, a position vector from the ankle to the COM location was determined. The COM for the pelvis provided by the Simi software did not lie on the triangular plane defined by the hip and lumbar joint centers. The pelvis COM value used as an input to the dynamic model is the perpendicular projection of the Simi pelvis COM onto the triangular plate from below.

Chapter 5: Experimental Results

5.1 Experiment #1

5.1.1 Kinematic Analysis

In order to assess the effect of changing the treadmill speed, each subject was processed separately with each of the slower and faster trials being compared with the natural speed trial. The average kinematic trajectories of the leg joint angles for Subject #1 are given in Figure 5.1 for the right leg and Figure 5.2 for the left leg. These figures show the joint angle trajectories for the slow (dashed line), natural (solid line) and fast (dotted line) walking trials. The orientation of the HAT segment and the height and anterior posterior location of the pelvis COM are given in Figure 5.3. Finally, angular trajectories given in Figure 5.4 are the Euler angles specifying the orientation of the pelvis. The plotted results are shown for Subject #1.

As can be seen in Figures 5.1-2, the right and left joint angle trajectories are similar in shape but shifted by 50% of the gait cycle. This makes sense since the subjects for this experiment were healthy with no known neuromotor deficits, and as such their gait should be symmetrical. The most significant speed-related changes occur in the ankle angle trajectories, while less significant changes are seen in the hip angle. This intuitively makes sense since the ankle angle in closest to the ground and therefore experiences more dramatic changes in motion due to changing GRF levels. The ankle and knee joints,along with the soft tissues in the legs act as shock absorption damping out the effects of the GRF changes by the time they reach the hip.

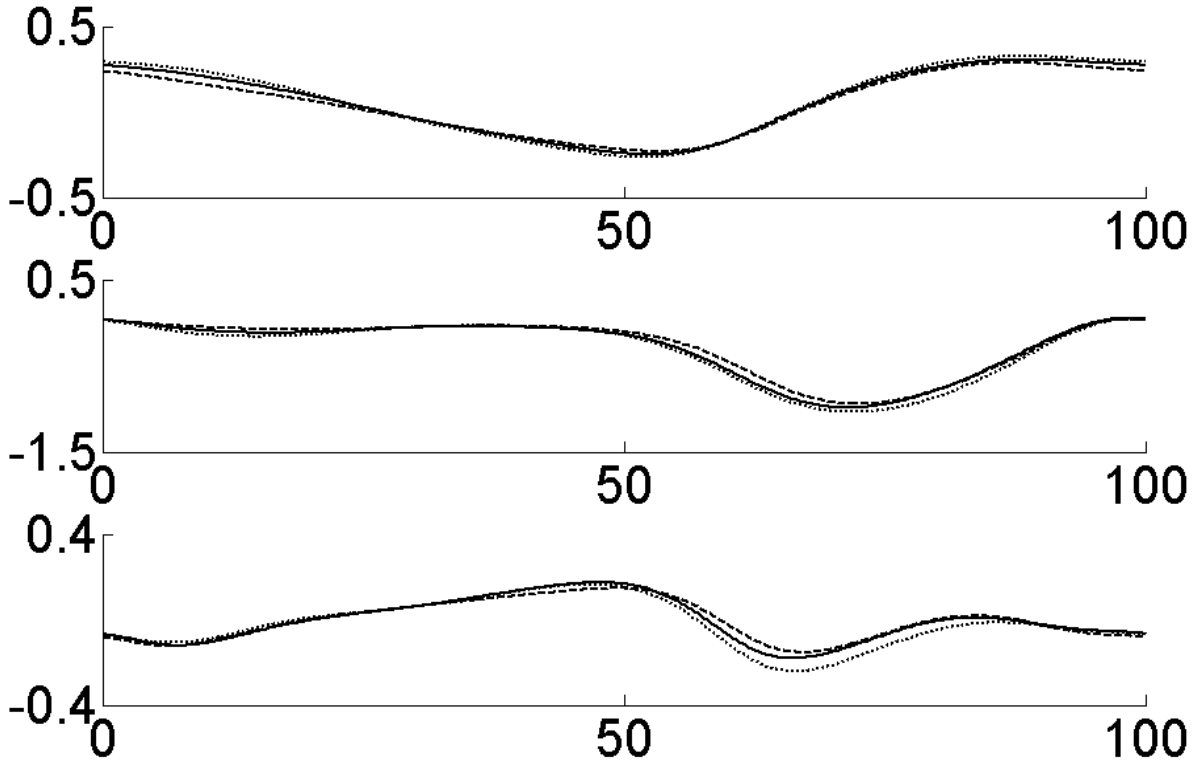

Figure 5.1: Right leg joint angle trajectories. Top - Hip joint angle. Middle – Knee joint angle. Bottom – Ankle joint angle The dark solid line is for the natural walking speed, the dashed line for the slow speed and the dotted line for the fast speed. The horizontal time axis represents gait cycle percentage and all angles are in radians.

The location of the pelvis COM seen in Figure 5.3 is related closely to the location of the hip joints as the subject walks. While it may appear that both the fast and slow trials show large decreases in the anterior-posterior pelvis COM location, it must be noted that the downward shift of the trajectories is the result of the subject walking at a slightly different location over the treadmill. Therefore, only the shape of these trajectories is of importance when considering changes due to walking speed. In this regard, there are some variations in the height of the pelvis COM in the last half of the gait cycle, during left leg stance. The height of the COM undergoes large changes as the result of changes in walking speed. The peak pelvis COM height during the swing phase of each leg is similar for all three walking

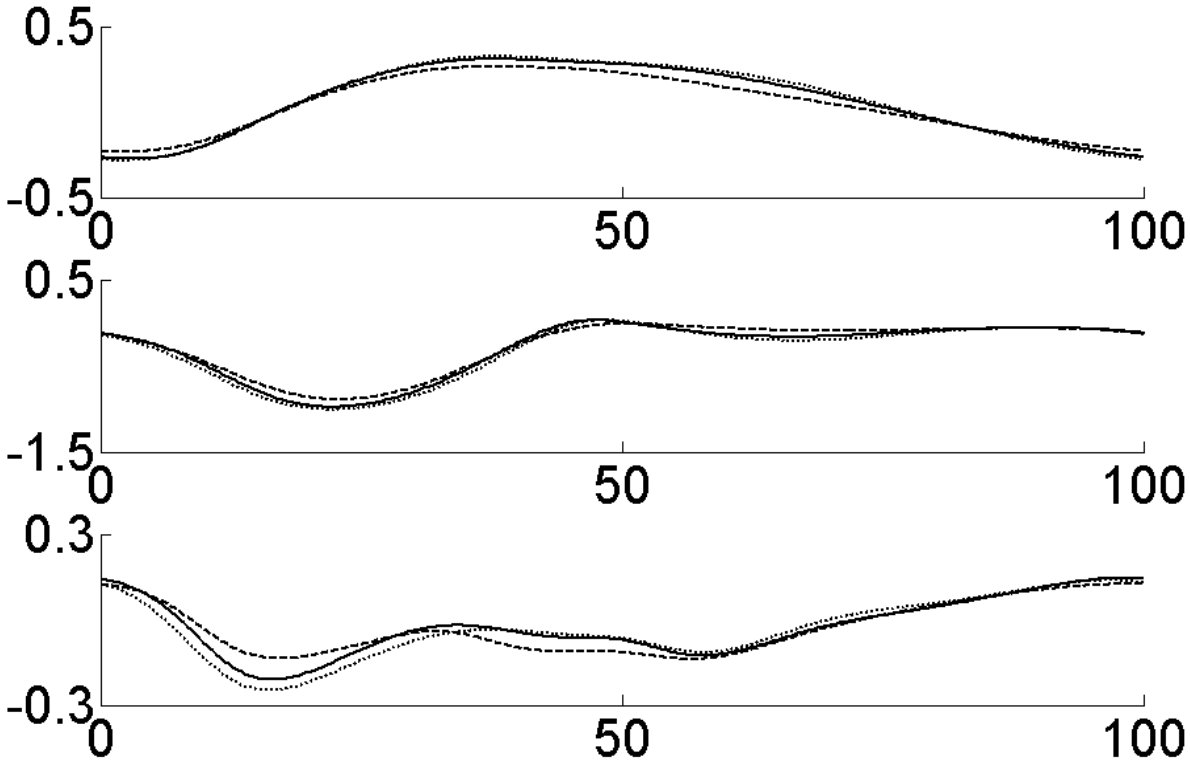

Figure 5.2: Left leg joint angle trajectories. Top - Hip joint angle. Middle – Knee joint angle. Bottom – Ankle joint angle The dark solid line is for the natural walking speed, the dashed line for the slow speed and the dotted line for the fast speed. The horizontal time axis represents gait cycle percentage and all angles are in radians.

speeds. This is due to the relationship between the stance leg functional length and the height of the pelvis at this point. Since there is no significant difference in peak knee flexion of the stance leg (smaller valley in the knee flexion trajectory in Figure 5.1), the height of the stance leg hip joint (and by extension the pelvis COM) will be similar for all three walking speeds. There are, however, significant changes in the height of the pelvis COM shortly following the heel strike of each leg. These are the locations at which the most significant changes in ankle angle occur in Figure 5.1.

The orientation of the torso in Figure 5.3 appears to exhibit significant changes in the second half of the gait cycle. This may be related to the difference in pelvis COM anterior-posterior location. It

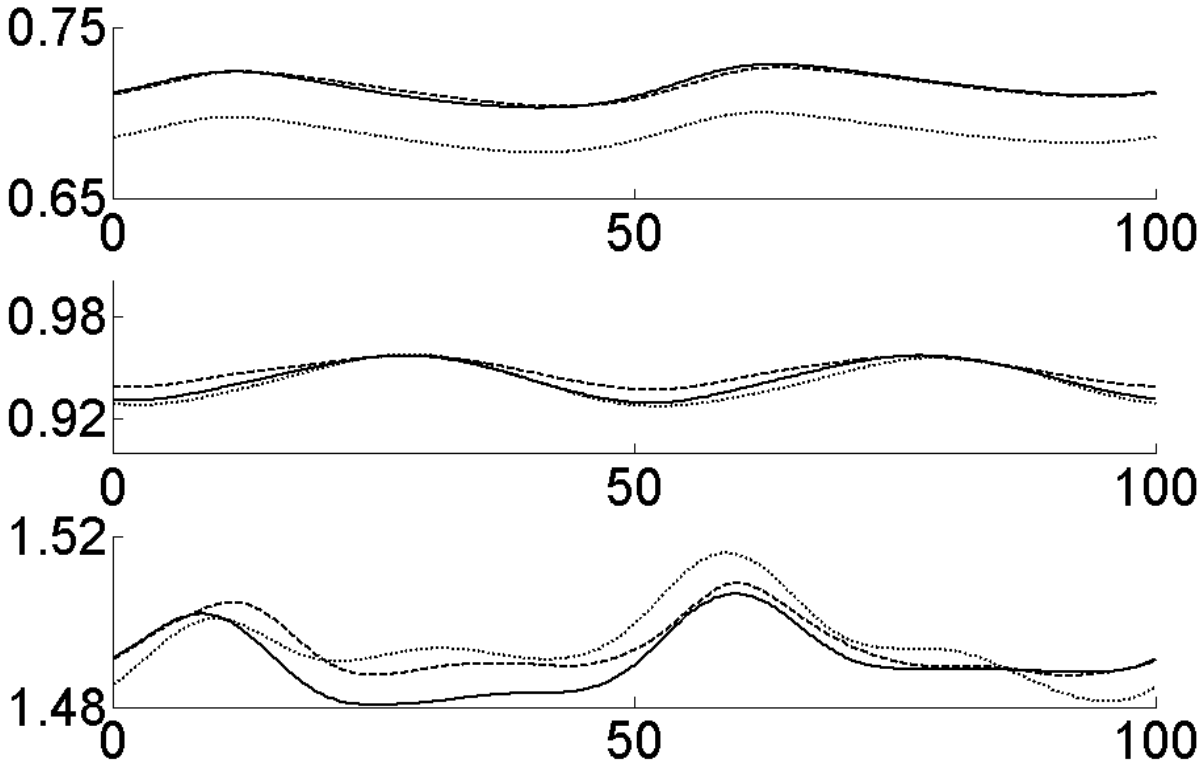

Figure 5.3: HAT segment angle and COM location of the pelvis. Top - Anterior-posterior pelvis COM location. Middle – Pelvis COM height. Bottom – Torso orientation about the X-axis measured from the Y-axis. The dark solid line is for the natural walking speed, the dashed line for the slow speed and the dotted line for the fast speed. The horizontal time axis represents gait cycle percentage. The COM location values are in meters and the torso angle is in radians.

appears that, when walking at the slower speed, this particular subject allowed the treadmill to pull them backwards. As the pelvis at the base of the torso moves further back, the torso exhibits a forward (negative) rotation. This asymmetry is apparent at all three walking speeds, but is more pronounced at slower speeds.

Overall, the trajectories given in Figures 5.1-4 demonstrate that there are definite differences resulting from the changes in walking speed for several of the kinematic trajectories considered. However, the exact nature of these differences cannot be read directly from the Figures.

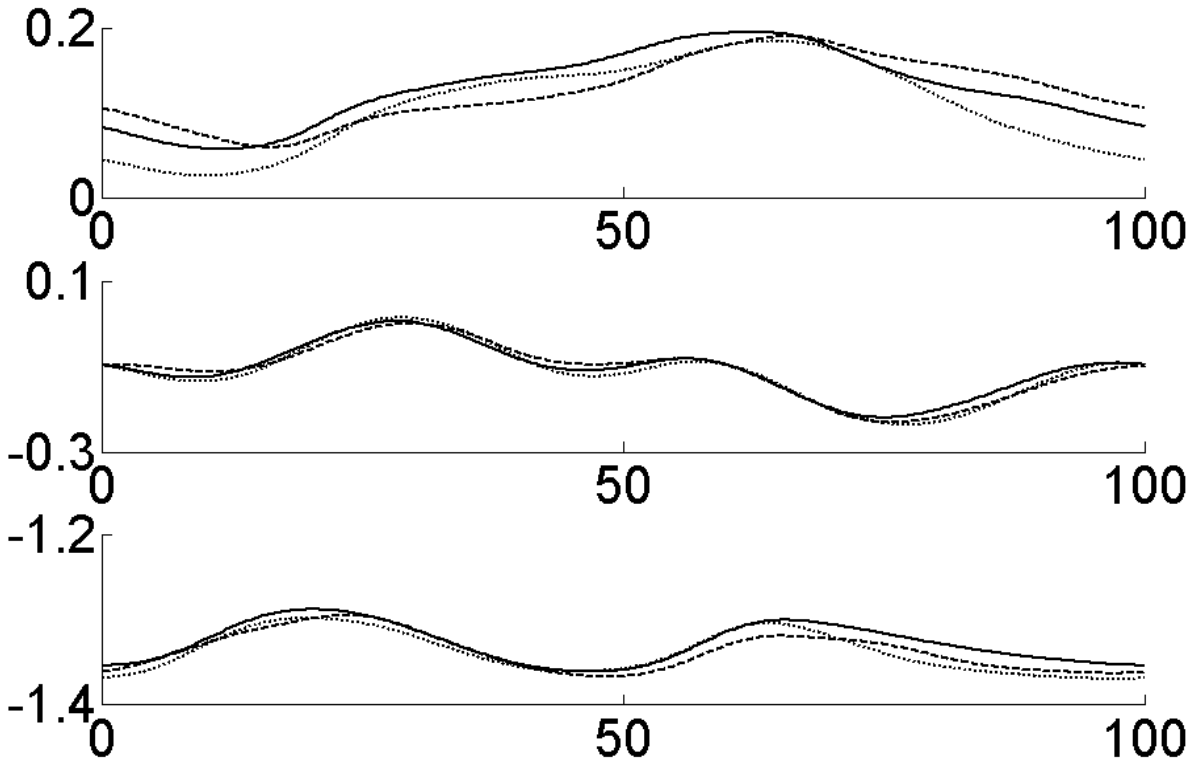

Figure 5.4: Pelvis orientation Euler angles. Top - X-axis Euler angle. Middle – Y-axis Euler angle. Bottom – Z-axis Euler angle. The dark solid line is for the natural walking speed, the dashed line for the slow speed and the dotted line for the fast speed. The horizontal time axis represents gait cycle percentage and all angles are in radians.

In order to assess the nature of the changes to the kinematic patterns, several performance metrics were selected and their average values determined for the different walking speeds. In particular, the following metrics were chosen.

- Stride time (seconds)
- Stance phase percentage (%)
- Stride length (meters)
- Peak knee flexion (radians)
- Peak hip extension (radians)

- Peak hip flexion during swing phase (radians)
- Ankle angle at toe off (radians)
- Ankle angle at heel strike (radians)
- Peak toe clearance (meters)
- Hip joint height during stance (radians)
- Hip joint height during swing (radians)

Table 5.1 shows the means and standard deviations for the above metrics for the right legs of all of the subjects. The results for each of the slow and fast trials were compared to those of the corresponding natural speed trial. Those results showing statistically significant differences are presented in the Table 5.1 in italics. This data is also given in Figures 5.5-7 to provide a more clear view of any trends present in the data.

As expected, the stride times for all of the subjects decreased as their walking speed increased. As subjects walk faster, they walk with a higher cadence thus reducing the step time. There is also a significant decrease in the amount of time spent in the stance phase as subjects walk faster. Counter-intuitively, there was a decrease in stride length for all subjects as they walked faster, which is not the general relationship seen in the literature for overground walking. This difference may be related to the changes in the anterior-posterior location of the pelvis COM from Figure 5.3. If the asymmetry in the COM position was indeed the result of subjects allowing the treadmill to pull them backwards when walking at slower speeds, then the corresponding calculated stride length could increase. This may also be related to the larger stance times seen during the slower walking trials.

Table 5.1: Average (± std dev) performance metric values for three subjects and three speeds.

Subject	**1**			**2**			**3**		
Trial	**Slow**	**Natural**	**Fast**	**Slow**	**Natural**	**Fast**	**Slow**	**Natural**	**Fast**
Stride Time	*1.27±.022*	1.17±.02	*1.04±.01*	*1.25±.03*	1.18±.027	*1.11±.03*	*1.37±.051*	1.2±.021	*1.1±.024*
Stance %	*64.3±1.03*	62.8±.81	*62.0±.53*	*66.6±.88*	64.9±1.13	*64.0±1.0*	*68.4±1.78*	66.6±1.54	*66.0±1.37*
Stride Length	*1.15±.023*	1.06±.017	*0.95±.013*	*1.09±.036*	1.03±.028	*0.97±.032*	*1.22±.051*	1.07±.027	*0.98±.029*
Knee Flexion	*0.95±.023*	0.99±.015	*1.04±.014*	*1.01±.037*	1.07±.025	1.08±.044	*0.84±.023*	0.83±.019	*0.94±.021*
Hip Extension	*0.23±.009*	0.25±.01	*0.27±.009*	*0.22±.017*	0.24±.014	*0.26±.017*	*0.33±.02*	0.36±.017	*0.37±.018*
Hip Flexion	*0.29±.011*	0.31±.011	*0.33±.009*	0.42±.017	0.43±.015	*0.45±.014*	*0.26±.013*	0.24±.011	*0.31±.013*
Ankle Toe Off	*-0.14±.034*	-0.15±.026	*-0.18±.024*	*0.05±.05*	-.04±.047	*-0.09±.082*	*-0.11±.028*	-0.08±.026	*-0.10±.035*
Ankle Heel Strike	*-0.08±.017*	-0.07±.011	-0.07±.01	0.06±.021	0.04±.012	*0.04±.013*	*-0.06±.016*	-0.05±.015	*-0.02±.015*
Toe Clearance	*.056±.003*	.064±.002	*.07±.003*	*.031±.013*	.049±.007	.049±.012	*.019±.016*	.011±.013	.011±.01
Hip Height Stance	*.939±.002*	.937±.002	*.939±.002*	*.881±.003*	.878±.002	.878±.003	*1.00±.002*	.999±.002	*.998±.003*
Hip Height Swing	*.923±.001*	.921±.001	*.923±.001*	*.904±.002*	.899±.002	*.905±.003*	*.996±.001*	.993±.001	*.994±.001*

*italics – Statistically significant difference from natural speed trial

The levels of peak hip flexion and extension exhibit small yet statistically significant increases as the result of walking faster (Figure 5.6A-B). At faster walking rates, the hip angle extremes would generally correlate with a longer stride length and a lower pelvis COM height at heel strike. The second of these characteristics is seen to be true from Figure 5.3 However, the correlation in stride length is not apparent. This is further evidence in support of the idea that the subjects' stride lengths are artificially lengthened by allowing the treadmill to pull them backwards slightly during the stance phase at slower walking speeds. This would affect the stride time, but would not have a significant effect on the thigh

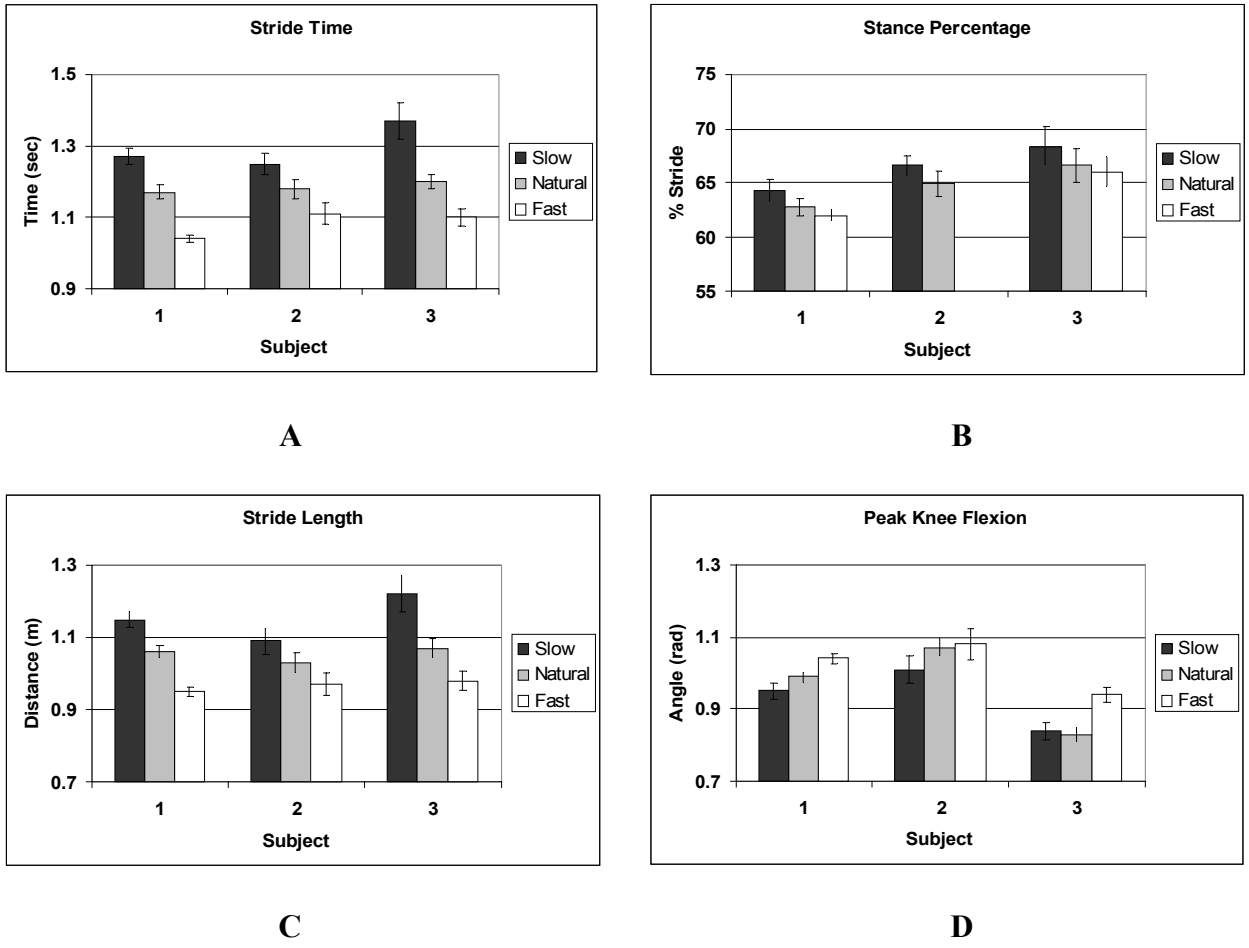

Figure 5.5: Average performance metrics for three subjects at three different speeds. Vertical error bars represent standard deviation A – Stride time, B – Stance percentage, C – Stride length, D – Peak knee flexion.

orientation at the moment of heel strike. For two of the three subjects, there is a decrease in the ankle angle at toe-off. This corresponds to the ankle undergoing extra plantarflexion at this time. The faster speed and larger ankle moments required for push-off would results in the foot experiencing extra plantarflexion. There is however, no clear pattern of change in the ankle angle during heel strike resulting from changes in walking speed.

While the pelvis COM exhibits significant changes due to changes in walking speed, the peak hip joint heights during stance and swing remained relatively constant. In healthy non-impaired subjects

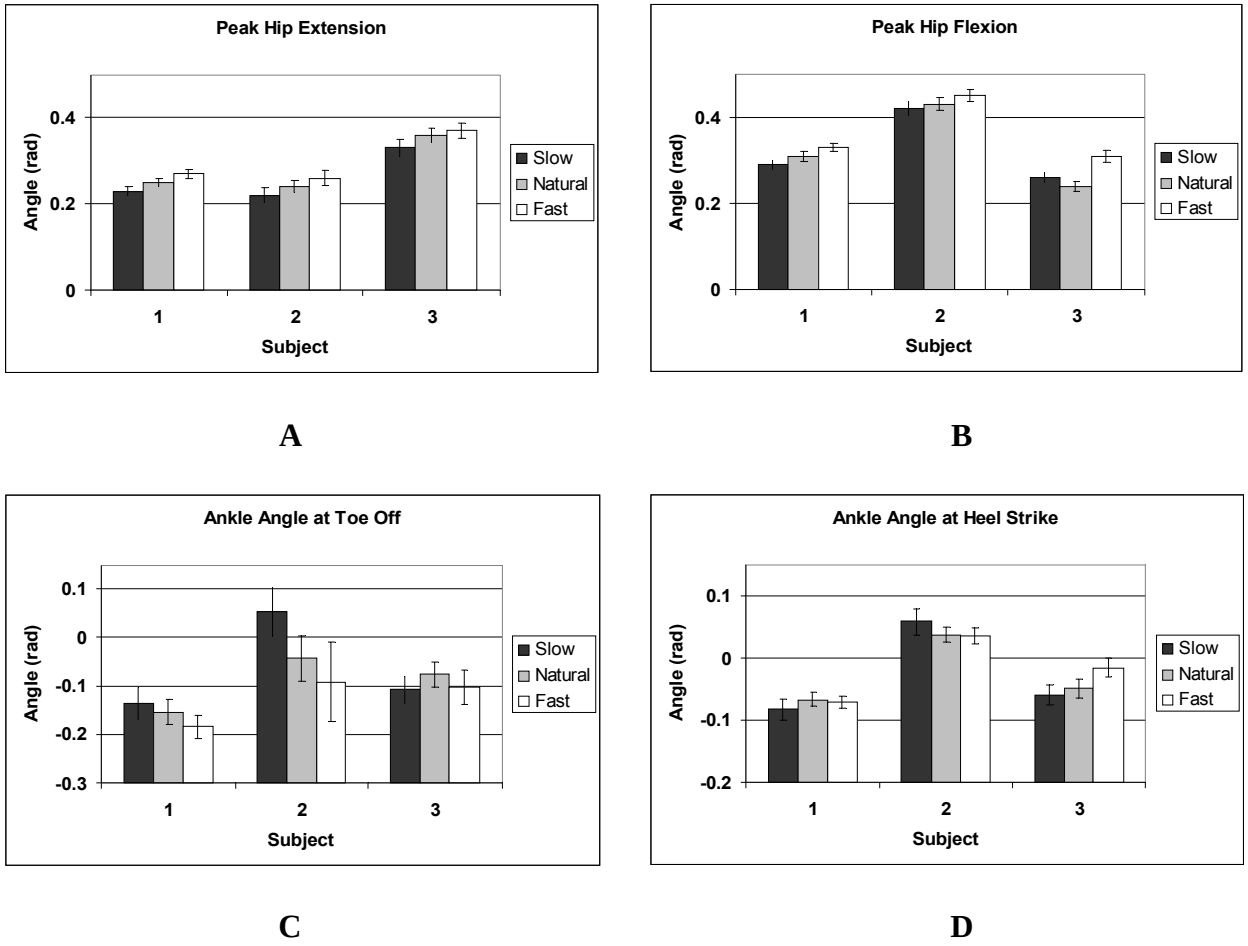

Figure 5.6: Average performance metrics for three subjects at three different speeds. Vertical error bars represent standard deviation A – Peak hip extension, B – Peak hip flexion, C – Ankle angle at toe off, D – Ankle angle at heel strike.

the peak hip heights at these time may not change much since the height is mostly dictated by the length of the stance leg. However, it is expected that patients with drop foot who must lift their foot higher to achieve toe clearance may see a change in these values resulting from vaulting and steppage gait patterns. Finally, the toe clearance increase for two of the three subjects as is expected with the increases in peak knee flexion. However, one subject showed a decrease in peak toe clearance. This is also the subject who exhibit the least prominent trend in increasing knee flexion.

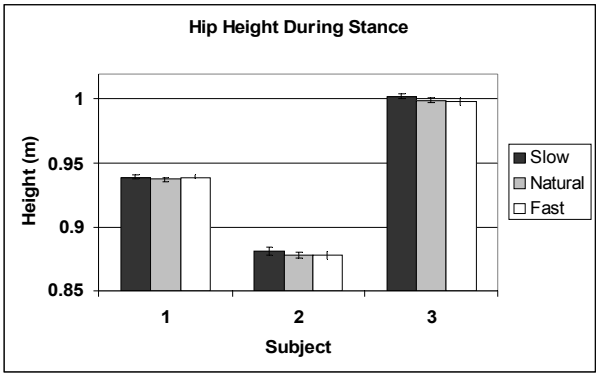

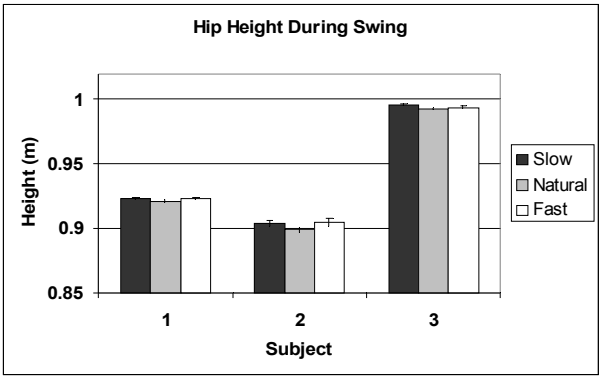

A **B**

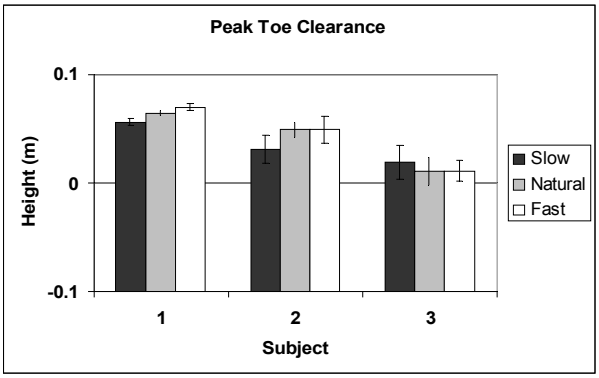

C

Figure 5.7: Average performance metrics for three subjects at three different speeds. Vertical error bars represent standard deviation A – Hip height during stance, B – Hip height during swing, C – Peak toe clearance.

After analyzing the changes in kinematics above, the changes in the ground reaction forces were also studied. Figure 5.8 shows the GRF values for the right leg and Figure 5.9 presents the GRF plots for the left leg. Once gain, the results are shown for Subject #1. As with the leg joint angles, the GRF data for the left and right legs is symmetrical. There are clear significant increase in the peak force levels in both the anterior and posterior direction and in the vertical direction for faster walking speeds. The most prominent changes occur as the result of heel strike and toe-off changes.

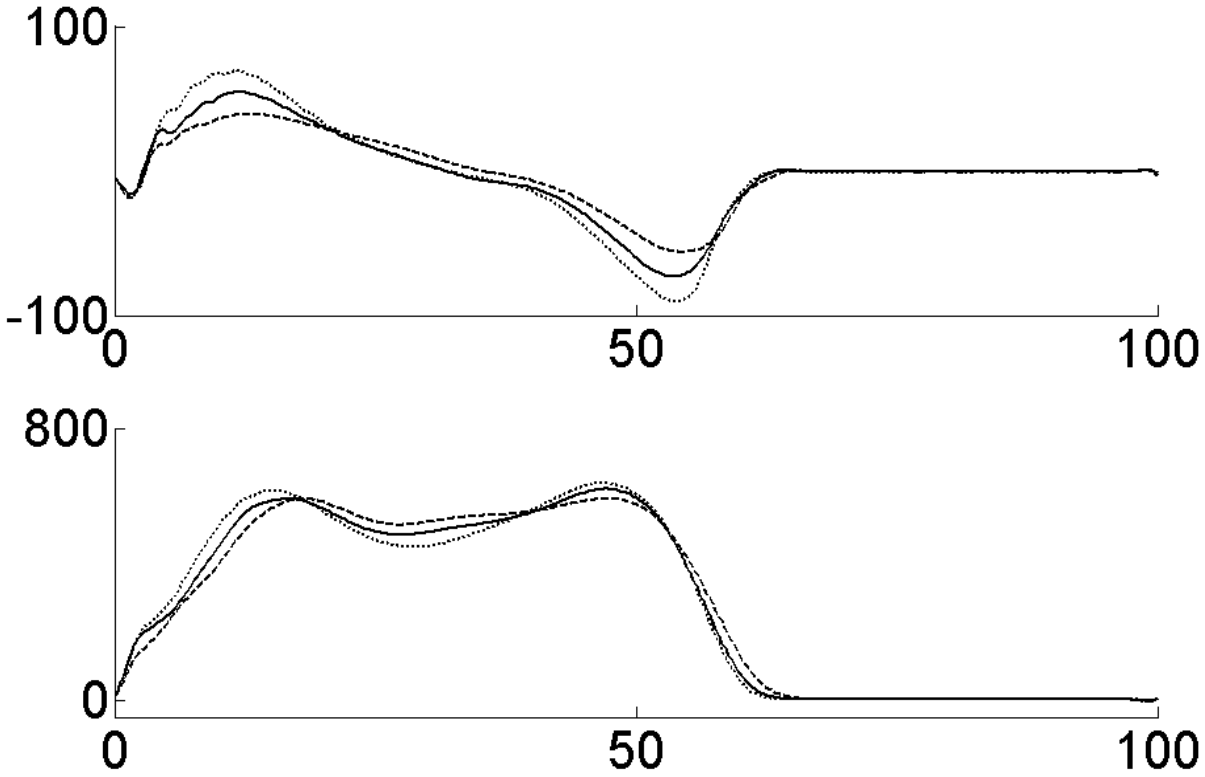

Figure 5.8: Average GRF values acting on the right foot. Top – Anterior posterior force. Bottom – Vertical force. The dark solid line is for the natural walking speed, the dashed line for the slow speed and the dotted line for the fast speed. The horizontal axis is the gait cycle percentage and the force values are in Newtons.

At heel strike the forward progression of the leg must be stopped to allow for placement of the foot into stance. The faster the walking speed, the more deceleration is required and thus the larger GRF value in the both the horizontal and vertical direction. At toe off, more force is required to swing the leg forward, therefore an increase in the ground reaction forces is also seen. In the midstance phase, a lower valley is seen in the vertical ground reaction forces. Examination of the GRF plots also demonstrates the longer stance time seen for slower walking speeds since the GRF values go to zero earlier in the gait cycle.

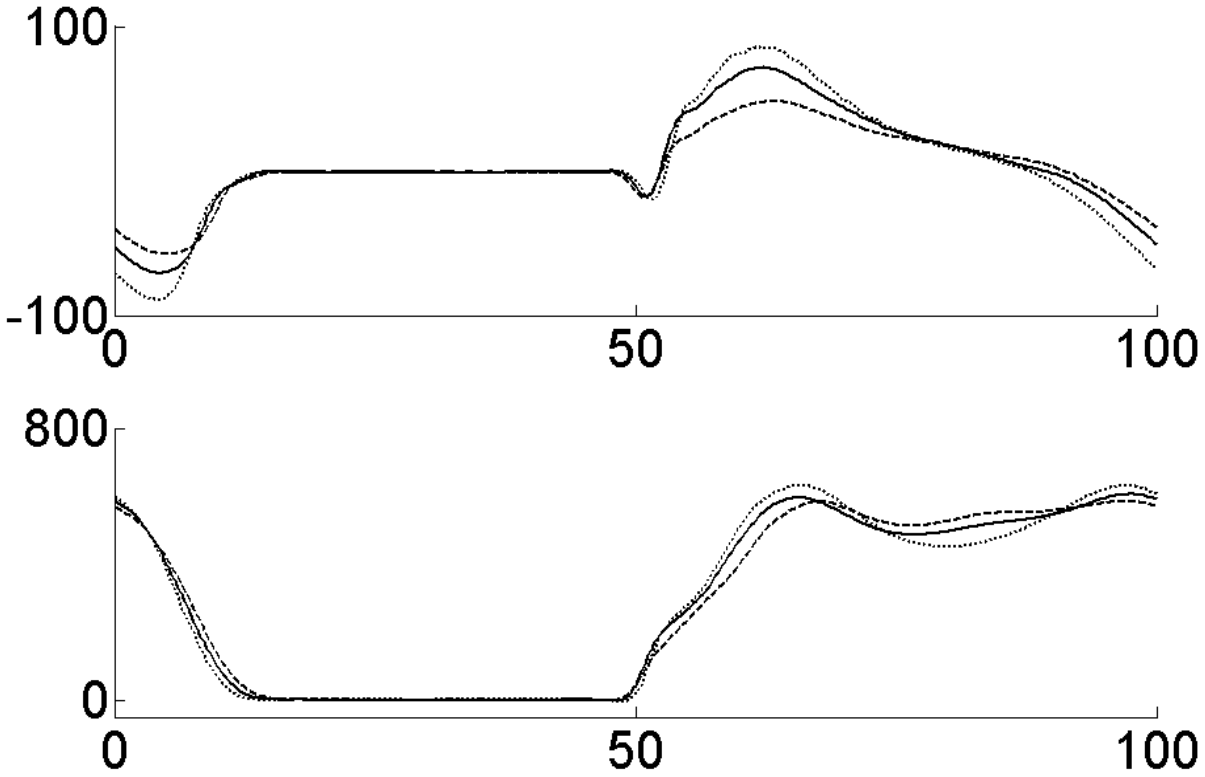

Figure 5.9: Average GRF values acting on the left foot. Top – Anterior posterior force. Bottom – Vertical force. The dark solid line is for the natural walking speed, the dashed line for the slow speed and the dotted line for the fast speed. The horizontal axis is the gait cycle percentage and the force values are in Newtons.

5.1.2 Inverse Dynamic Analysis

The results of the inverse dynamics analysis for Subject #1 are given in Figures 5.10-12. In particular, the results for the right leg, left leg and pelvis motion are given in Figures 5.10, 5.11 and 5.12 respectively. In Figures 5.10-11, the natural walking speed results follow typical joint moment trajectories for healthy non-impaired subjects [RPCP06]. All three joints exhibit larger moments at faster speeds during much of the stance phase in order to move progress the body over the limb and to generate additional force during push-off. Additionally, immediately after toe-off, faster walking speeds show larger moments in order to move the swing leg forward at a faster rate.

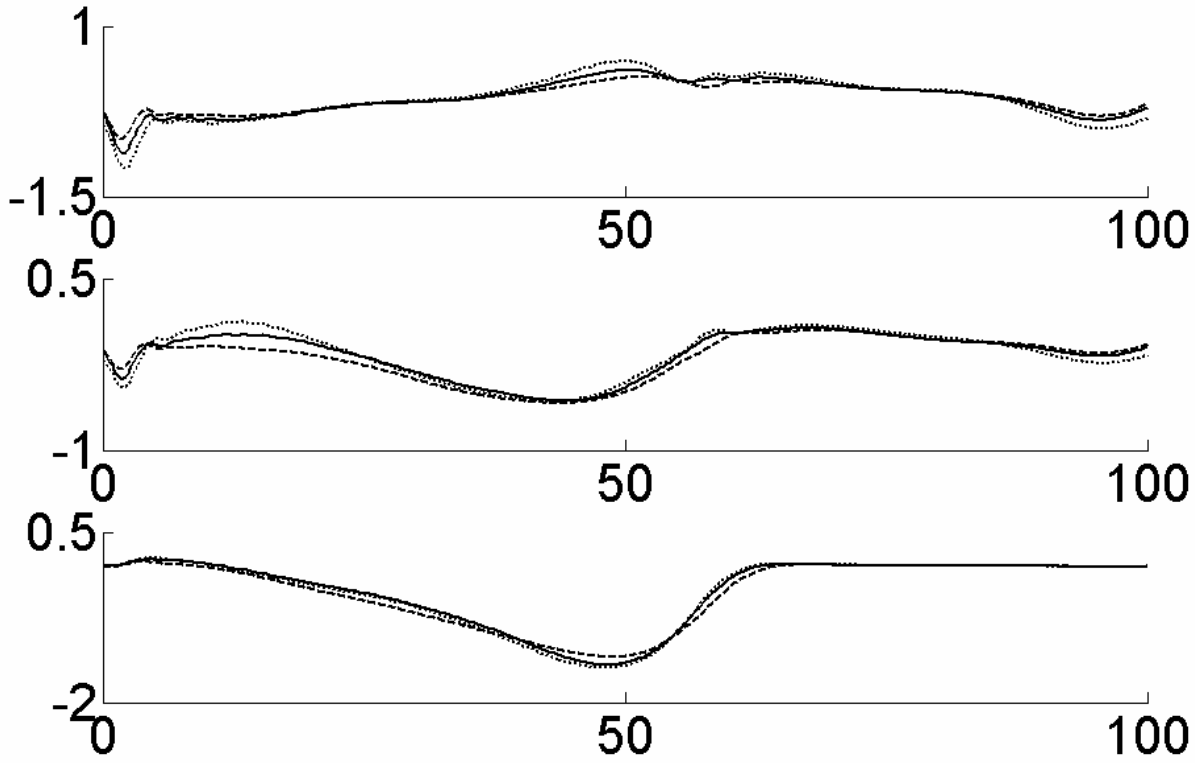

Figure 5.10: Average joint moments for the right leg determined using an inverse dynamics analysis. From top to bottom the plots show the moments for the hip, knee and ankle. The solid line represents the natural walking speed, the dashed line the slow speed and the dotted line the fast speed. The horizontal axes give gait cycle percentage and the vertical axes are the moments in Nm/kg (normalized by subject mass).

The results for the pelvis moments are presented in Figure 5.12. Recall that the order of rotation follows the XYZ sequence. The positive X-axis is along the subject's walking direction, with positive moments following the right-hand rule (counter-clockwise when looking towards the subject from the front). The Y-axis closely correlates with coronal plane rotation of the pelvis with positive moments working to move the right side of the pelvis forward and the left side of the pelvis backwards. Finally, the Z-axis of rotation closely correlates with the sagittal plane rotation of the pelvis. The moment about this axis is typically closer to a constant value, as the pelvis is not rotating by as much in this plane when

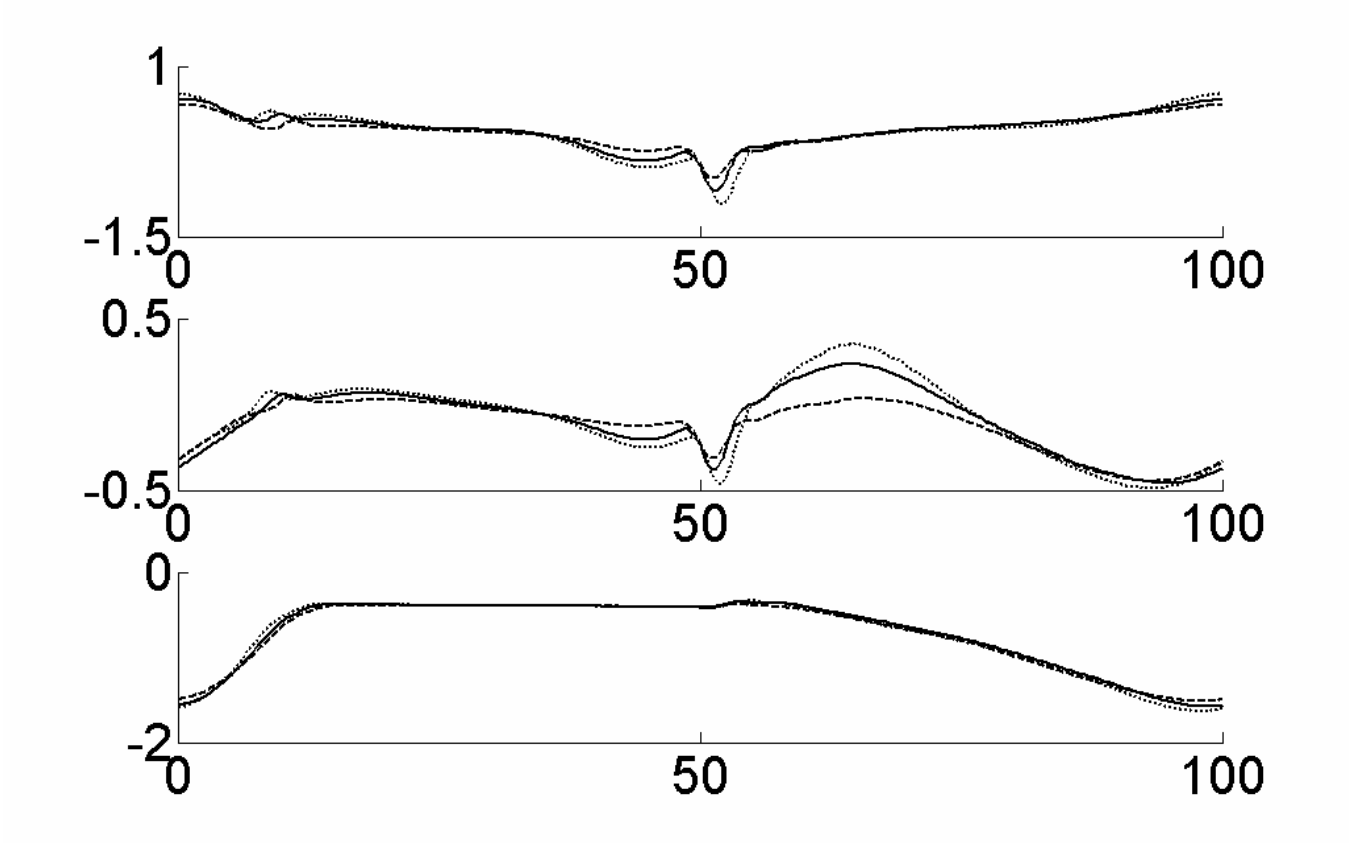

Figure 5.11: Average joint moments for the left leg determined using an inverse dynamics analysis. From top to bottom the plots show the moments for the hip, knee and ankle. The solid line represents the natural walking speed, the dashed line the slow speed and the dotted line the fast speed. The horizontal axes give gait cycle percentage and the vertical axes are the moments in Nm/kg (normalized by subject mass).

compared to the other two Euler rotations. There are no clear patterns resulting from changes in walking speed exhibited in the pelvis moment results. However, there does appear to be larger magnitude X and Y moments at the heel strike times (0% and 50% gait cycle) to counteract the effects of larger ground reaction forces.

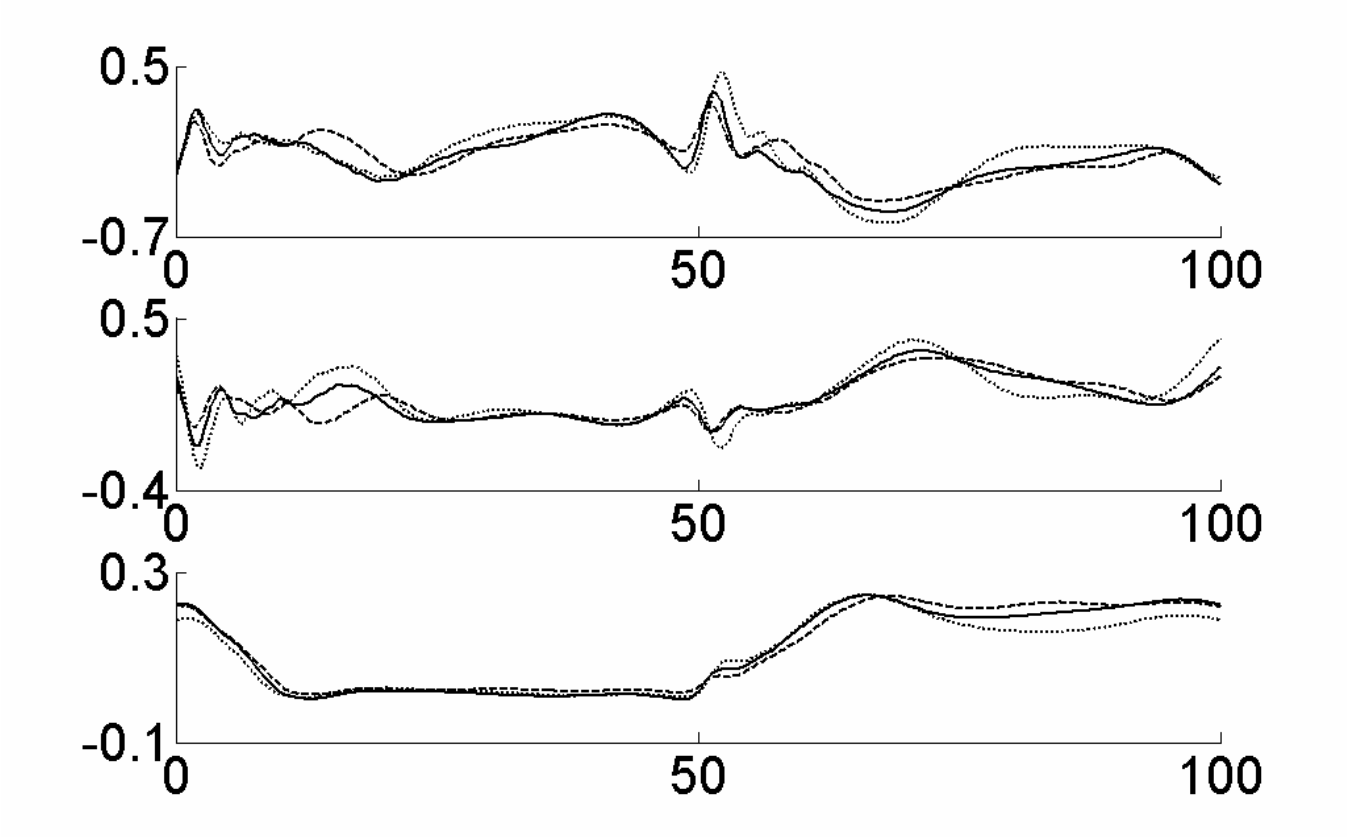

Figure 5.12: Average joint moments for the pelvis DOF determined using an inverse dynamics analysis. From top to bottom the plots show the moments for the X, Y and Z Euler rotations. The solid line represents the natural walking speed, the dashed line the slow speed and the dotted line the fast speed. The horizontal axes give gait cycle percentage and the vertical axes are the moments in Nm/kg (normalized by subject mass).

5.2 Experiment #2

5.2.1 Kinematic Analysis

The kinematic analysis of the adaptation experiments presented here focuses primarily on the behaviour of the performance metrics from Table 5.1 throughout the adaptation process. In all instances, the adaptation and after-effect results are shown together and compared with the average performance during the corresponding null field trial. Once again, the figures presented show the results for Subject #1. In all of the figures in this section, the right leg is shown in the top plot and the left leg

in the bottom plot. Recall that the leg with the AFO was the right leg and that the right tread was moving faster for the different tread speeds experiment. In all cases, the only difference between the adaptation and after-effect experiment conditions is the removal of the gait task modification between the trials.

Locked in Plantarflexion

The adaptation results for Subject #1 during the plantarflexed experiment are outlined in Figures 5.13-16. In Figure5.13 the stride time and stride length adaptation trials do not appear to show any changes from the null trial performance. However, once the AFO was unlocked, there is a clear after-effect of adaptation. Both the stride time and length show a decrease in the early after-effect trials, which gradually returns to the null trial levels within about 25 trials. This after-effect pattern is typical of the internal models investigated in motor adaptation literature. The lack of an initial change during the adaptation trial is unusual, though may be the result of the nature of the experiments. Traditional adaptation experiments impose unknown force-fields onto the subjects and therefore the subjects have no opportunity to predict what is going to happen. In the current work, thee nature of the gait task modification was apparent to the subject immediately after it was applied. Therefore the subjects could form an initial prediction of what modifications would be necessary to compensate for the modification. Therefore, there would be less chance for an initial error in performance that would need to be corrected.

It is worth noting the clear similarities between the stride length and stride time plots for the left and right legs. This is due to the fact that stride lengths and stride times are naturally going to be the same for both legs, since a full stride incorporates a step from each leg. The stance percentage however, should provide insight into gait asymmetries resulting from the adaptation process. In Figure 5.13C, there is a clear decrease in the right leg stance time at the beginning of the adaptation trial. This then increases towards the end of the trial. The corresponds with a small decrease in the stance time for the

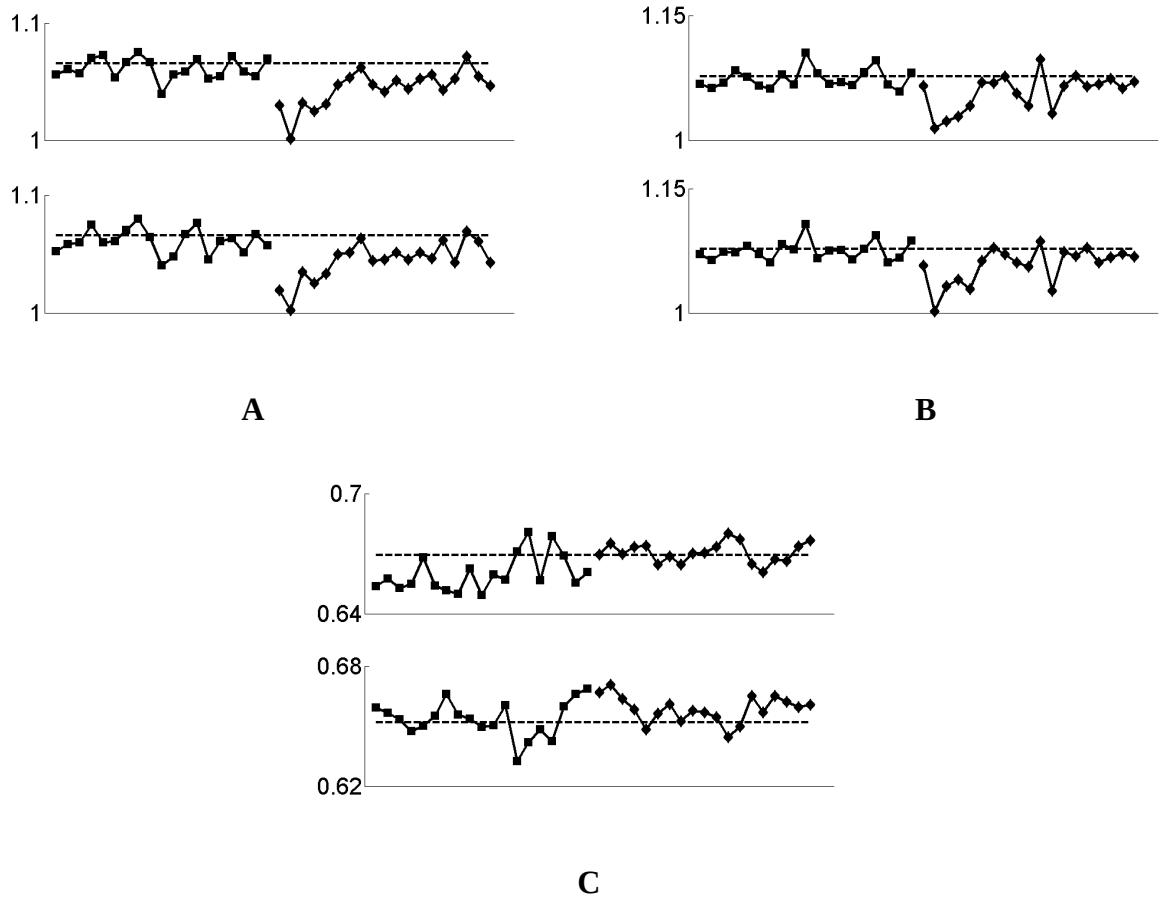

Figure 5.13: Stride time (A), stride length (B) and stance percentage (C) kinematic data through adaptation to AFO locked in plantarflexed position. For each performance metric, the top plot is for the right leg and the bottom plot is for the left leg. Each data point represents the average value for three strides. The square data points are for the adaptation stage and the diamonds are for the after-effect stage. The dashed horizontal line shows the null stage average performance. The units for the vertical axes are seconds, meters and % for A, B and C respectively.

left leg near the end of the adaptation trial. The after-effect of the learning process is seen in the increase in larger stance time for the left leg at the beginning of the after-effect trial. Again, there is a gradual return to the null trial levels within 20 strides.

In Figure 5.14A, there is a clear pattern of changes associated with the adaptation process. During the adaptation stage the peak hip extension levels are higher than the null stage. This is the case for both the left and right legs, although the effect is more pronounced on the right leg with the AFO.

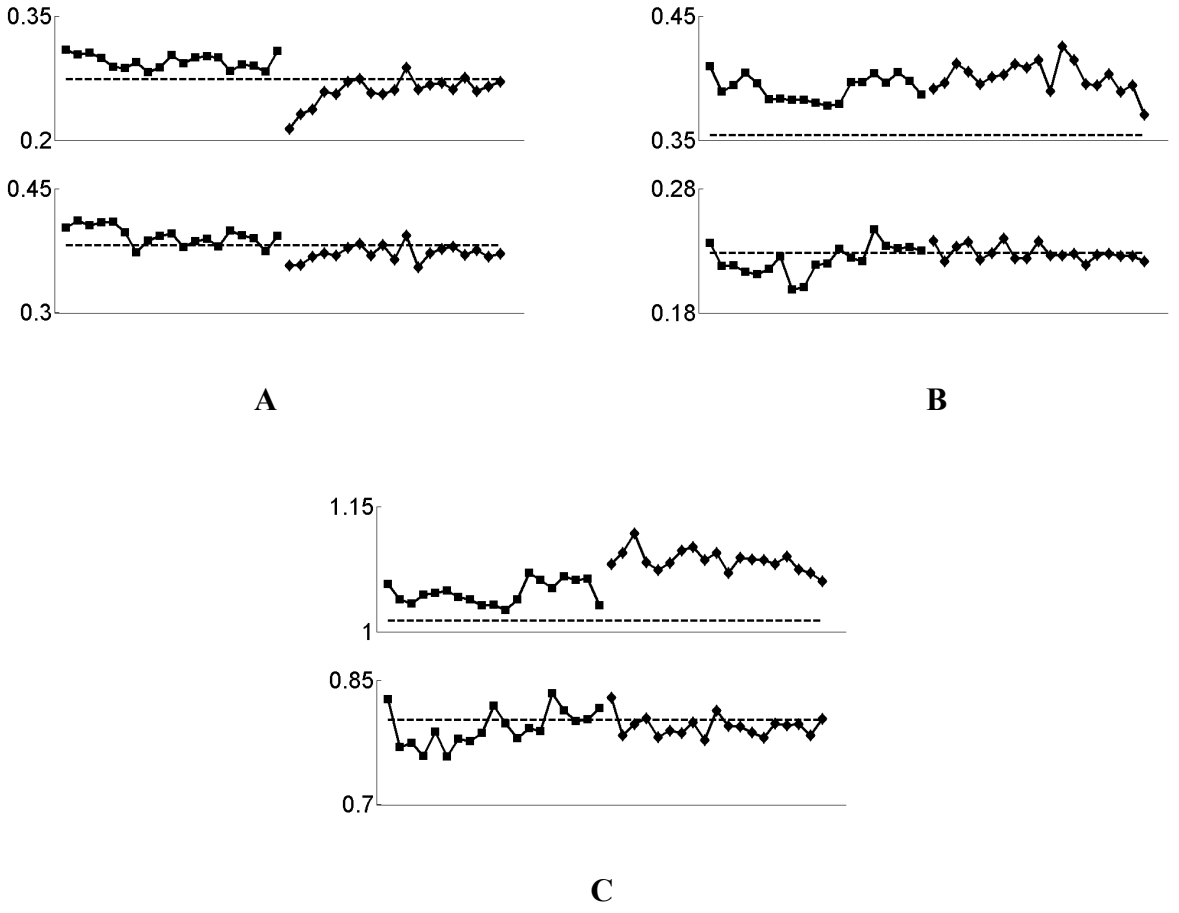

Figure 5.14: Hip extension (A), hip flexion (B) and knee flexion (C) kinematic data through adaptation to AFO locked in plantarflexed position. For each performance metric, the top plot is for the right leg and the bottom plot is for the left leg. Each data point represents the average value for three strides. The square data points are for the adaptation stage and the diamonds are for the after-effect stage. The dashed horizontal line shows the null stage average performance. The units for the vertical axes are radians.

Then the peak hip flexion angle shows a sharp decrease as an after-effect of the internal model formation, which gradually decreases to null trial levels within about 20 strides. As in previous adaptation research, the after-effect is in the opposite direction as the changes resulting from the adaptation tot he new task dynamics. For hip flexion, there is an slight decrease in peak flexion for the left leg and a distinct increase for the right leg. Throughout the adaptation trial the left leg hip flexion gradually returns to the null trial average, however the right leg hip flexion does not. In fact the right leg

flexion remains significantly higher than the null trial average through the entire after-effect trial as well, though there appears to be a slight decrease towards the end of the after-effect trial. The increase in flexion as a result of locking the foot in a plantarflexed position is similar to the increased hip flexion seen during steppage gait in patients with drop foot. However, the reason the subject did not quickly (within 25 strides) return to the null trial performance levels after the AFO lock was removed is not readily apparent.

As expected, the peak knee flexion angle of the right leg increased during the adaptation trial. This change was required to allow proper toe clearance during the swing phase and is consistent with the gait patterns seen in patient populations with drop foot. Also, there is a decrease in the left leg peak knee flexion during the initial strides of the adaptation trial. Since the subject's foot is locked with the toes down, the right leg stance phase should involve some degree of tip-toe walking which in turn raises the level of the pelvis and thus the left knee would require less flexion to achieve toe clearance during swing. As with the peak knee hip flexion, the knee flexion increase in the right leg did not return to null field levels during the after-effect trial, though it did show a clear decrease.

In Figure 5.15A there is a clear increase in the peak hip height during the swing phase. As with the previous adaptations, this is consistent with gait patterns seen in patient populations. In order for toe clearance to be achieved, the subject compensates for the plantarflexed foot by rotating the pelvis to lift the hip joint on the affected limb. Also, in line with the results seen for hip[and knee flexion peak values during the swing phase, the peak hip height also does not return to the null trial average during the after-effect trial. For the left leg, there are no significant changes seen for the swing phase hip height.

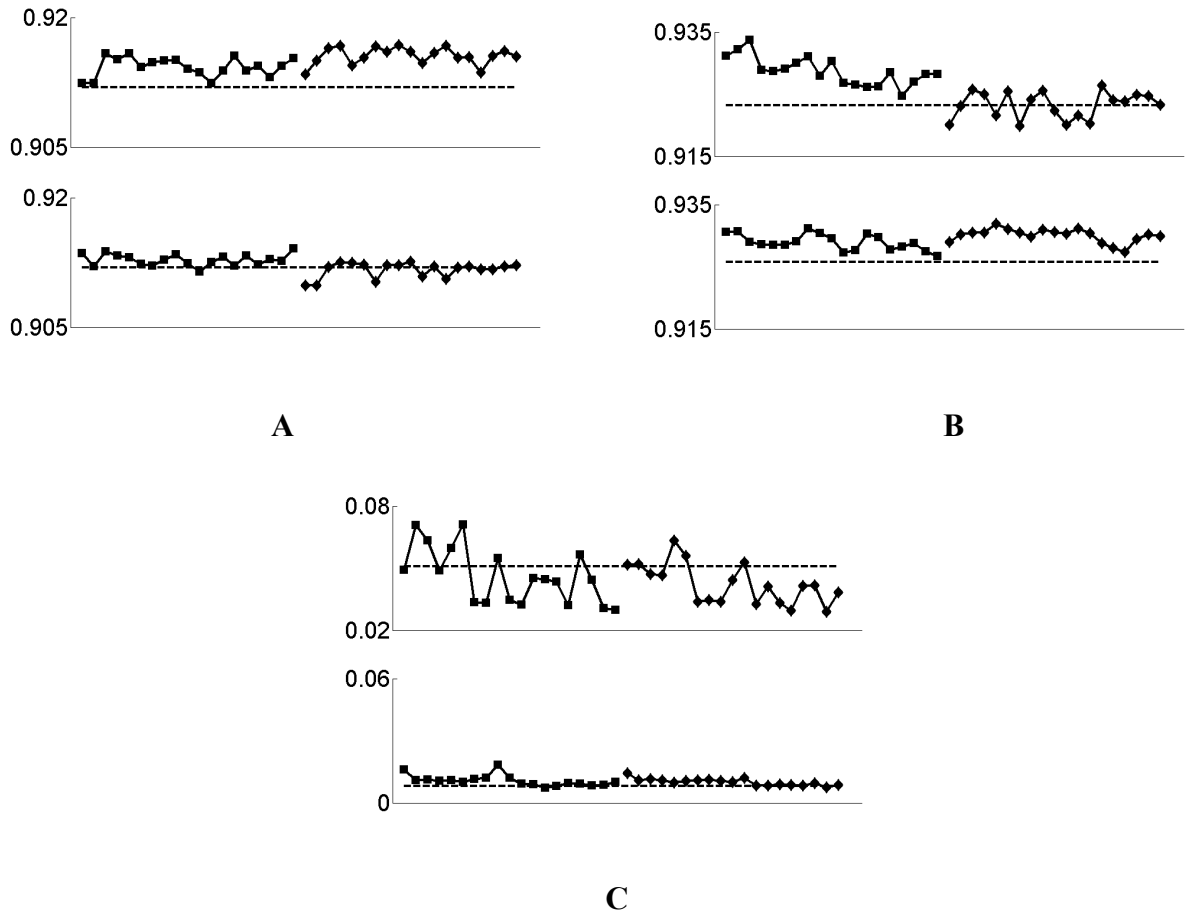

Figure 5.15: Hip joint height during swing (A), hip joint height during stance (B) and peak toe clearance (C) kinematic data through adaptation to AFO locked in plantarflexed position. For each performance metric, the top plot is for the right leg and the bottom plot is for the left leg. Each data point represents the average value for three strides. The square data points are for the adaptation stage and the diamonds are for the after-effect stage. The dashed horizontal line shows the null stage average performance. The units for the vertical axes are meters.

The height of both the left and right hips show clear increases during the adaptation trial and the height for both decrease by the end of the adaptation trial, although the decrease is more significant on the right side. The right hip height change is most likely the result of a tip-toe stance phase for the right foot. The increase on the left is not as significant as that on the right, however, the increase does make sense in terms of compensation for drop foot. Occasionally patients will increase the functional length

of the unaffected leg during stance (vaulting) to effectively increase the height of the pelvis and thus allow for easier toe clearance. Again, as with the other adaptations for improving toe clearance, this adaptation does not reduce to null trial levels during the after-effect trial. The right leg stance phase hip height however, immediately returns to the null trial level during the after effect trial, since there is no longer a tip-toe gait being imposed on the right foot.

Figure 5.15C shows the toe clearance levels for both legs. The toe peak toe clearance for the left leg remains at the null trial levels throughout the adaptation and after-effect trials. However, the right leg toe clearance shows a significant increase from the beginning of the adaptation trial. This is the most clear evidence that the subject formed an initial estimate of the modifications required for walking with a plantarflexed ankle before the adaptation trial began. Then as the subject realized that their initial estimate was too conservative and they became comfortable walking with the plantarflexed foot, the toe clearance decreased by the end of the adaptation trial. In fact for the after effect trial, the toe clearance levels continued to decrease below the null trial average levels.

Figure 5.16 shows the angles of the ankles at the moments of heel strike and toe off. There is no significant change for the left leg during either of the adaptation or after-effect trials. However, the ankle does exhibit lower levels than the null trial values during the adaptation phase. This demonstrates the plantarflexion locking of the ankle, since any ankle locked in such a position would show a decrease in ankle angle. After the modification was removed the ankle returned to null trial levels.

Locked in Dorsiflexion

The results in Figure 5.17 show clear gait timing adaptations when the ankle is locked in a dorsiflexed position. The stance phase percentage is lower than the null trial level since the ankle cannot plantarflex during push off and the foot is therefore lifted early to start the swing phase. This is accompanied by a corresponding increase in the stance phase percentage for the left leg. Since the right

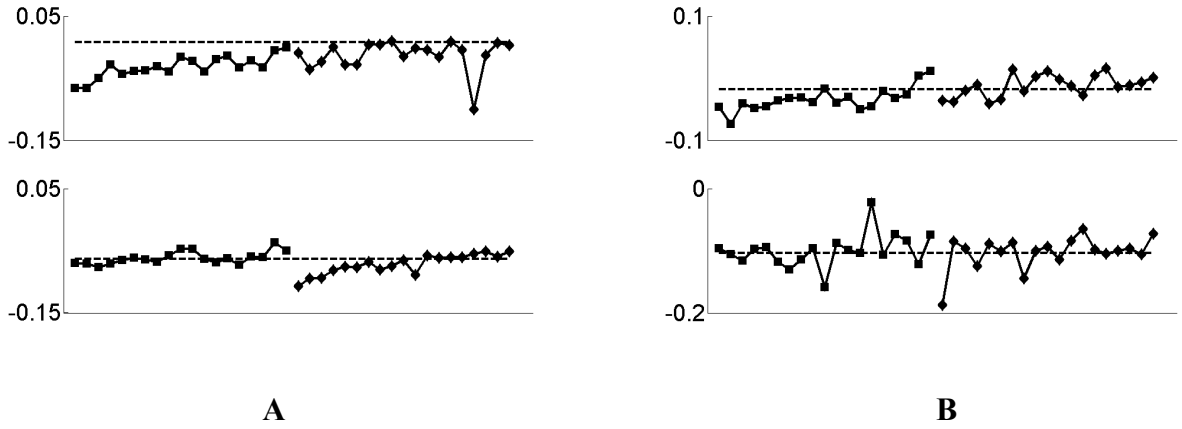

Figure 5.16: Ankle angle at heel strike (A) and toe-off (B) kinematic data through adaptation to AFO locked in plantarflexed position. For each performance metric, the top plot is for the right leg and the bottom plot is for the left leg. Each data point represents the average value for three strides. The square data points are for the adaptation stage and the diamonds are for the after-effect stage. The dashed horizontal line shows the null stage average performance. The units for the vertical axes are radians.

right stance is shortened, the left swing will also be shortened to move the left leg forward faster for the next heel strike, this results in more time being spent in stance. Both of these adaptations return to null field levels during the after-effect trial.

As a result of the short stance phase for the right leg, there is a decrease in both the stride time and the stride length. Assuming that the stance time of the left leg remains relatively constant, and shortening of the left leg swing phase will result in a shorter stride time and an associated drop in the stride time. Both of these metrics show clear after-effects following the removal of the AFO lock. The Stride time and stride length both increase at the start of the after-effect trial and return gradually to null field levels within 20 strides.

Figure 5.18A shows the clear increase in peak hip extension for the right leg at the start of the adaptation trial. This is the result of an initial estimate of the adaptation required for dorsiflexed ankle walking. It can be seen that this value drops as the subjects corrects for the apparent error in this initial estimate. For the after-effect trial, there is no significant change in the hip extension levels though they

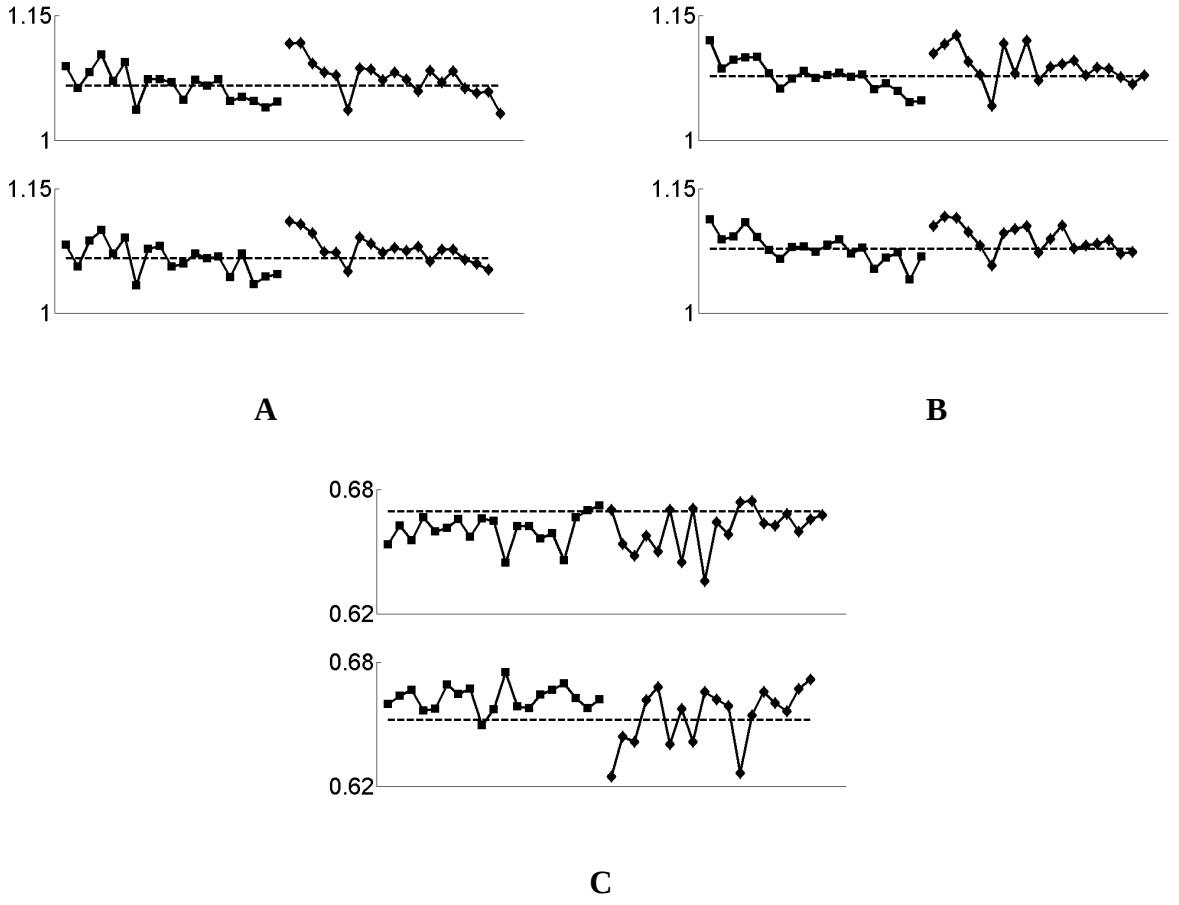

Figure 5.17: Stride time (A), stride length (B) and stance percentage (C) kinematic data through adaptation to AFO locked in dorsiflexed position. For each performance metric, the top plot is for the right leg and the bottom plot is for the left leg. Each data point represents the average value for three strides. The square data points are for the adaptation stage and the diamonds are for the after-effect stage. The dashed horizontal line shows the null stage average performance. The units for the vertical axes are seconds, meters and % for A, B and C respectively.

do remain higher than the null trial average level. The early toe-off time required by the dorsiflexed ankle would appear to contradict the need for increased hip extension during push-off. However, the transition from heel strike to flat foot is significantly affected by locking the ankle in dorsiflexion. The ability to control this transition in a faster forward motion of the limb over the foot which leads to extra hip extension. This should also lead to increased knee flexion and a drop in the hip height for the right leg.

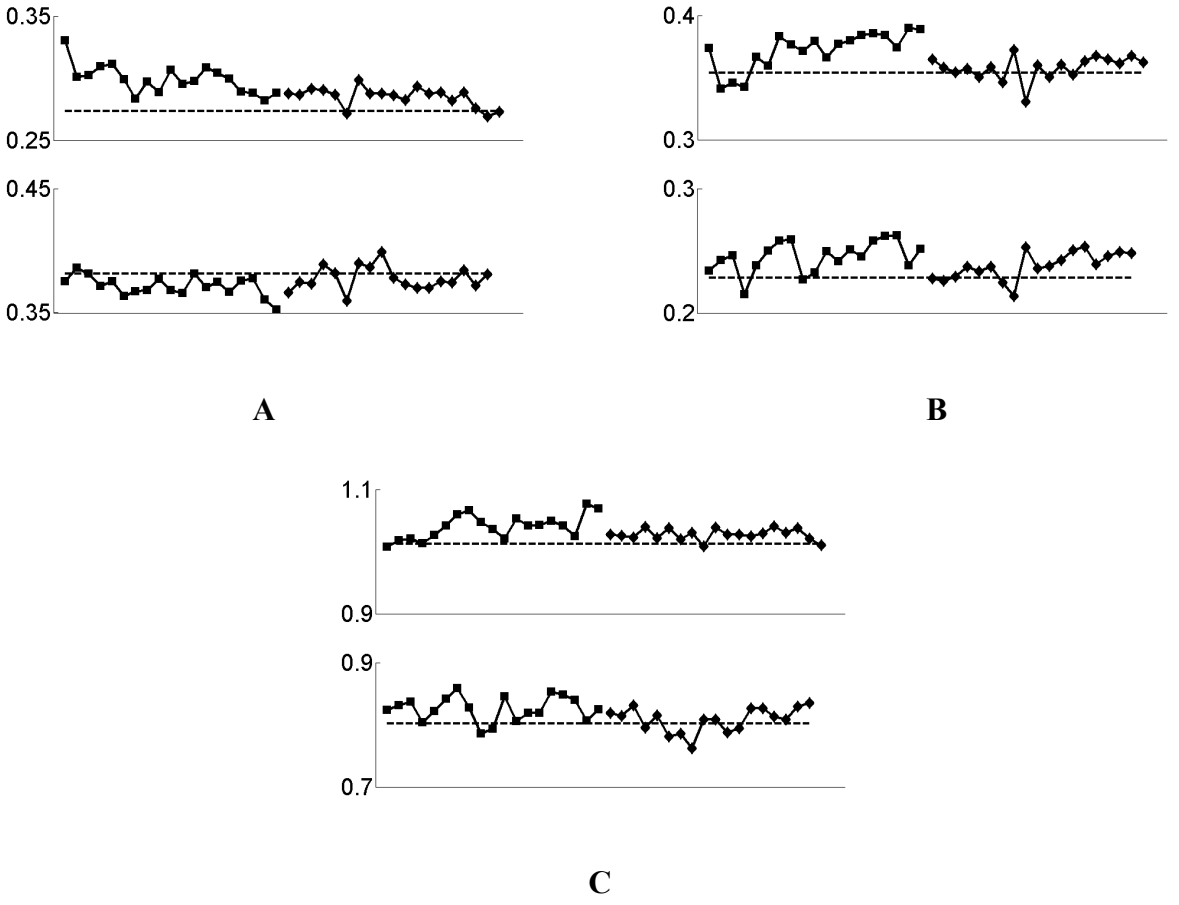

Figure 5.18: Hip extension (A), hip flexion (B) and knee flexion (C) kinematic data through adaptation to AFO locked in dorsiflexed position. For each performance metric, the top plot is for the right leg and the bottom plot is for the left leg. Each data point represents the average value for three strides. The square data points are for the adaptation stage and the diamonds are for the after-effect stage. The dashed horizontal line shows the null stage average performance. The units for the vertical axes are radians.

For the right leg, both hip flexion and knee flexion show increases throughout the adaptation trial, but show no evidence of the after-effects resulting from the formation of an internal model. The left leg shows slight increases for both of these angles as well, though the increases are present from the beginning of the adaptation trial.

Figure 5.19A shows that there is a decrease in the hip height during swing for the right leg. This decrease correlates well with increased hip flexion shown in Figure 5.18A. At the start of the adaptation

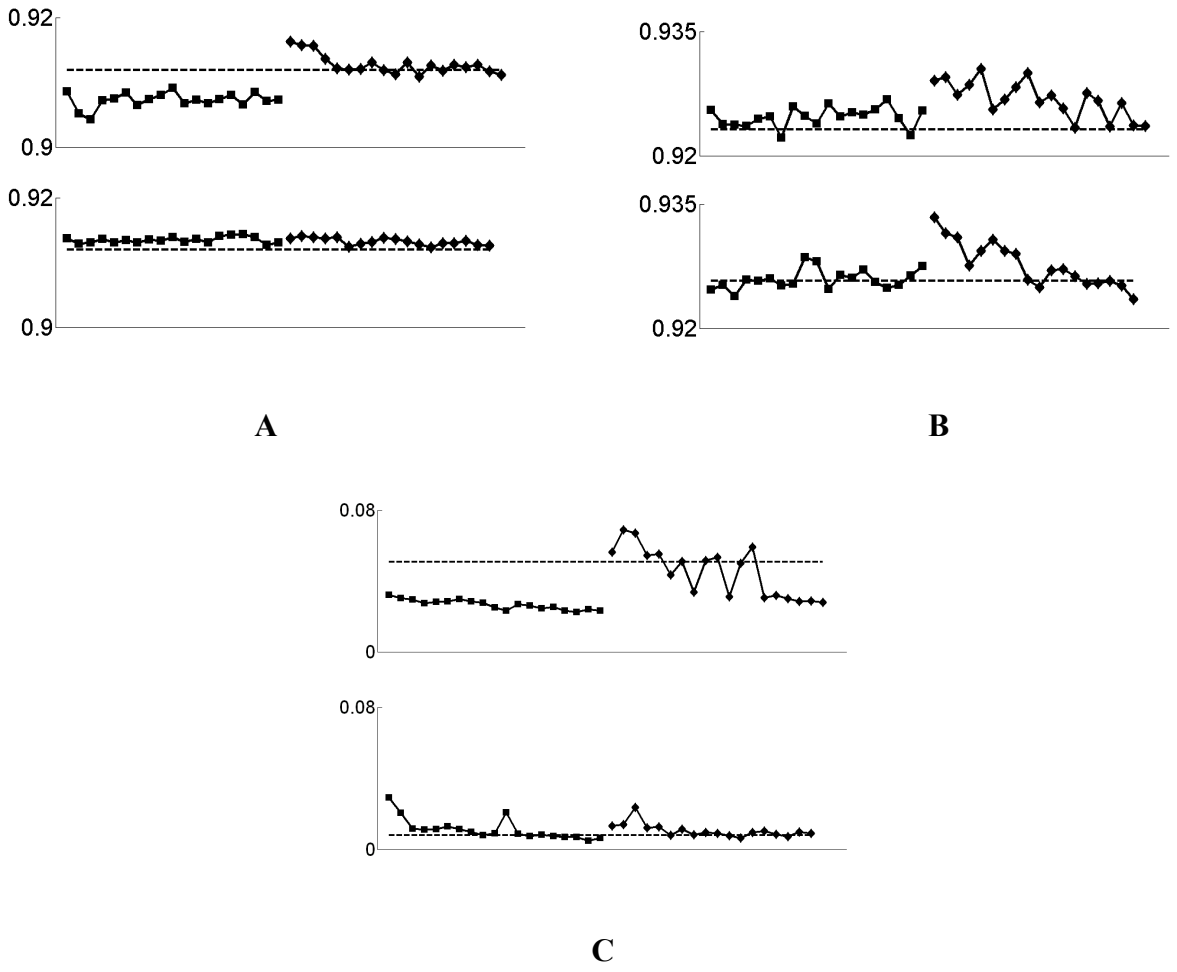

Figure 5.19: Hip joint height during swing (A), hip joint height during stance (B) and peak toe clearance (C) kinematic data through adaptation to AFO locked in dorsiflexed position. For each performance metric, the top plot is for the right leg and the bottom plot is for the left leg. Each data point represents the average value for three strides. The square data points are for the adaptation stage and the diamonds are for the after-effect stage. The dashed horizontal line shows the null stage average performance. The units for the vertical axes are meters.

trial, a clear after-effect and gradual return to null trial behaviour is seen. This is due to the subject adjusting their performance to compensate for the heel to flat foot transition. Once the adaptations were not required anymore, the modified behaviour results in an after-effect in the opposite direction of the original task modification. There are no clear changes to the peak hip height during stance for either the

right or left legs. However, both show after-effects when the ankle was unlocked. These changes are most likely related to the increased swing phase hip increase for the right leg.

There were no significant changes in the toe clearance levels for the left leg. However, the peak toe for the right leg had a significant decrease during the adaptation trial. The decrease of the toe clearance corresponds with the swing phase hip joint height drop discussed previously. Intuitively, a drop in hip height should lead to a decrease in toe clearance level. This is further supported by the increase and gradual decrease of the toe clearance during the after-effect trial, which also happens with the swing phase hip height.

In Figure 5.20, the only clear changes from the null trial behaviour occurs during the adaptation trial and only for the right angle. This reflects the locked position of the ankle, since a dorsiflexed position results in a positive joint angle orientation. The increased joint angle is immediately gone at the start of the after-effect trial.

No Dorsiflexion

In this experimental condition, the AFO was set to limit the range of motion of the ankle but not lock it in a single position. Specifically, the ankle was able to plantarflex but zero dorsiflexion was permitted. Given that there was more ankle movement capability, it is expected that the effects of adaptation will be less pronounced.

Figure 5.21 shows the results for the stride length, stride time and stance phase percentage when no dorsiflexion of the ankle is permitted. Not having the ability to dorsiflex the ankle at heel strike would lead to a shorter transition time to flat foot and have the result of reducing the stance ratio at the start of the adaptation trial. This may have also been affected by the lack of dorsiflexion through midstance that would have slowed the progression of the limb over the foot. The subject then adapts to the change and gradually returns to the null trial performance. However, no clear after-effects can be

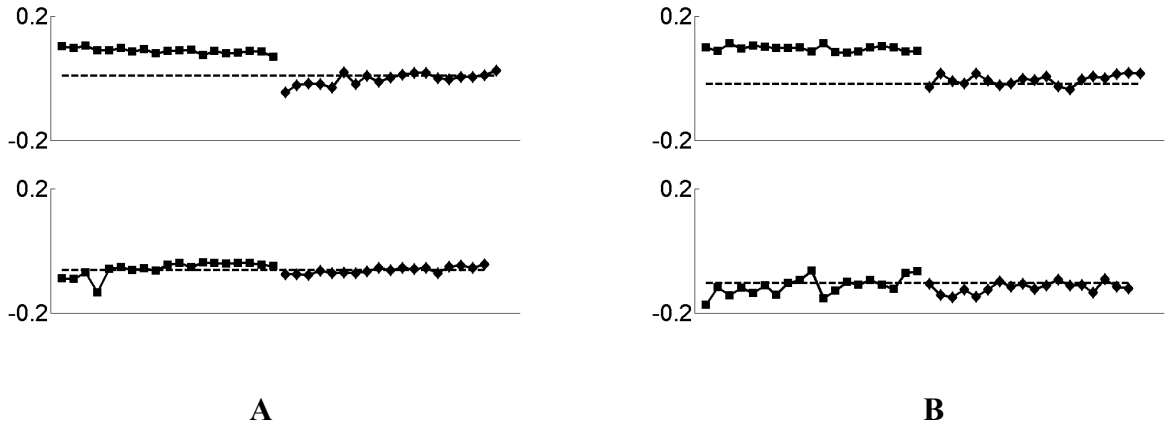

Figure 5.20: Ankle angle at heel strike (A) and toe-off (B) kinematic data through adaptation to AFO locked in dorsiflexed position. For each performance metric, the top plot is for the right leg and the bottom plot is for the left leg. Each data point represents the average value for three strides. The square data points are for the adaptation stage and the diamonds are for the after-effect stage. The dashed horizontal line shows the null stage average performance. The units for the vertical axes are radians.

seen in the trial that followed. The stride length was increased at the start of the adaptation trial and then decreased gradually. This change in performance also crated an after-effect in the following trial. This is accompanied by a slight increase in the stride time at the start of the adaptation trial. There is also the possibility of a slight after-effect at the very beginning of the after-effect trial in Figure 5.21A.

There is a very clear adaptation of the subject to a large increase in the hip extension adaptation plot in Figure 5.22A. This adaptation also resulted in an after-effect in the following trial. There is also a similar result for the left leg, which exhibits a clear after effect in the hip flexion plot. There is an increase in the peak hip flexion levels throughout the entire adaptation trial that persists during the after effect trial for the right leg. This accompanied by a similar, though smaller, decrease in the in the left leg hip flexion level. However, both results appear to be quite small.

There is a clear significant increase in the knee flexion angle in the adaptation trial for the right leg in Figure 5.22C. Additionally, there appears to be an after-effect resulting in even larger knee angles at the start of the after-effect trial that decreases to the level of knee flexion seen in the adaptation trial

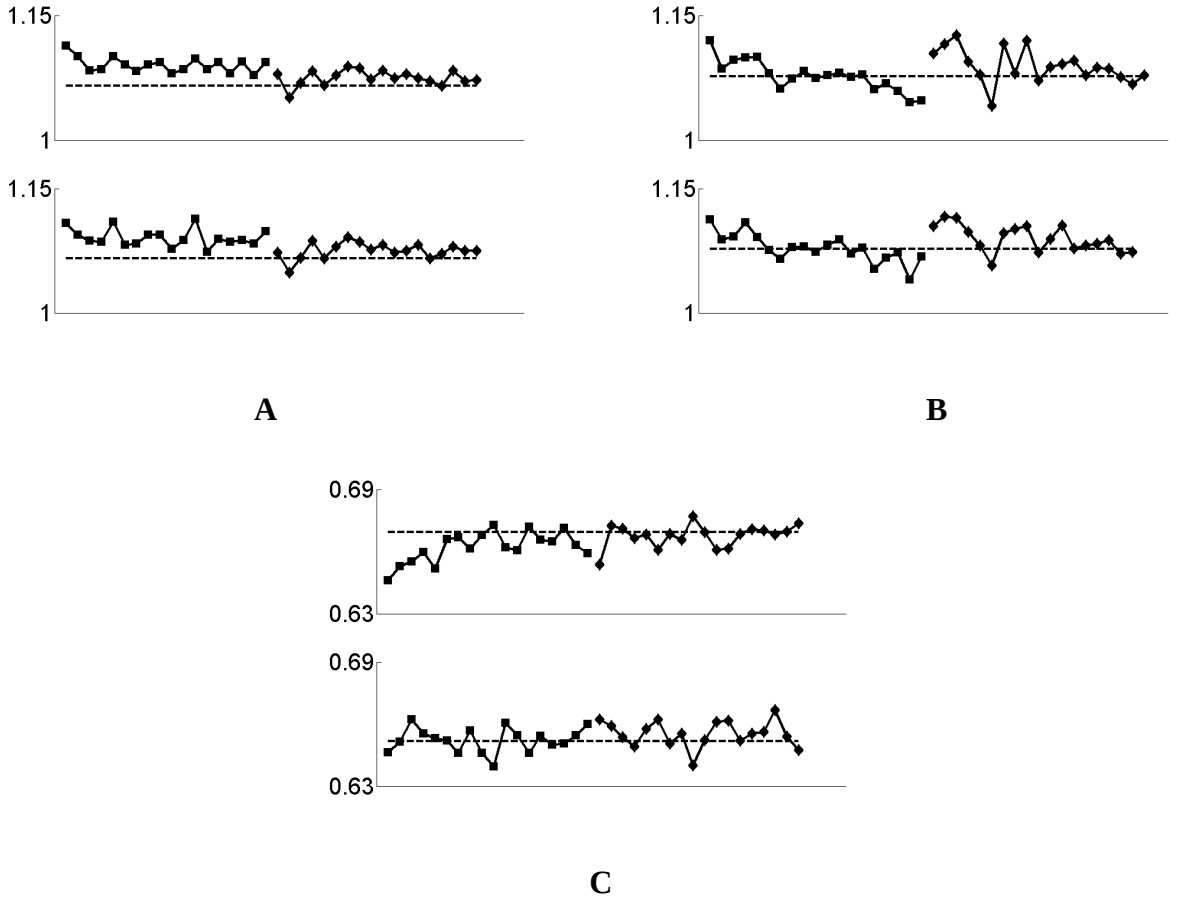

Figure 5.21: Stride time (A), stride length (B) and stance percentage (C) kinematic data through adaptation to AFO not allowing dorsiflexion. For each performance metric, the top plot is for the right leg and the bottom plot is for the left leg. Each data point represents the average value for three strides. The square data points are for the adaptation stage and the diamonds are for the after-effect stage. The dashed horizontal line shows the null stage average performance. The units for the vertical axes are seconds, meters and % for A, B and C respectively.

The inability to dorsiflex the foot leads to a greater possibility of toe drag during swing. An increase in knee flexion has the result of lifting the foot higher to prevent such dragging. This may also be the reason for the increased right leg hip flexion seen in Figure 5.22B.

In similar manner, the hip joint height during the right leg swing phase increases to prevent the toes from contacting the floor in Figure 5.23A. This effect persists through the after-effect trial as well. Both the right and left legs exhibit an increase in the hip height during the stance phase. This may be the

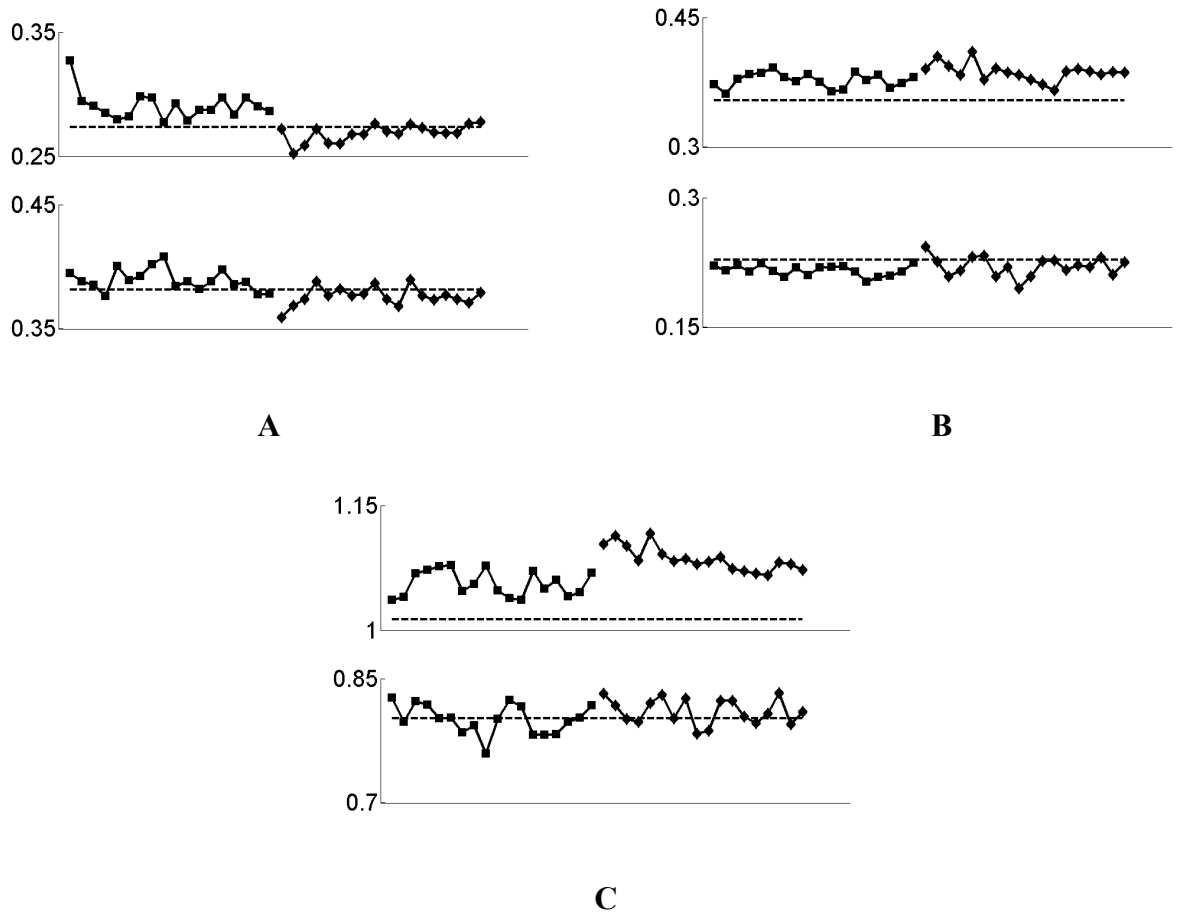

Figure 5.22: Hip extension (A), hip flexion (B) and knee flexion (C) kinematic data through adaptation to AFO not allowing dorsiflexion. For each performance metric, the top plot is for the right leg and the bottom plot is for the left leg. Each data point represents the average value for three strides. The square data points are for the adaptation stage and the diamonds are for the after-effect stage. The dashed horizontal line shows the null stage average performance. The units for the vertical axes are radians.

result of the reduced dorsiflexion of the ankle leading to a tip-toe motion near the end of the right leg stride. This adaptation occurs to allow progression of the limb over the foot when dorsiflexion is not possible. The subject shows an adaptation to this height change through the adaptation trial. The peak toe clearance shows a similar pattern to the trial in Figure 5.15C for the plantarflexed lock on the AFO. The initial increase appears to be due to the subject predicting that toe clearance will be more difficult and the correction of an over-estimate throughout the adaptation trial.

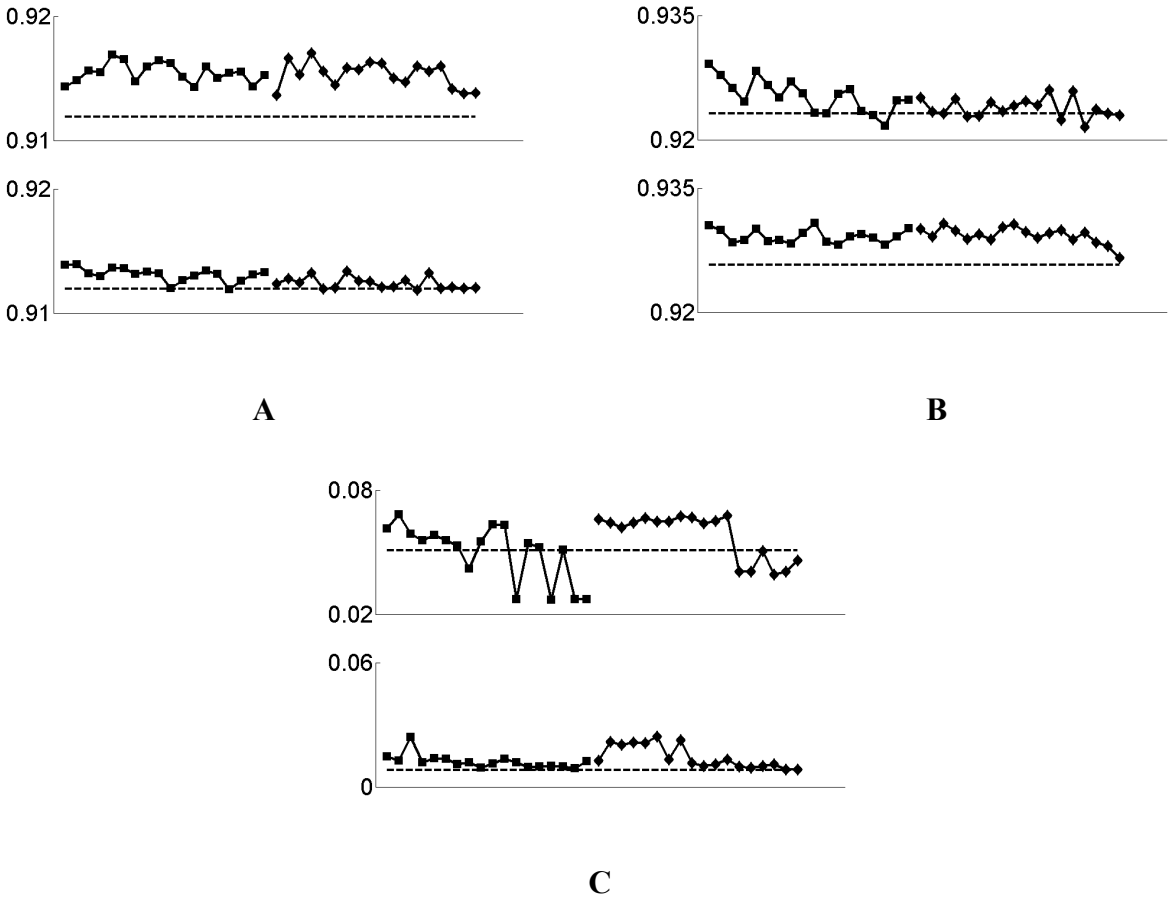

Figure 5.23: Hip joint height during swing (A), hip joint height during stance (B) and peak toe clearance (C) kinematic data through adaptation to AFO not allowing dorsiflexion. For each performance metric, the top plot is for the right leg and the bottom plot is for the left leg. Each data point represents the average value for three strides. The square data points are for the adaptation stage and the diamonds are for the after-effect stage. The dashed horizontal line shows the null stage average performance. The units for the vertical axes are meters.

Figure 5.24 shows the behaviour of the ankle joint at heel strike and toe off when the foot in unable to plantarflex. The right leg ankle shows a clear decrease in the plantarflexion direction during heel strike compared to the null trial performance since the foot is not able to move into a positive rotation. The subject adapts to this situation and shows an after-effect that decreases during the after-effect trial. At toe-off there is a slight increase in the ankle ankle at the start of the adaptation trial that is quickly decreased during the adaptation process. The reason for this decrease is not readily apparent

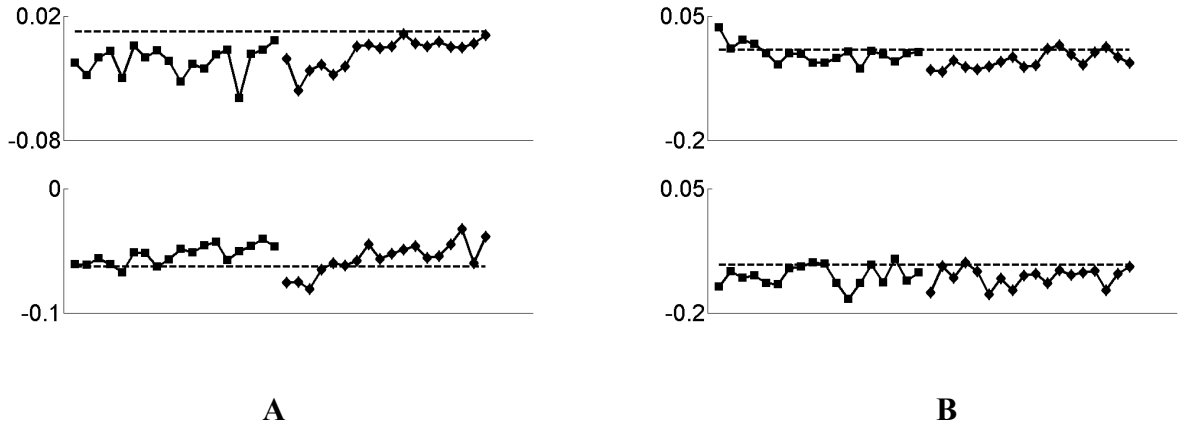

Figure 5.24: Ankle angle at heel strike (A) and toe-off (B) kinematic data through adaptation to AFO not allowing dorsiflexion. For each performance metric, the top plot is for the right leg and the bottom plot is for the left leg. Each data point represents the average value for three strides. The square data points are for the adaptation stage and the diamonds are for the after-effect stage. The dashed horizontal line shows the null stage average performance. The units for the vertical axes are radians.

No Plantarflexion

In this experimental condition the foot is not able to plantarflex while still being able to dorsiflex. Both the stride length and stride time show initial significant increases at the beginning of the adaptation stage as seen in Figures 5.25A-B. In both cases these decrease, though not down to the null trial levels. The stance phase percentage decreases for both the right and left legs as shown in Figure 5.25C. The inability to plantar flex should lead to an earlier toe off time as the amount of ankle motion will be restricted during the push-off stage. This would have the effect of reducing the stance phase length. Also, in a similar manner to the locked dorsiflexion trial, the initial heel contact does not cause plantarflexion of the foot and as a result the transition from heel strike to foot flat is affected.

In Figure 5.26A, the hip extension of the right leg is increased during the adaptation trials and a clear after-effect of adaptation can be seen at the start of the next trial. The inability to plantarflex the foot prevents the full range of motion of the foot during push-off, which is the moment of peak hip

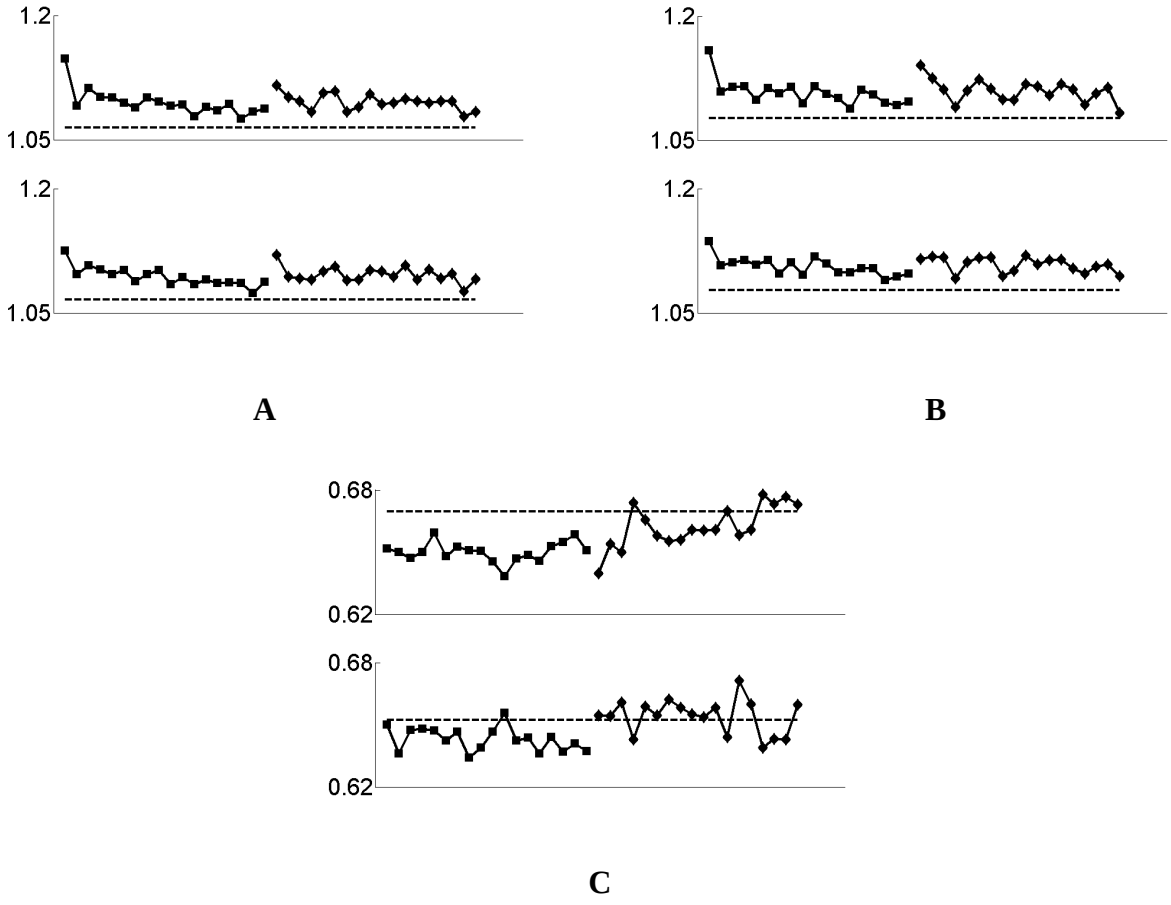

Figure 5.25: Stride time (A), stride length (B) and stance percentage (C) kinematic data through adaptation to AFO not allowing plantarflexion. For each performance metric, the top plot is for the right leg and the bottom plot is for the left leg. Each data point represents the average value for three strides. The square data points are for the adaptation stage and the diamonds are for the after-effect stage. The dashed horizontal line shows the null stage average performance. The units for the vertical axes are seconds, meters and % for A, B and C respectively.

extension. There is an increase in right leg hip flexion seen for both the adaption and after-effect trials and a decrease in hip flexion for the left leg. The increase in hip flexion/extension and the corresponding increase in the stride length may be due to the shortening of the right leg stride percentage and therefore the shortening of the left leg swing time. This requires faster hip motion to move the swing leg forward for heel strike. As a result the flexion of the left leg hip and the extension of the right leg hip would exhibit increases associated with increased stride length and stride time.

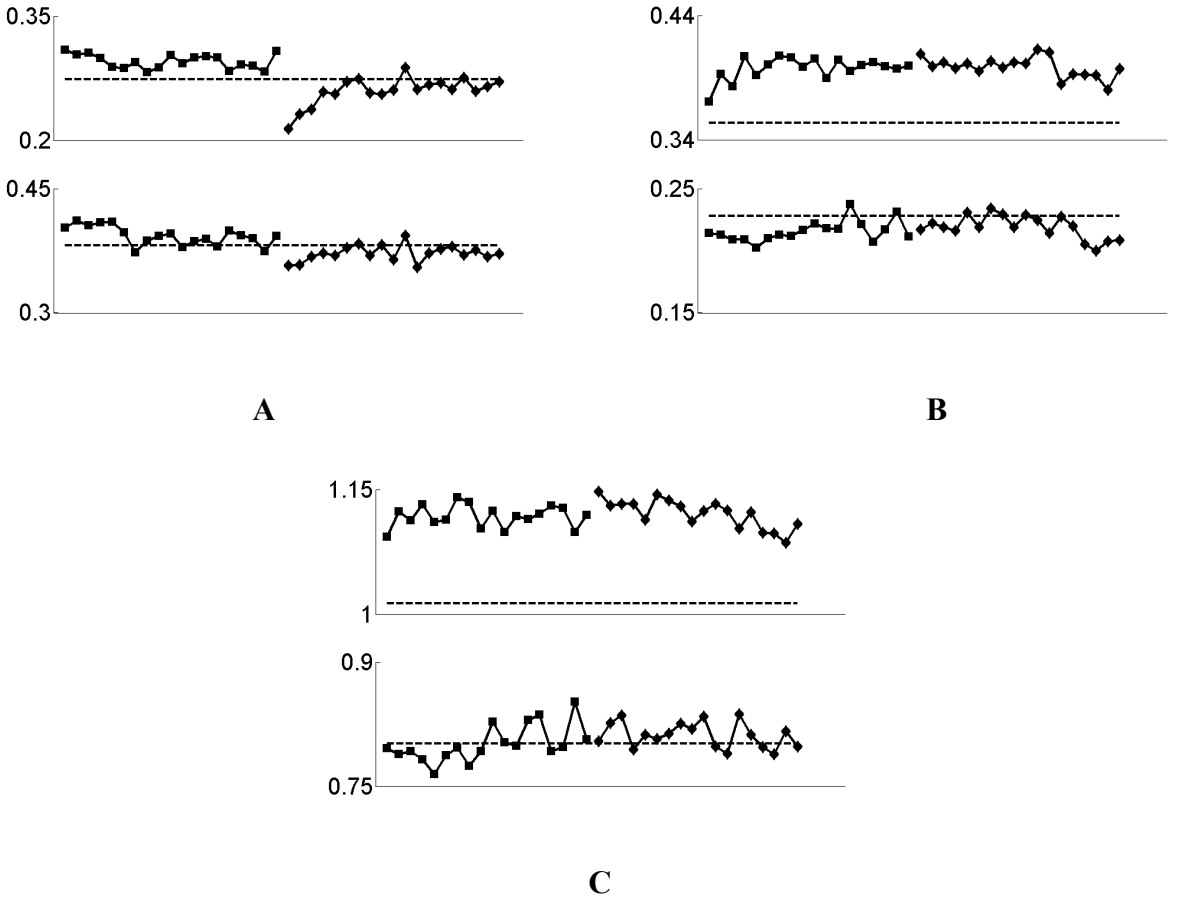

Figure 5.26: Hip extension (A), hip flexion (B) and knee flexion (C) kinematic data through adaptation to AFO not allowing plantarflexion. For each performance metric, the top plot is for the right leg and the bottom plot is for the left leg. Each data point represents the average value for three strides. The square data points are for the adaptation stage and the diamonds are for the after-effect stage. The dashed horizontal line shows the null stage average performance. The units for the vertical axes are radians.

The left leg knee flexion shows an initial decrease and subsequently increases through the adaptation trial, though with no evidence of after-effects. The right leg exhibits a very significant increase in knee flexion throughout both trials. This, along with the large increase in the hip flexion angle, leads to the conclusion that the subject may have been exhibiting steppage gait, though the reason for this is not initially apparent.

In Figure 5.27, the swing phase hip heights for both the left and right side show no significant change during the adaptation trial. This continues into the after-effect trial for the left leg, but there is an increase in height for the right leg during the after-effect trial. This may be the result of compensation for the newly unlocked plantarflexion in order to prevent toe dragging. There are slight increases in the stance phase hip heights for both hip joints. The peak toe clearance shows a very large decrease during the adaptation trials and a significant after-effect in the following trial. Not allowing dorsiflexion would initially make toe clearance easier and this the peak toe swing phase height would be higher at the start of the adaptation. But as the subject adapted, they were able to reduce this height.

Figure 5.28 shows the adaptation results for the ankle angles at heel strike and toe off times. The ankle of the right leg shows a decrease in the angle of the ankle at heel strike which should not be possible with the AFO not allowing plantarflexion. This is particularly evident with the joint angle actually going to negative (plantarflexion) values. The reason for this issue is not identifiable and may be the result of measurement error or with the AFO design itself.

Different Tread Speeds

This final adaptation a experiment was the one for which the most significant gait changes and adaptations would occur. This is because walking at two different tread speeds is a very novel and unpredictable task for people who have not done it before. This is apparent in the fact that several subjects stumbled slightly during their initial steps both the adaptation and after-effect trials. Also, for this particular gait modification, the subjects said they subjectively felt the most extreme changes in their walking and that they were able to "feel" the result of their learning during the start of the after-effect trial. For example, all subjects felt that the left tread was moving faster during the after-effect trial even though the treads were moving at the same speed. During this experiment subjects appeared to exhibit

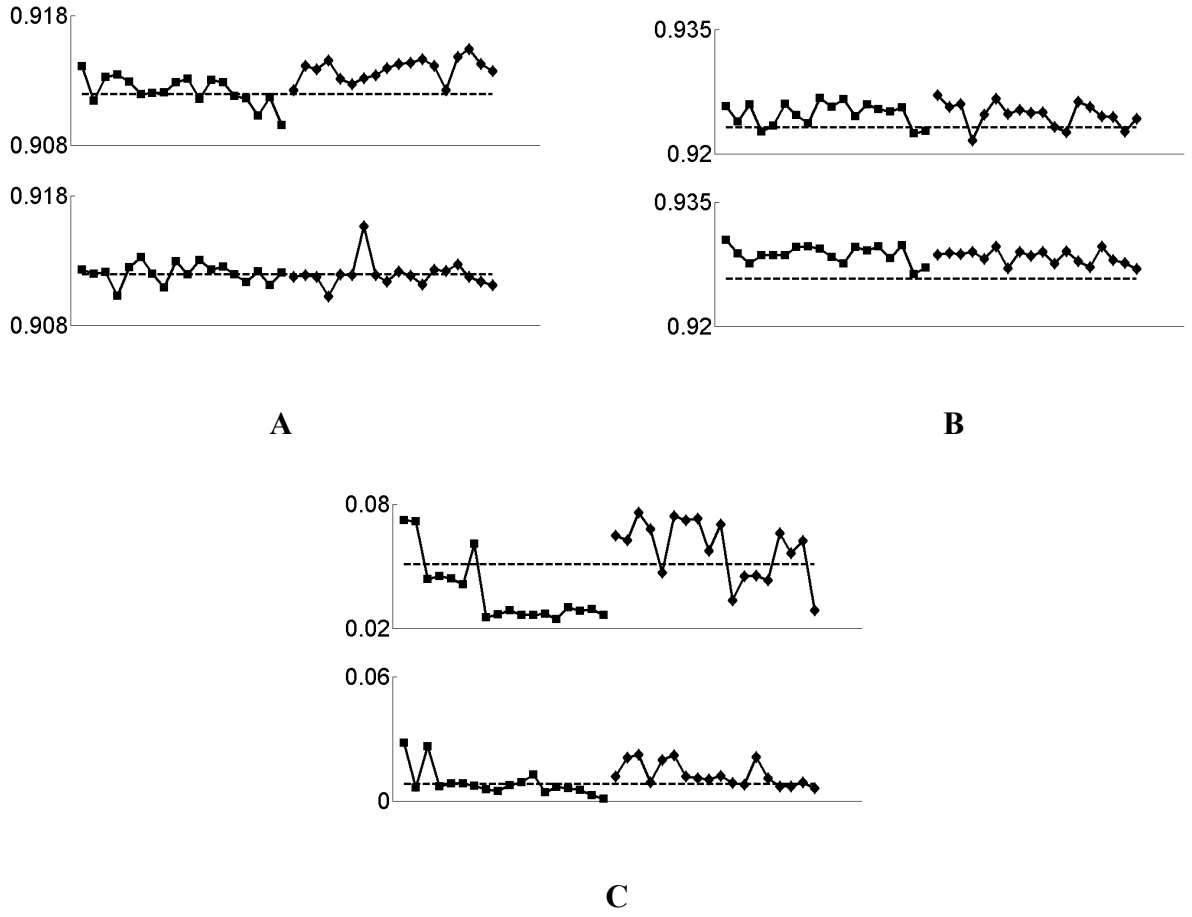

Figure 5.27: Hip joint height during swing (A), hip joint height during stance (B) and peak toe clearance (C) kinematic data through adaptation to AFO not allowing plantarflexion. For each performance metric, the top plot is for the right leg and the bottom plot is for the left leg. Each data point represents the average value for three strides. The square data points are for the adaptation stage and the diamonds are for the after-effect stage. The dashed horizontal line shows the null stage average performance. The units for the vertical axes are meters.

an artificial "limp" as the result of the right tread moving faster. The limp subjectively appeared to be reversed for the start of the after-effect trial.

Figure 5.29 shows the results for the stride length, stride time and stance phase percentage. Both stride length and stride time show significant decreases at the start of the adaptation process and both increase throughout the adaptation trial. The initial decrease most likely is the result of the uncertainty of the tasks reducing stride length and time. As the subject became more comfortable they

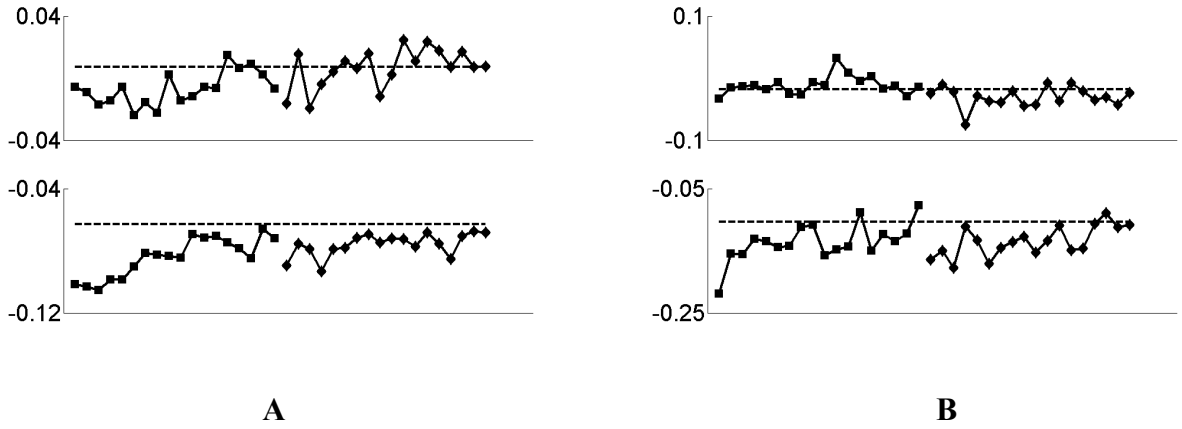

Figure 5.28: Ankle angle at heel strike (A) and toe-off (B) kinematic data through adaptation to AFO l not allowing plantarflexion. For each performance metric, the top plot is for the right leg and the bottom plot is for the left leg. Each data point represents the average value for three strides. The square data points are for the adaptation stage and the diamonds are for the after-effect stage. The dashed horizontal line shows the null stage average performance. The units for the vertical axes are radians.

were able to return to a longer stride closer in length to the null trial performance. In both of these cases, there was also a decrease in the metrics at the start of the after-effect trial. Though this decrease took place after a short (three or less strides) increase. This initial increase was most likely due to the subject stumbling and the sudden decrease after this point is the subject compensating for the uncertainty of the gait task. There is a very clear asymmetry in the stance phase timing for the adaptation trial in Figure 5.29C. The stance percentage for the right leg dropped significantly and the stance percentage increased for the slower tread. During the after effect trial, both legs show stance percentages in the opposite change direction as the adaptation stage percentages, however to a much smaller degree.

Figure 5.30 also shows clear asymmetry during the adaptation process. The hip extension for the right leg is greatly increased for the right leg and decreased for the left leg. The right leg, being pulled back faster by the treadmill, is forced to extend the hip to a greater degree. The left tread does not extend as much since it is moving slower. Basically, each leg exhibits changes characteristic of their respective changes in speed. The adaptation to this task is clearly evidenced by the after-effect present

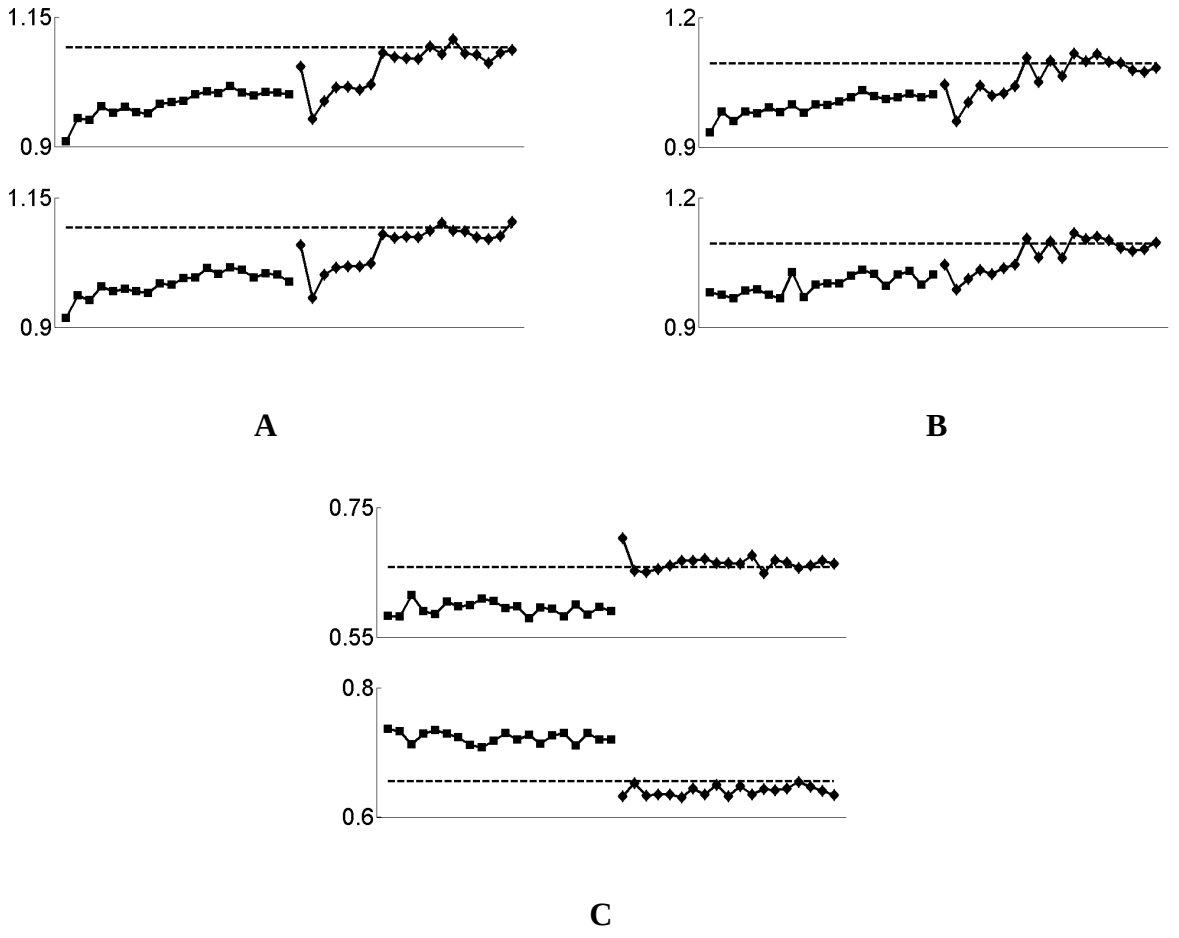

Figure 5.29: Stride time (A), stride length (B) and stance percentage (C) kinematic data through adaptation to treads moving at different speeds. For each performance metric, the top plot is for the right leg and the bottom plot is for the left leg. Each data point represents the average value for three strides. The square data points are for the adaptation stage and the diamonds are for the after-effect stage. The dashed horizontal line shows the null stage average performance. The units for the vertical axes are seconds, meters and % for A, B and C respectively.

in the hip extension data. For both the right and left legs, the after-effects are in the opposite direction of the task modification and they decreased gradually as the effects of the internal model are washed-out.

During the adaptation trial, the right leg shows a decrease in the hip flexion level that gradually returns close to the null trial behaviour. The transition from walking on the slower tread to walking on the faster tread means that the swing leg is moving forward at a rate similar to the backwards motion of the slow-moving stance leg. Therefore, when the heel strike occurs, there is not as much opportunity for

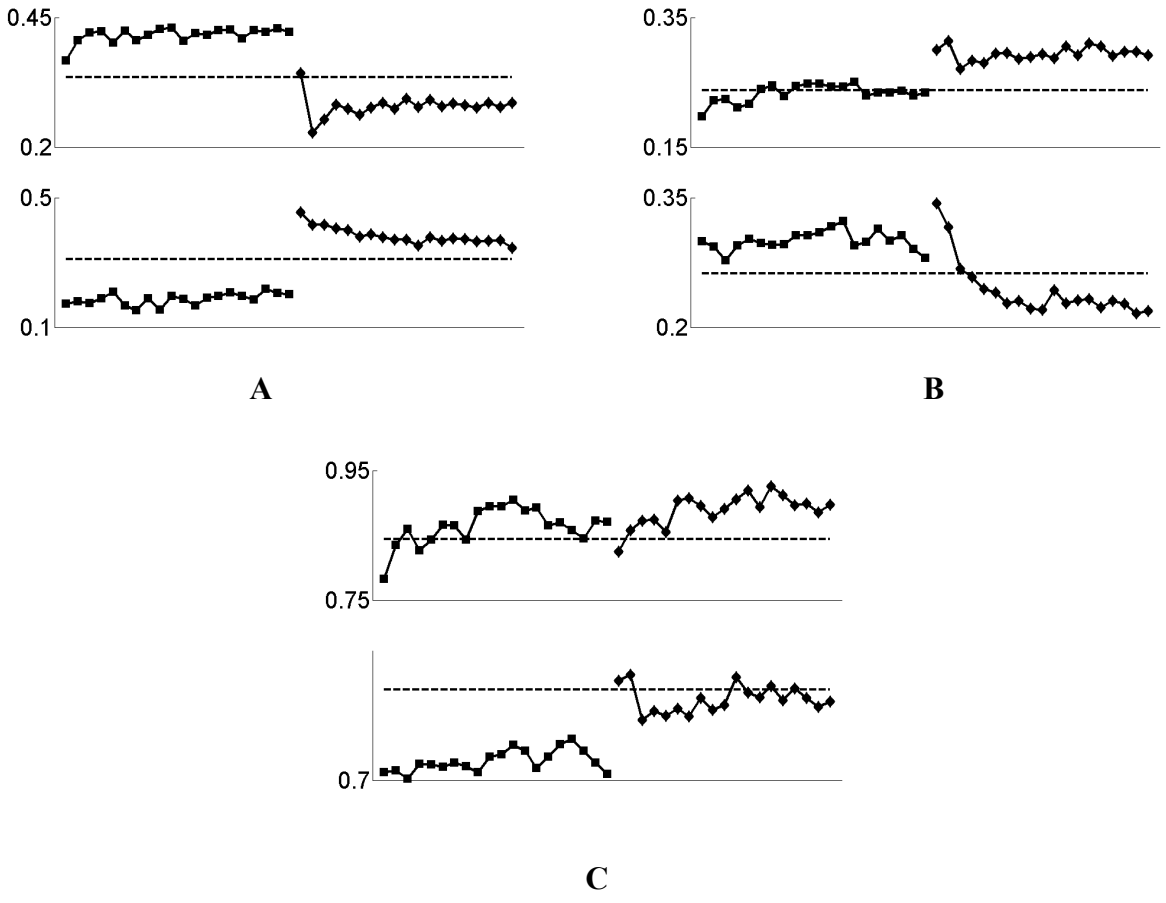

Figure 5.30: Hip extension (A), hip flexion (B) and knee flexion (C) kinematic data through adaptation to treads moving at different speeds. For each performance metric, the top plot is for the right leg and the bottom plot is for the left leg. Each data point represents the average value for three strides. The square data points are for the adaptation stage and the diamonds are for the after-effect stage. The dashed horizontal line shows the null stage average performance. The units for the vertical axes are radians.

the swing leg to flex forward. The reverse case holds for the fast-to-slow tread transition. The subjects then learn to adjust the flexion level of the legs for the transition times reducing the error. This adaptation is evidenced by the significant presence of after-effects, particularly for the left leg.

The knee flexion results also show clear changes due to the tread speed modifications. The left leg exhibits less flexion and the right leg exhibits more flexion. Again, these changes correlate with the respective speed change adaptations similar to those seen in Experiment #1.

In Figure 5.31A, there doesn't appear to be any significant change to the swing phase hip heights of either leg during the adaptation trial. However, when the treads were returned to the same speed for the after-effect trial, the subject shows a large decrease (up to 3 cm) in the swing phase height of both hips. A similar pattern occurs with the stance phase hip height. Therefore, there is a general decrease in the height of the pelvis COM during the after-effect trial. From this, it is clear that the subject adapts to the change in tread speeds and the after-effects of the internal model formation are so significant, the subject has drastic changes in performance even when there were no apparent changes during the adaptation itself. The peak toe clearance values seen in this experimental condition show little change for the left leg but a large change in the right leg for the adaptation trial. The increase in speed results in an increase in the toe clearance level to prevent toe drag.

Figure 5.32 shows the results for the ankle angles at heel strike and toe off. During the adaptation trial, the right leg exhibits greater levels of plantarflexion during the toe-off time. This is the result of the tread pulling the foot back at a faster rate and the need to generate more push-off force to Move the leg forward in the swing phase. The opposite condition occurs for the left leg since the left tread is moving slower. However, in both cases the lack of clear after-effects implies less adaptation to this particular performance metric. At heel strike, the right leg ankle dorsiflexes more throughout the adaptation but with little in the way of after-effects.

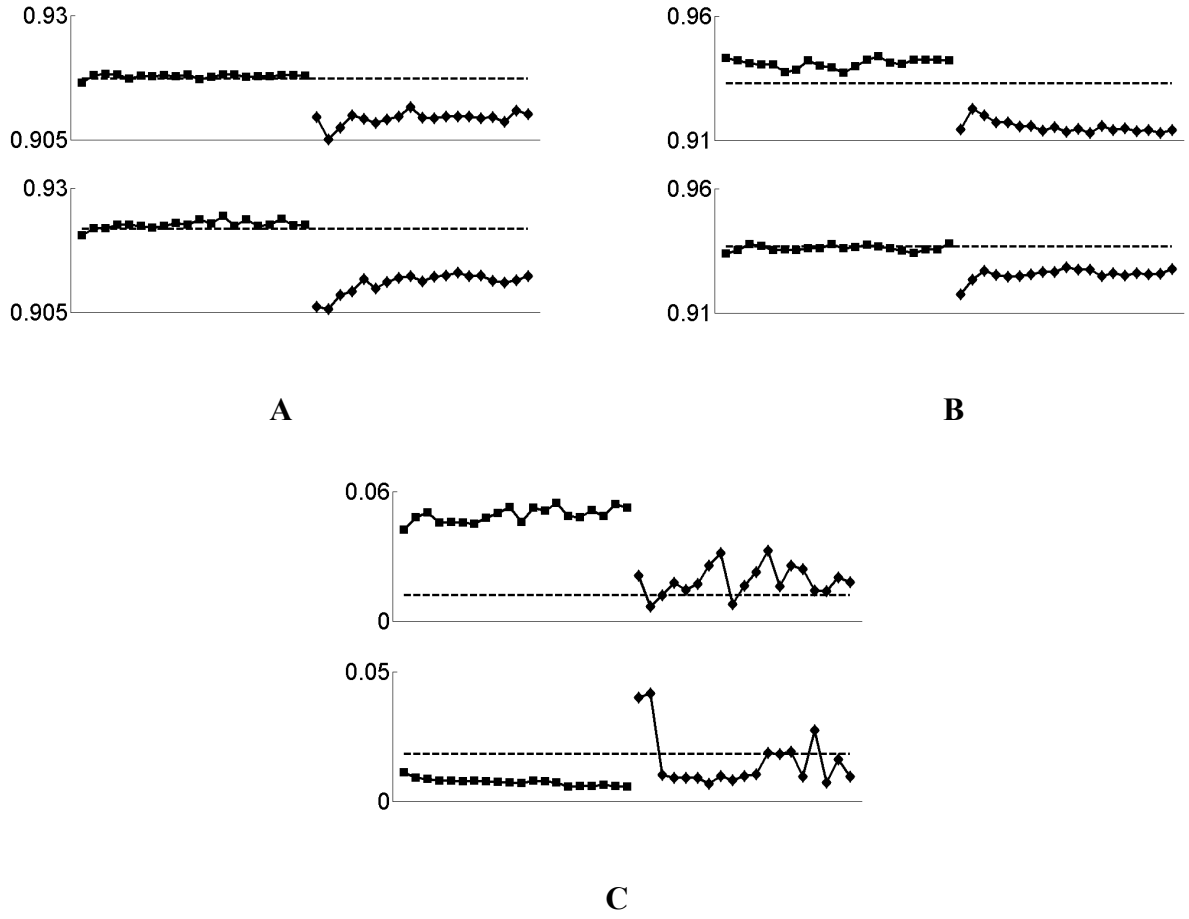

Figure 5.31: Hip joint height during swing (A), hip joint height during stance (B) and peak toe clearance (C) kinematic data through adaptation to treads moving at different speeds. For each performance metric, the top plot is for the right leg and the bottom plot is for the left leg. Each data point represents the average value for three strides. The square data points are for the adaptation stage and the diamonds are for the after-effect stage. The dashed horizontal line shows the null stage average performance. The units for the vertical axes are meters.

5.2.2 Inverse Dynamic Analysis

Locked in Plantarflexion

The joint moments results from the inverse dynamics analysis for the locked in plantarflexion experimental condition are shown in Figures 5.33-5. Each of these figures gives the results for the right leg, the left leg and the pelvis respectively. For each plot, the plot on the top (A) shows the adaptation

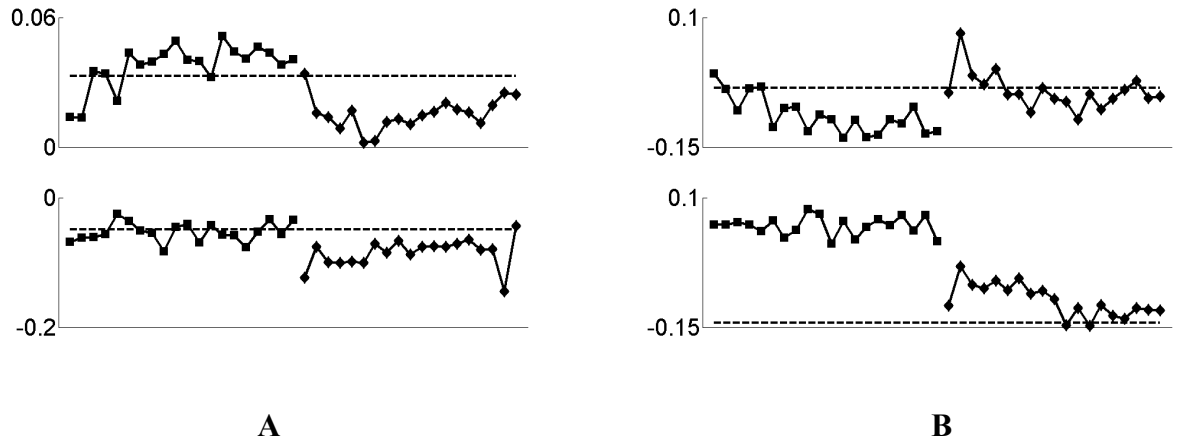

Figure 5.32: Ankle angle at heel strike (A) and toe-off (B) kinematic data through adaptation to treads moving at different speeds. For each performance metric, the top plot is for the right leg and the bottom plot is for the left leg. Each data point represents the average value for three strides. The square data points are for the adaptation stage and the diamonds are for the after-effect stage. The dashed horizontal line shows the null stage average performance. The units for the vertical axes are radians.

stage joint moments and the plot on the bottom shows the after-effects stage moments. Each of the subplots shows the null-field average as a solid line, the average of the first five strides of the trial as a dashed line and the average of the last five strides of the trial as a dotted line.

Within these inverse dynamics results, there is clear evidence of adaptation. There is additional stance knee flexion at the start of the adaptation trial that drops by the end of the adaptation trial (Figure 5.33A). This decrease in moments demonstrates that the subject is learns to adapt to the modification locking the foot in a plantarflexed position. This is supported further by the after-effect seen in the following trial (Figure 5.33B). At the beginning of the after-effect trial, there is an extra right knee extension moment during the stance phase. The fact that this change is of similar magnitude and in the opposite direction as the initial change in the adaptation trial is evidence that the adaptation was the result of the creation of an internal model. This after-effect moment then gradually decreases demonstrating the unlearning of the gait task modification. This sequence of changes is analogous to the classic adaptation/after-effect paradigm seen in past adaptation research.

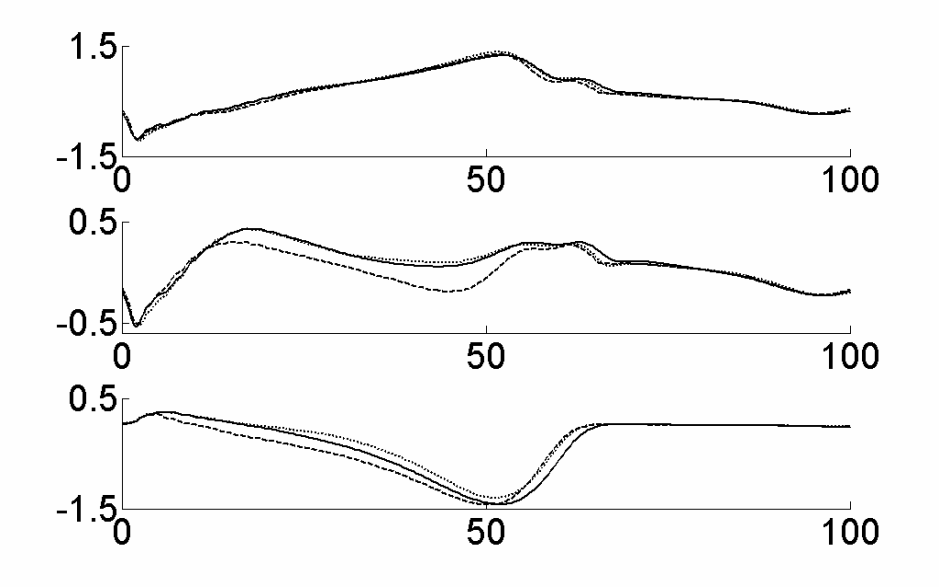

A

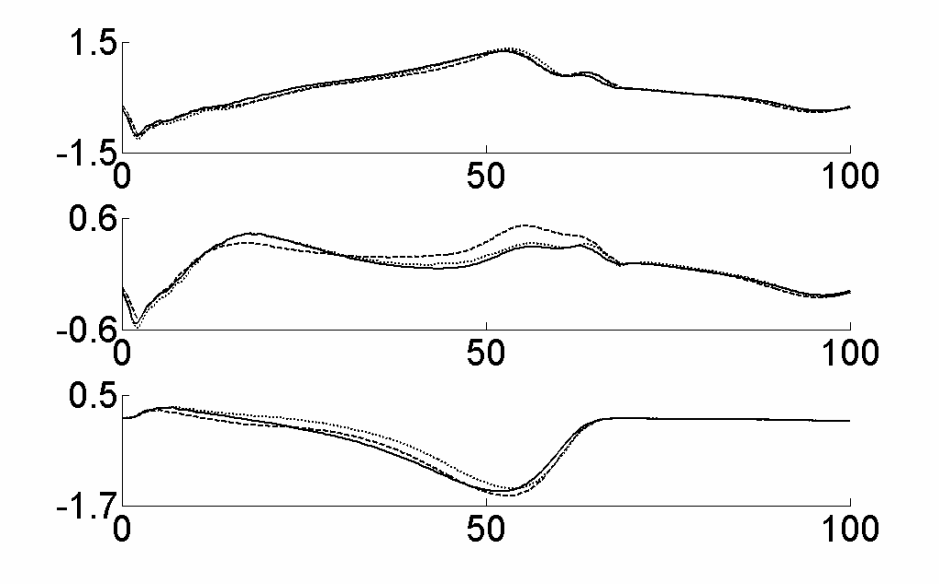

B

Figure 5.33: Right leg joint moments for locked in plantarflexion experimental condition. The top plot (A) shows the adaptation trial joint moments and the bottom plot (B) shows the after-effect trial joint moments. Each subplot shows results for the hip, knee and ankle (top to bottom). For each trial, the plot shows the null trial performance as a solid line, the average result for the first five strides as a dashed line and the average of the last five strides as a dotted line. The horizontal axes give gait cycle percentage and the vertical axes are the moments in Nm/kg (normalized by subject mass).

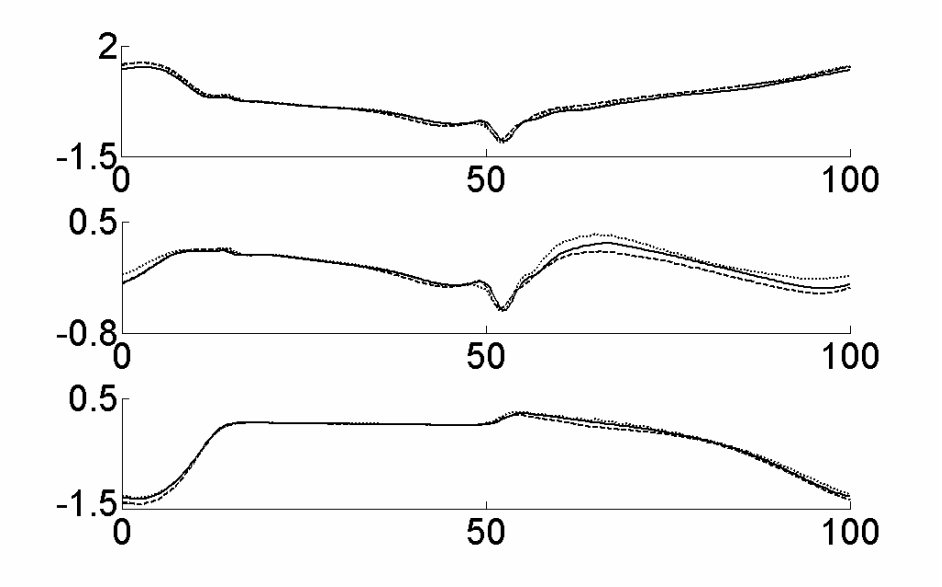

A

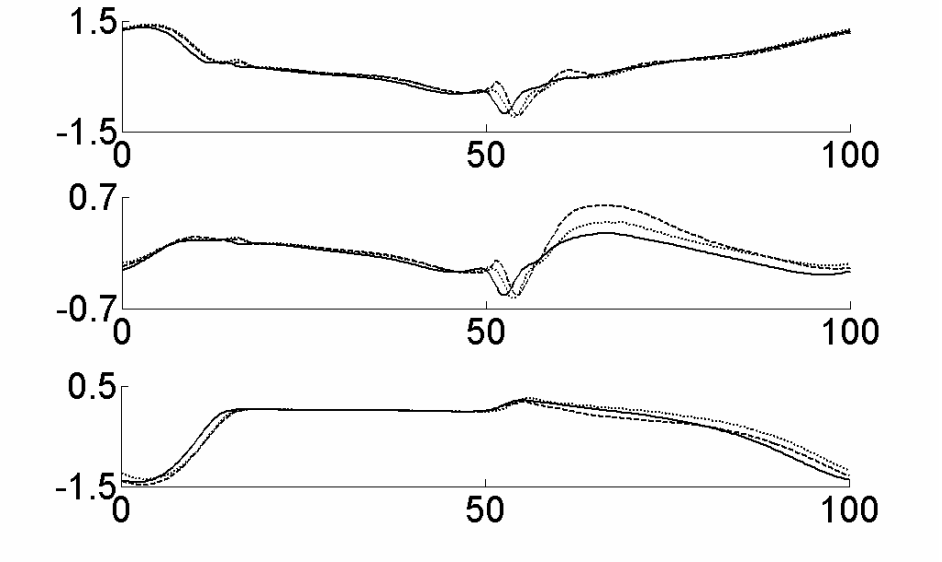

B

Figure 5.34: Left leg joint moments for locked in plantarflexion experimental condition. The top plot (A) shows the adaptation trial joint moments and the bottom plot (B) shows the after-effect trial joint moments. Each subplot shows results for the hip, knee and ankle (top to bottom). For each trial, the plot shows the null trial performance as a solid line, the average result for the first five strides as a dashed line and the average of the last five strides as a dotted line. The horizontal axes give gait cycle percentage and the vertical axes are the moments in Nm/kg (normalized by subject mass).

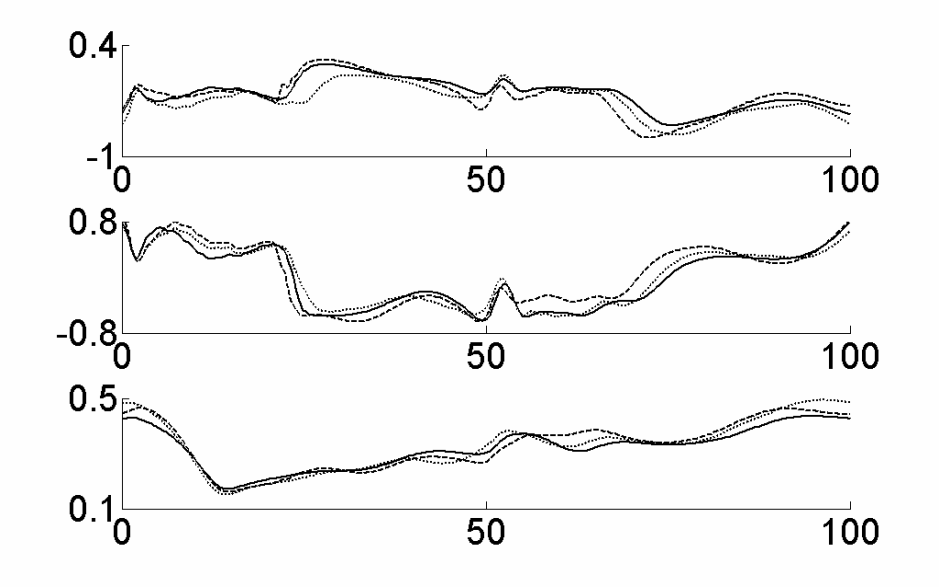

A

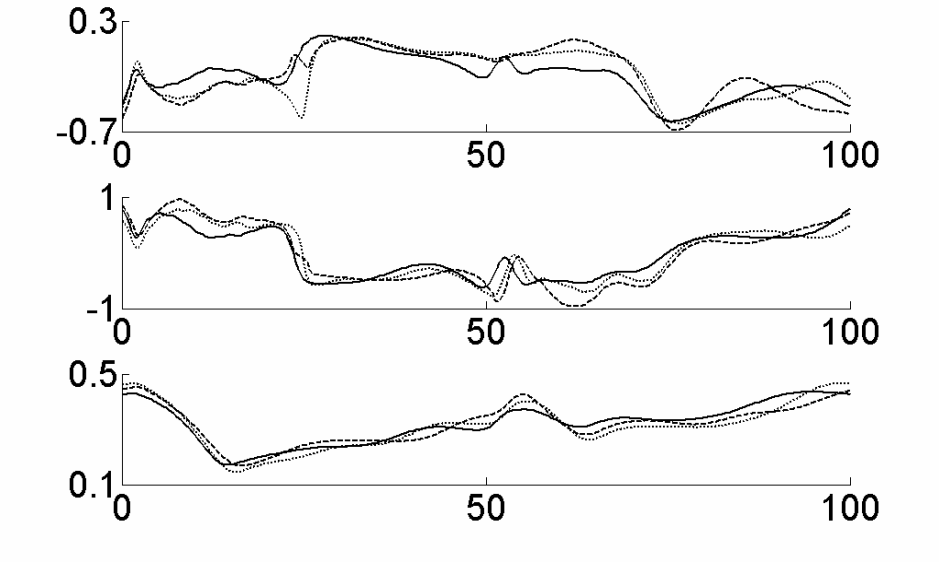

B

Figure 5.35: Pelvis moments for locked in plantarflexion experimental condition. The top plot (A) shows the adaptation trial joint moments and the bottom plot (B) shows the after-effect trial joint moments. Each subplot shows results for the X, Y and Z rotations (top to bottom). For each trial, the plot shows the null trial performance as a solid line, the average result for the first five strides as a dashed line and the average of the last five strides as a dotted line. The horizontal axes give gait cycle percentage and the vertical axes are the moments in Nm/kg (normalized by subject mass).

The effect of the AFO on the ankle moment can also be seen in the inverse dynamics of the right leg in Figure 5.33. There is an extra plantarflexion moment during the right stance phase. Therefore, it can be seen that the moments generated by the AFO locking mechanism appear in the net joint moments of the inverse dynamics results. So, care must be taken when considering with which moments the subject is controlling their motion and which moments are from other sources such as the AFO.

Early in the adaptation trial, there is a positive change in the Y-moment and a negative change in the X-moment (Figure 5.35A). By the end of the adaptation trial, these changes have decreased back to normal levels. This adaptation causes the opposite direction after-effect seen in the following trial (Figure 5.35B). The extra positive moment of the Y-moment appears to be for advancing the right hip faster and the negative change in the X-moment raises the right hip higher during the right leg swing phase. Both of these actions are required to allow adequate toe clearance and forward progression with when the toes of the right foot are locked in a plantarflexed position.

Locked in Dorsiflexion

The inverse dynamics results giving the joint moments resulting from locking the ankle in a dorsiflexed position are given in Figures 5.36-38. Evidence of adaptation due to internal model formation is seen in the extra stance phase right knee extension during the adaptation trial and the corresponding extra knee extension at the start of the after-effect trial. This after-effect then decreases throughout the after-effect trial showing the unlearning of the internal model.

The presence of the AFO on the right foot is apparent in the extra dorsiflexion moment seen for the right ankle during the stance phase. As a result of having the AFO apply this dorsiflexion moment, the subject adapted and altered the moments that it generated to control the ankle motion. This is apparent in the right ankle plantarflexion after-effect during the stance phase of the after-effect trial.

On the left side, there is significant extra ankle plantarflexion and knee flexion during the early

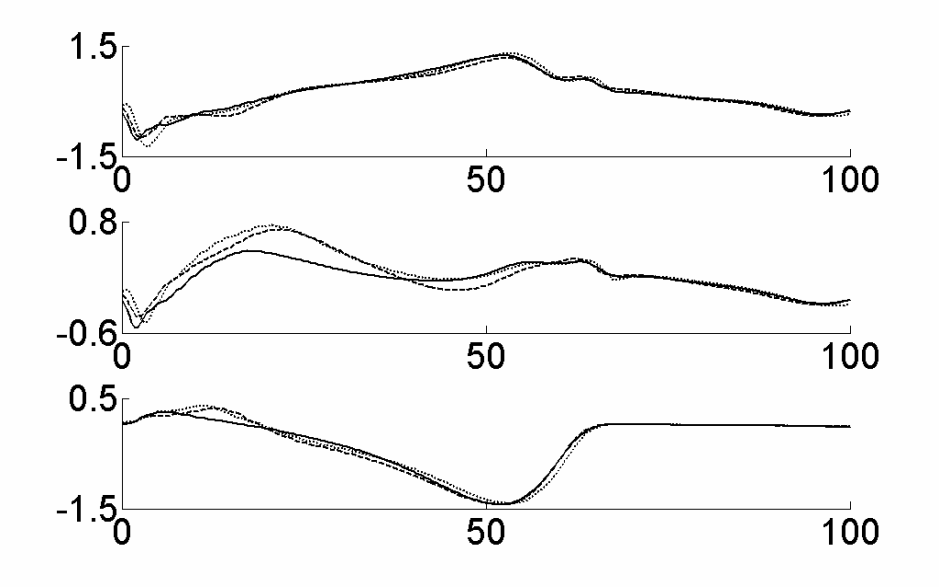

A

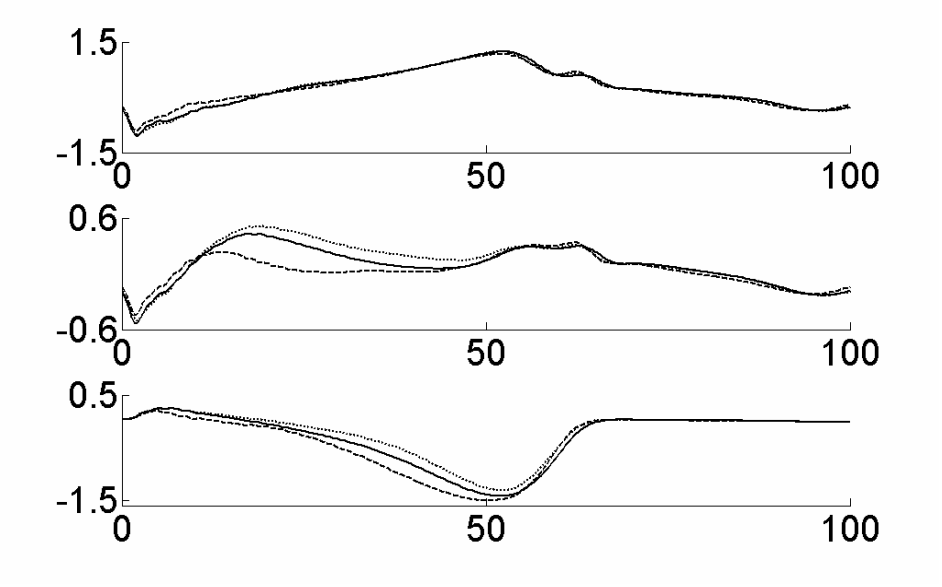

B

Figure 5.36: Right leg joint moments for locked in dorsiflexion experimental condition. The top plot (A) shows the adaptation trial joint moments and the bottom plot (B) shows the after-effect trial joint moments. Each subplot shows results for the hip, knee and ankle (top to bottom). For each trial, the plot shows the null trial performance as a solid line, the average result for the first five strides as a dashed line and the average of the last five strides as a dotted line. The horizontal axes give gait cycle percentage and the vertical axes are the moments in Nm/kg (normalized by subject mass).

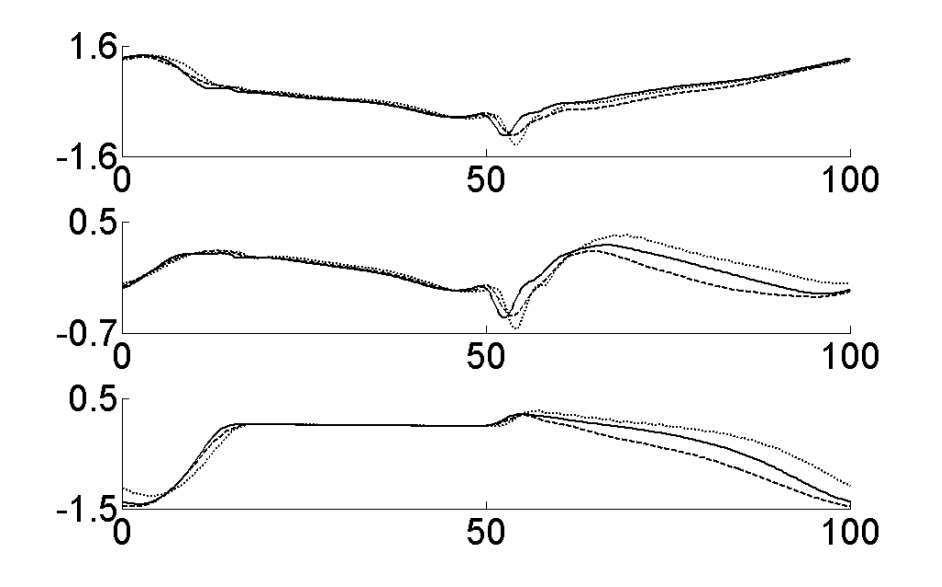

A

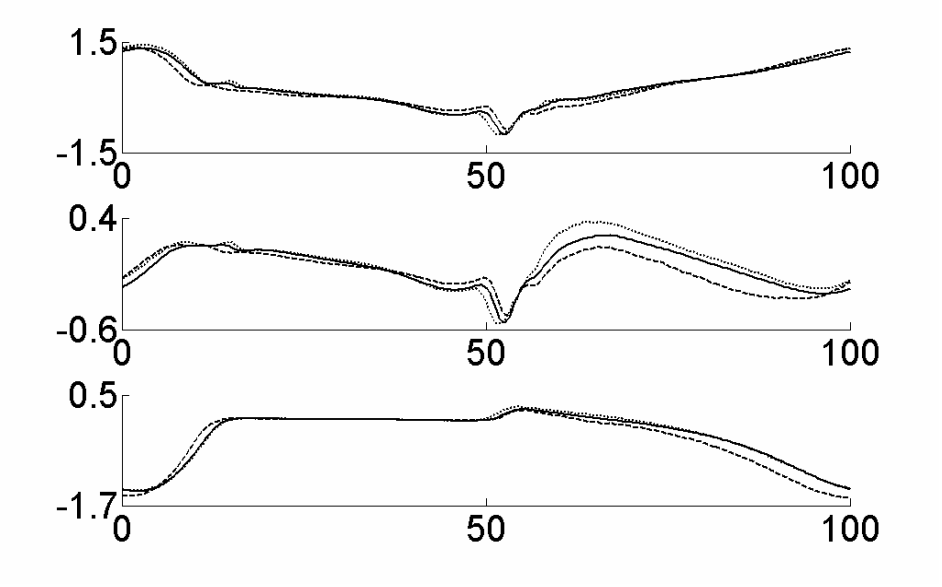

B

Figure 5.37: Left leg joint moments for locked in dorsiflexion experimental condition. The top plot (A) shows the adaptation trial joint moments and the bottom plot (B) shows the after-effect trial joint moments. Each subplot shows results for the hip, knee and ankle (top to bottom). For each trial, the plot shows the null trial performance as a solid line, the average result for the first five strides as a dashed line and the average of the last five strides as a dotted line. The horizontal axes give gait cycle percentage and the vertical axes are the moments in Nm/kg (normalized by subject mass).

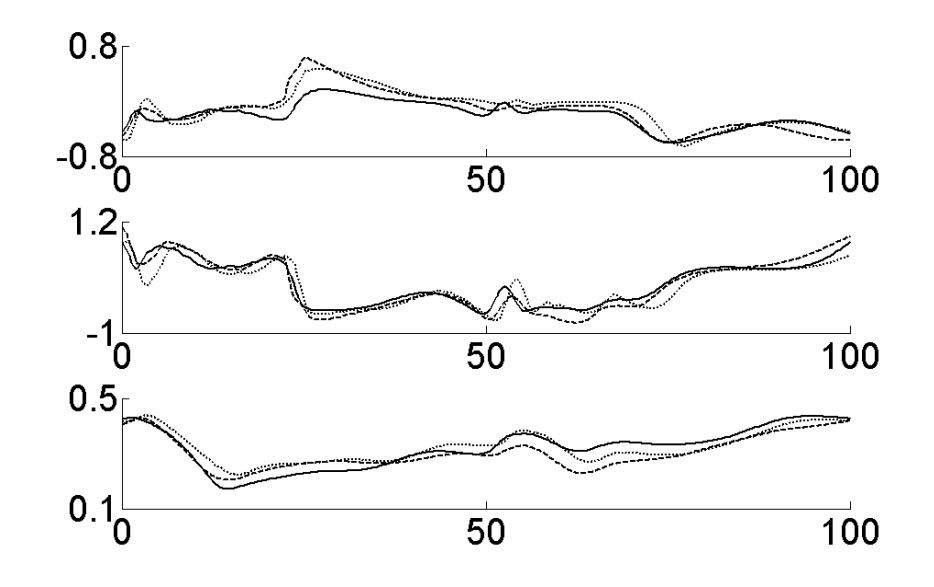

A

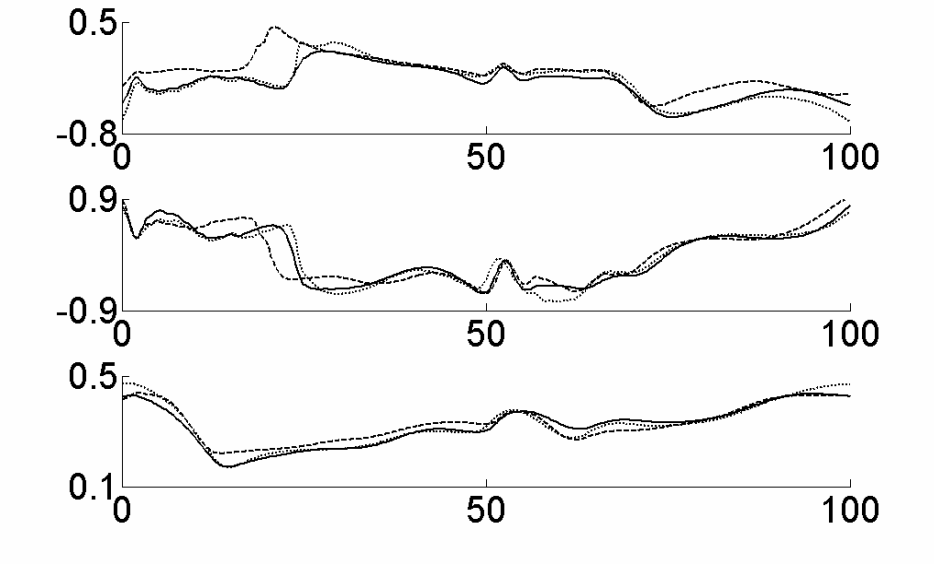

B

Figure 5.38: Pelvis moments for locked in dorsiflexion experimental condition. The top plot (A) shows the adaptation trial joint moments and the bottom plot (B) shows the after-effect trial joint moments. Each subplot shows results for the X, Y and Z rotations (top to bottom). For each trial, the plot shows the null trial performance as a solid line, the average result for the first five strides as a dashed line and the average of the last five strides as a dotted line. The horizontal axes give gait cycle percentage and the vertical axes are the moments in Nm/kg (normalized by subject mass).

strides of both the adaptation and after-effect trials. For the adaptation trials, the ankle plantarflexion moment becomes an extra dorsiflexion moment by the final strides of the trial. The knee flexion moment also changes direction by the end of the adaptation trial. This change shows an adaptation to the AFO being locked. The extra moments seen in the ankle and knee at the start of the after-effect trial further support this idea. Unlike the plantarflexion case, there are no clear patterns of adaptation seen in the pelvis moments for the dorsiflexion experiment (Figure 5.38).

No Dorsiflexion

For the AFO experiments, the most dramatic results were expected for the cases where the ankle was locked in either a plantarflexed or dorsiflexed position. Since the other experimental conditions allowed a given amount of ankle rotation, any results would not be as significant. This is indeed the case with the results for the experiment where there was no dorsiflexion allowed (Figures 5.39-41). While there are ankle moment changes associated with the AFO itself, there are no significant changes apparent in the hip moments for either leg. There are increases in right knee flexion for the early strides of both the adaptation and after-effect trials that returns to normal or even to knee extension by the end of the respective trials.

For the left leg (Figure 5.40), there is an increase in knee flexion during the stance phase of the first strides of the adaptation trial. This becomes extra knee flexion by the end of the adaptation trial and an after-effect is seen at the start of the after-effect trial. There is a general decrease in the pelvis X-moment at the start of the adaptation trial that returns to the null trial behaviour by the end of the trial. This correlates with an increase in the X-moment of the pelvis at the start of the after-effect trial. A decrease in the X-moment of the pelvis would lead to an increase in the moment lifting the right hip during the swing phase, which may help with toe clearance since the foot is unable to dorsiflex in this case.

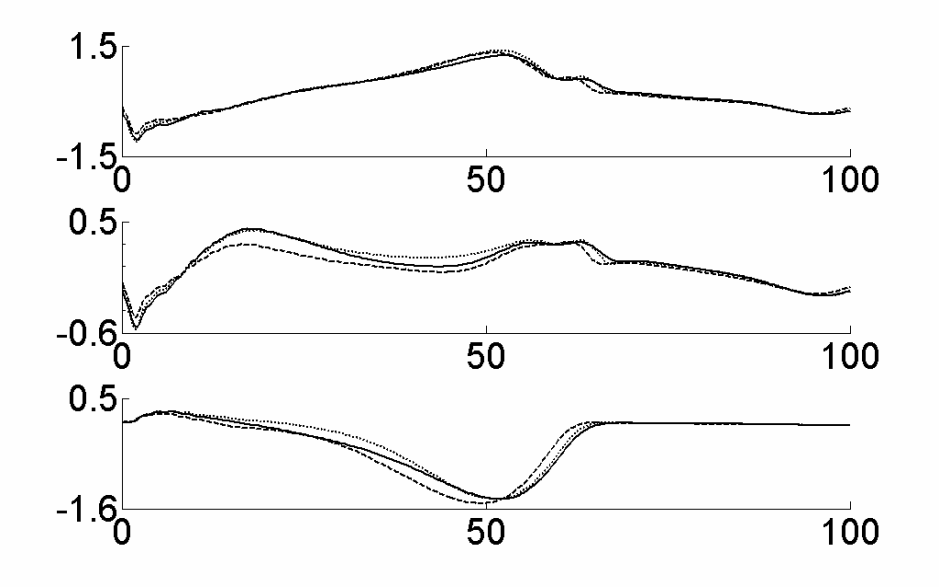

A

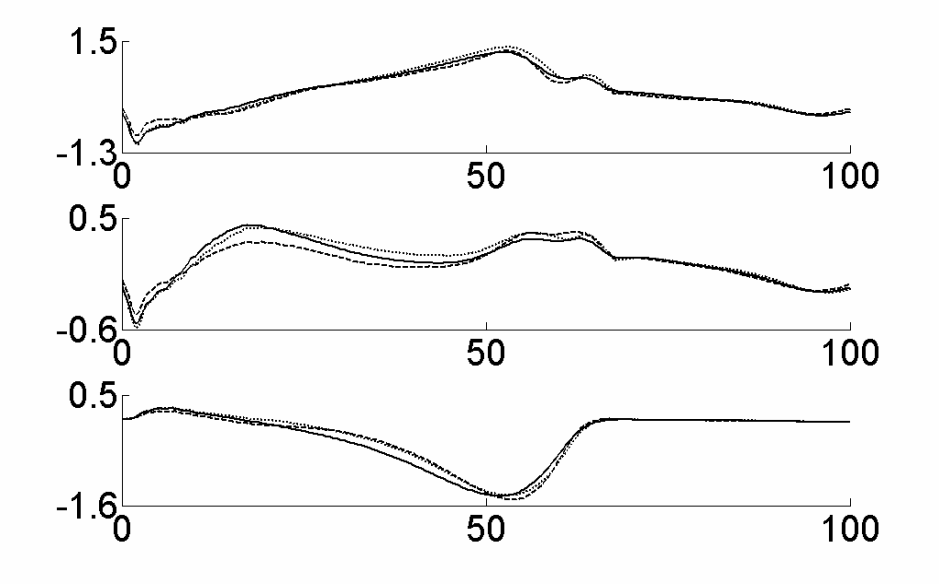

B

Figure 5.39: Right leg joint moments for the plantarflexion without dorsiflexion experimental condition. The top plot (A) shows the adaptation trial joint moments and the bottom plot (B) shows the after-effect trial joint moments. Each subplot shows results for the hip, knee and ankle (top to bottom). For each trial, the plot shows the null trial performance as a solid line, the average result for the first five strides as a dashed line and the average of the last five strides as a dotted line. The horizontal axes give gait cycle percentage and the vertical axes are the moments in Nm/kg (normalized by subject mass).

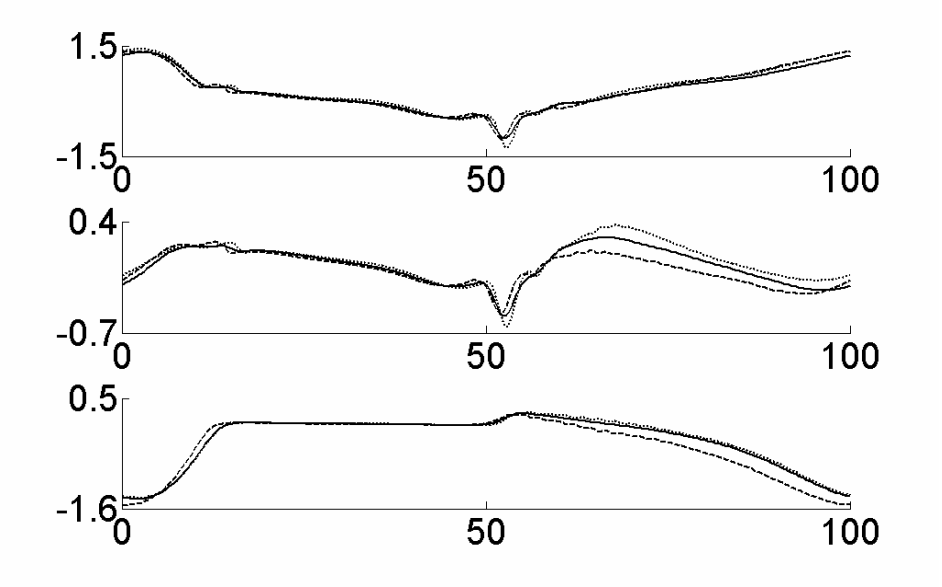

A

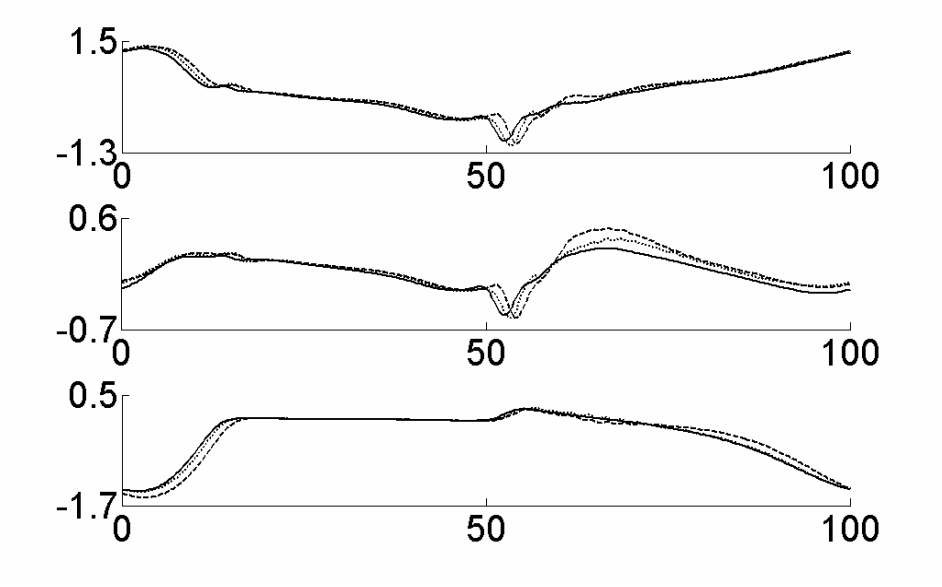

B

Figure 5.40: Left leg joint moments for the plantarflexion without dorsiflexion experimental condition. The top plot (A) shows the adaptation trial joint moments and the bottom plot (B) shows the after-effect trial joint moments. Each subplot shows results for the hip, knee and ankle (top to bottom). For each trial, the plot shows the null trial performance as a solid line, the average result for the first five strides as a dashed line and the average of the last five strides as a dotted line. The horizontal axes give gait cycle percentage and the vertical axes are the moments in Nm/kg (normalized by subject mass).

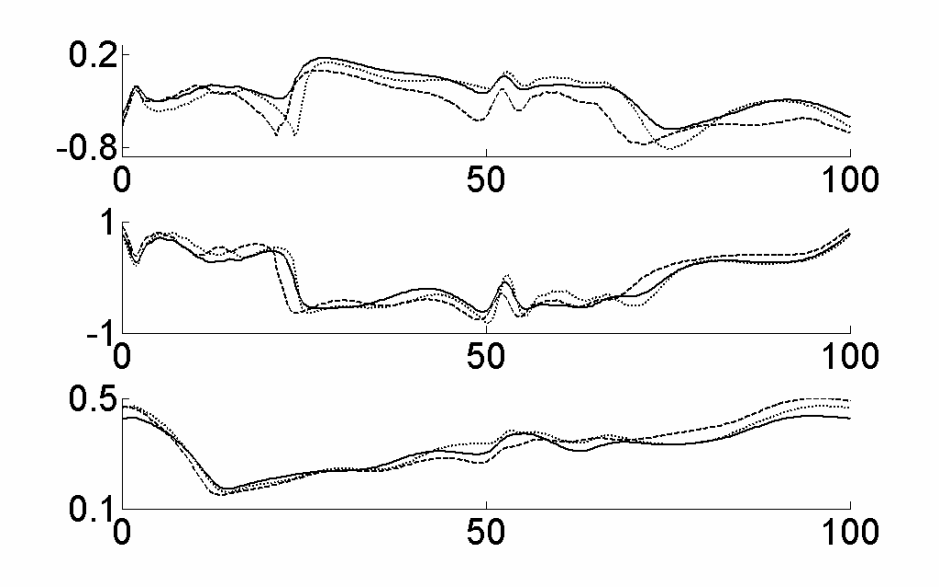

A

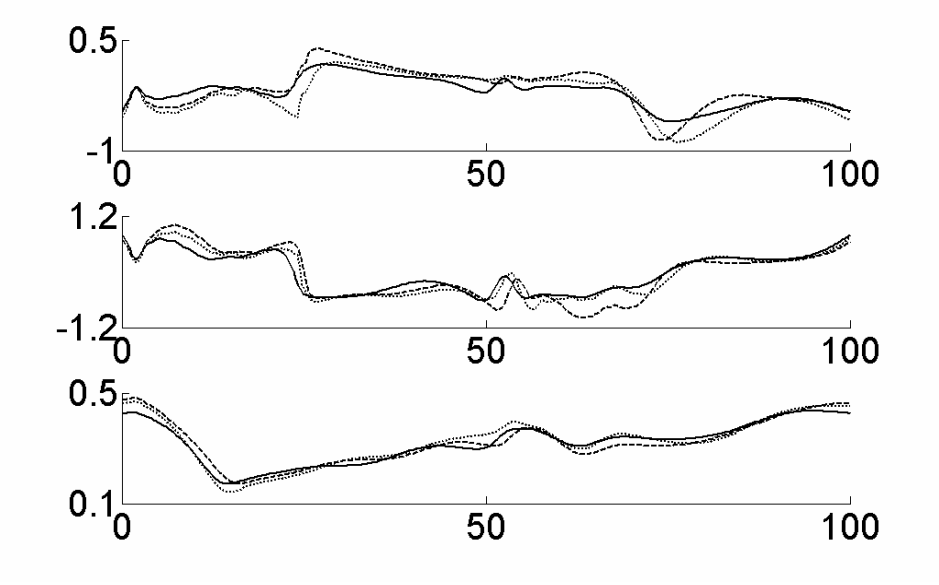

B

Figure 5.41: Pelvis moments for the plantarflexion without dorsiflexion experimental condition. The top plot (A) shows the adaptation trial joint moments and the bottom plot (B) shows the after-effect trial joint moments. Each subplot shows results for the X, Y and Z rotations (top to bottom). For each trial, the plot shows the null trial performance as a solid line, the average result for the first five strides as a dashed line and the average of the last five strides as a dotted line. The horizontal axes give gait cycle percentage and the vertical axes are the moments in Nm/kg (normalized by subject mass).

No Plantarflexion

For the inverse dynamics results for the experimental condition allowing dorsiflexion with no plantarflexion (Figures 5.42-44), there are no significant changes in the behaviour of the hips for either leg and also no clear pattern of changes in the moments for the pelvis. There is however, an increase in right knee stance phase extension moments during the adaptation trial with an associated flexion after-effect in the following trial. There are also stance phase knee extension moment increases for the left leg during both the adaptation and after-effect trials. Aside from the knee moment changes, there are few significant changes occurring for this particular experimental condition.

Different Tread Speeds

The results for the different tread speed experiment are presented in Figures 5.45-47. For the right leg, most of the changes during the adaptation trial are purely timing changes resulting from the asymmetry introduced by the different tread speeds. During the after-effect trial, both the right ankle and the right knee exhibit significant changes in their stance phase behaviour. The ankle shows an increase in dorsiflexion moments and the knee exhibits very significant knee extension moment increases. These significant changes occur as a result of the formation of an internal model of the tread speed task by the central nervous system. This model formation was also apparent in the subjective responses of the subjects after the experiment. All subjects stated that, at the start of the after-effect trial, they felt like the the left tread was going faster than the right tread, when they were in fact going at the same speed. This perception caused the subjects to generate extra compensatory torques when non were required.

For the left leg, there were significant increases in the ankle dorsiflexion moment and the knee extension moment leading up to toe-off during the adaptation trial. During the after-effect trial, significant changes before toe-off were in the opposite direction and provide evidence for the formation

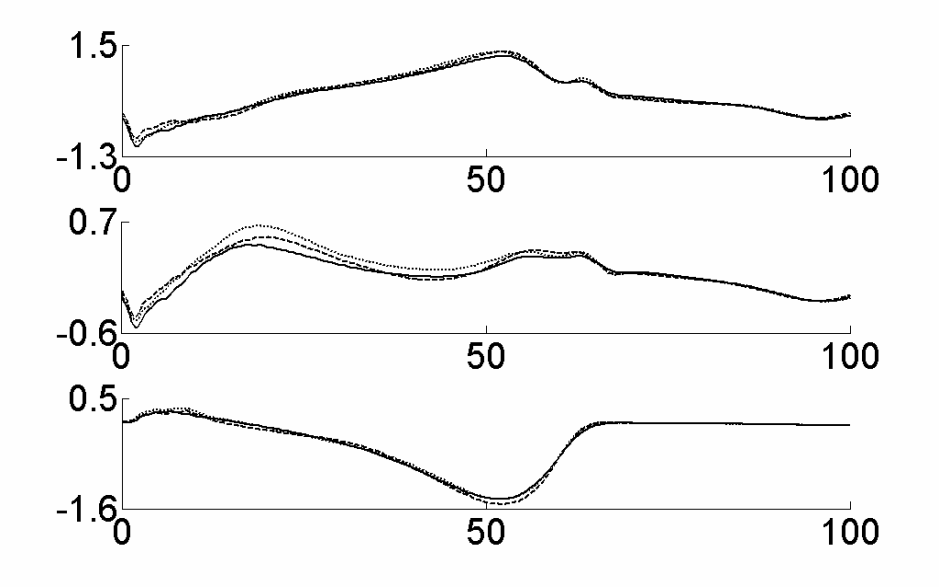

A

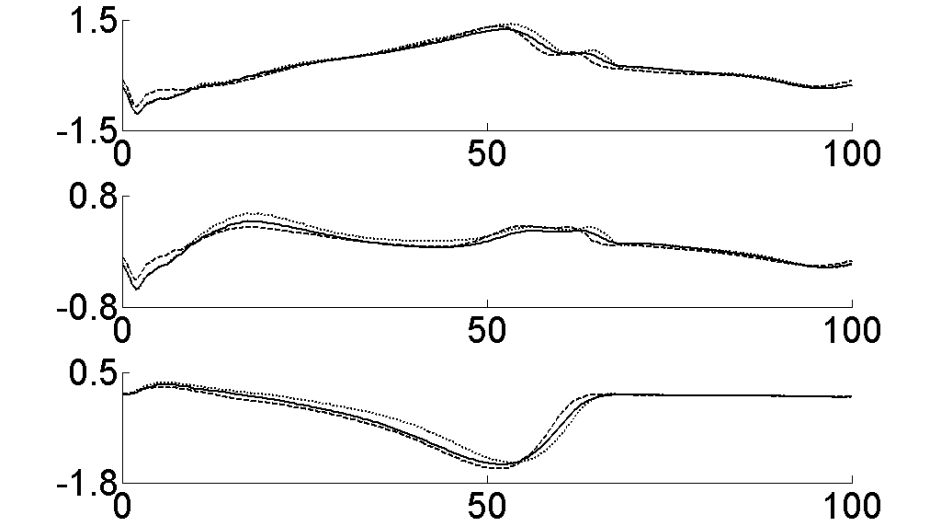

B

Figure 5.42: Right leg joint moments for the dorsiflexion without plantarflexion experimental condition. The top plot (A) shows the adaptation trial joint moments and the bottom plot (B) shows the after-effect trial joint moments. Each subplot shows results for the hip, knee and ankle (top to bottom). For each trial, the plot shows the null trial performance as a solid line, the average result for the first five strides as a dashed line and the average of the last five strides as a dotted line. The horizontal axes give gait cycle percentage and the vertical axes are the moments in Nm/kg (normalized by subject mass).

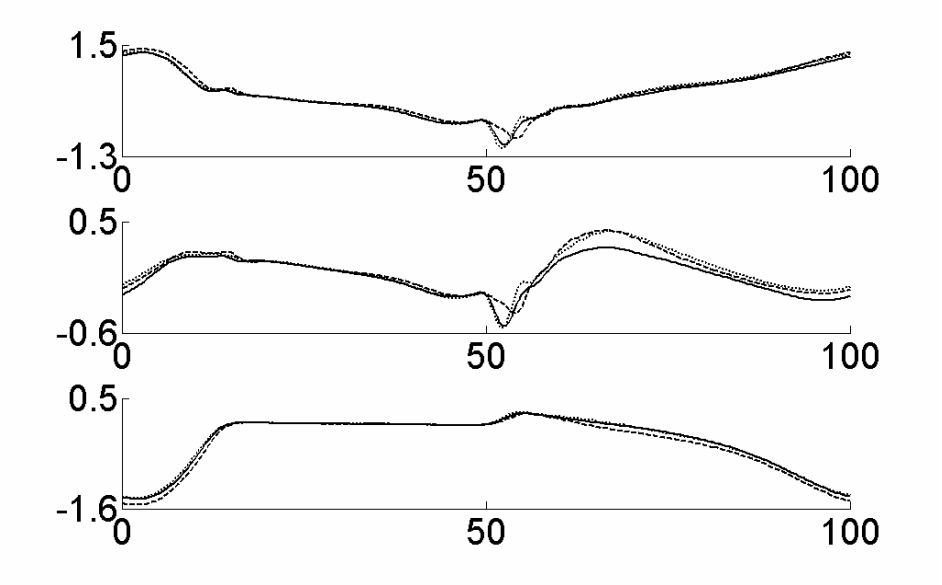

A

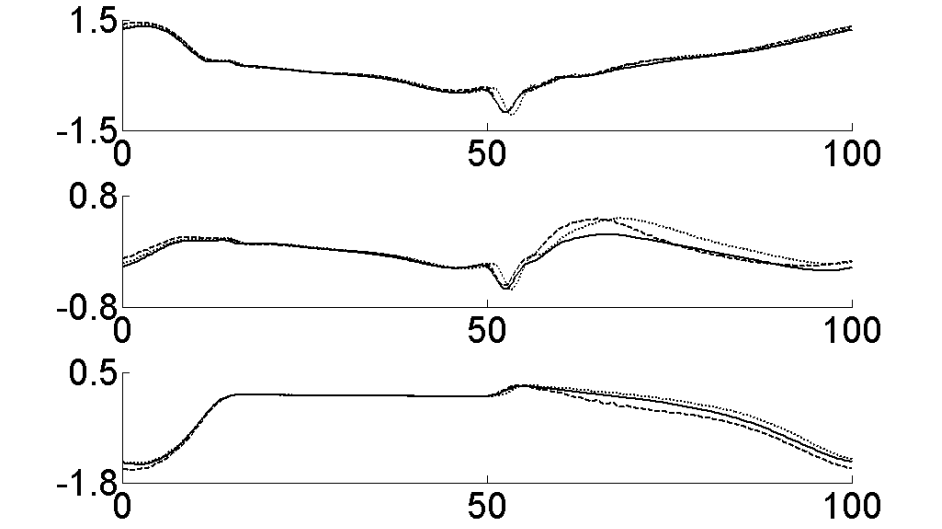

B

Figure 5.43: Left leg joint moments for the dorsiflexion without plantarflexion experimental condition. The top plot (A) shows the adaptation trial joint moments and the bottom plot (B) shows the after-effect trial joint moments. Each subplot shows results for the hip, knee and ankle (top to bottom). For each trial, the plot shows the null trial performance as a solid line, the average result for the first five strides as a dashed line and the average of the last five strides as a dotted line. The horizontal axes give gait cycle percentage and the vertical axes are the moments in Nm/kg (normalized by subject mass).

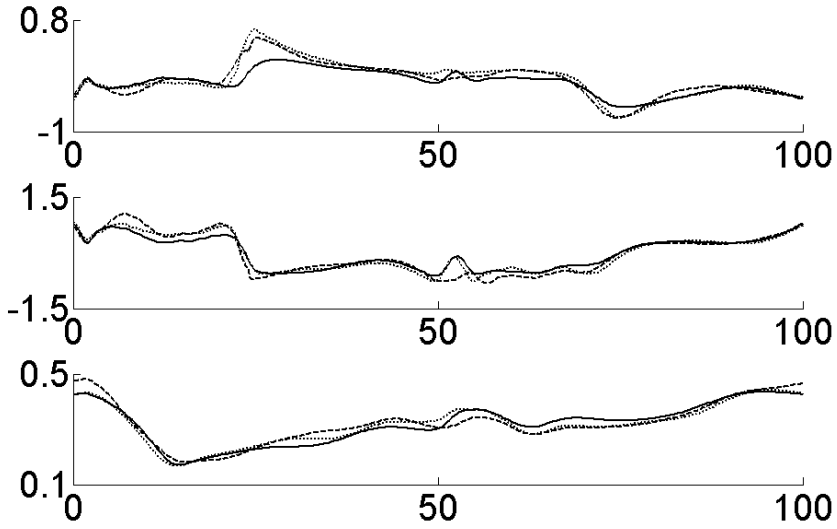

A

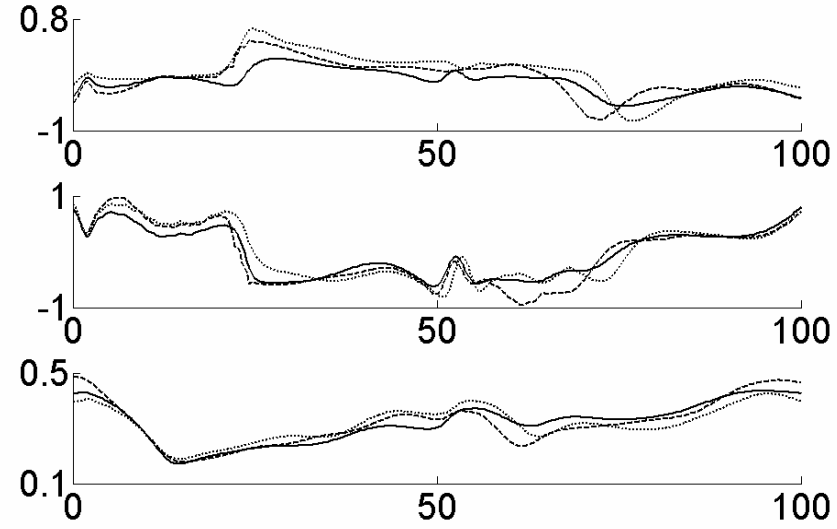

B

Figure 5.44: Pelvis moments for the dorsiflexion without plantarflexion experimental condition. The top plot (A) shows the adaptation trial joint moments and the bottom plot (B) shows the after-effect trial joint moments. Each subplot shows results for the X, Y and Z rotations (top to bottom). For each trial, the plot shows the null trial performance as a solid line, the average result for the first five strides as a dashed line and the average of the last five strides as a dotted line. The horizontal axes give gait cycle percentage and the vertical axes are the moments in Nm/kg (normalized by subject mass).

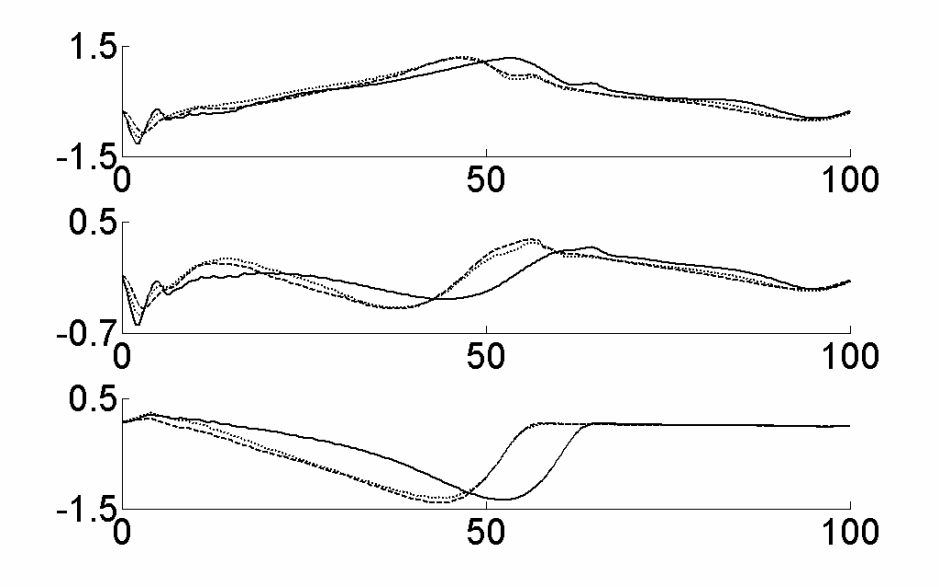

A

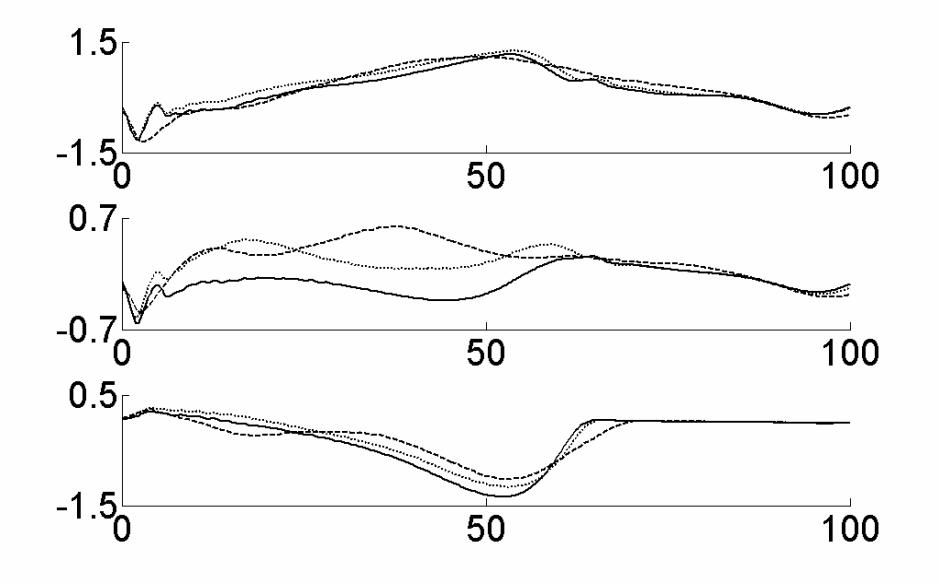

B

Figure 5.45: Right leg joint moments for the different tread speeds experimental condition. The top plot (A) shows the adaptation trial joint moments and the bottom plot (B) shows the after-effect trial joint moments. Each subplot shows results for the hip, knee and ankle (top to bottom). For each trial, the plot shows the null trial performance as a solid line, the average result for the first five strides as a dashed line and the average of the last five strides as a dotted line. The horizontal axes give gait cycle percentage and the vertical axes are the moments in Nm/kg (normalized by subject mass).

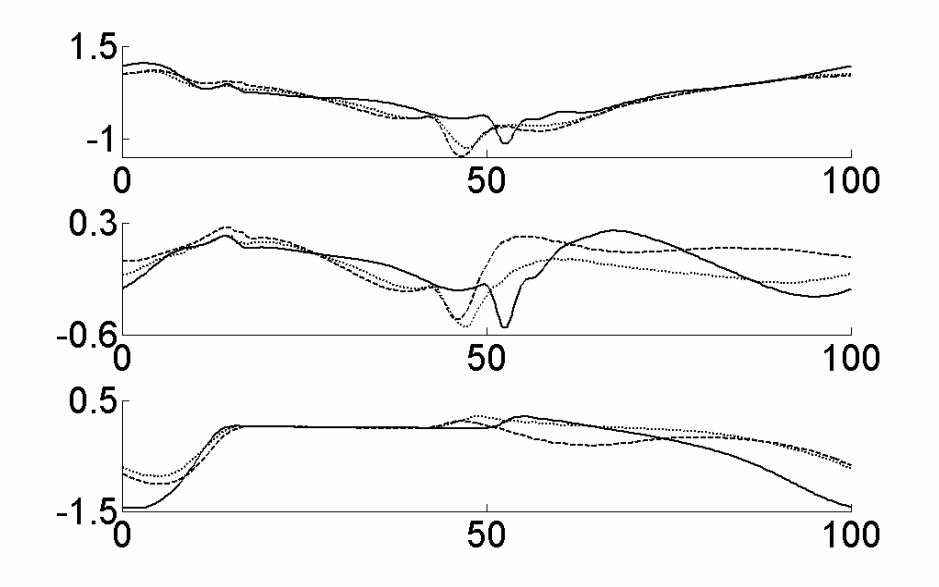

A

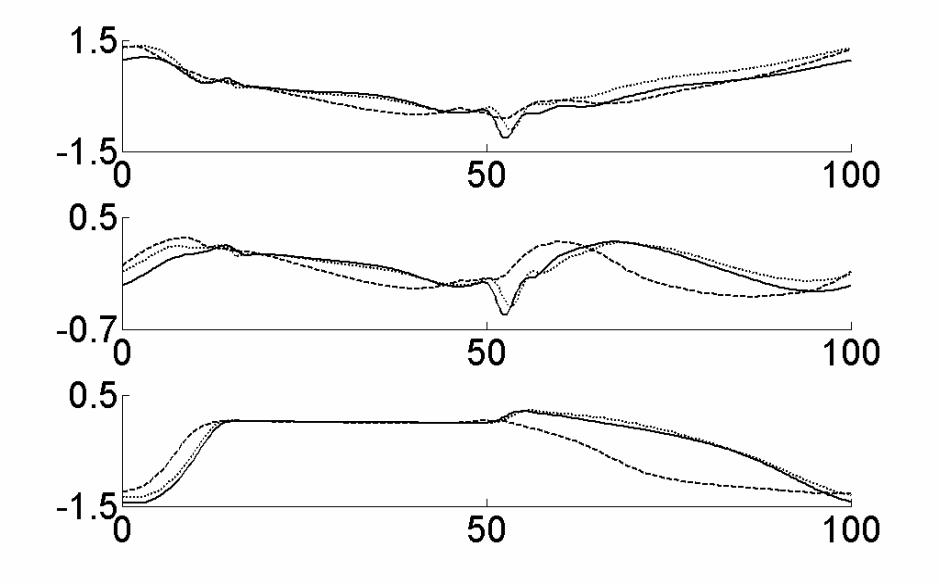

B

Figure 5.46: Left leg joint moments for the different tread speeds experimental condition. The top plot (A) shows the adaptation trial joint moments and the bottom plot (B) shows the after-effect trial joint moments. Each subplot shows results for the hip, knee and ankle (top to bottom). For each trial, the plot shows the null trial performance as a solid line, the average result for the first five strides as a dashed line and the average of the last five strides as a dotted line. The horizontal axes give gait cycle percentage and the vertical axes are the moments in Nm/kg (normalized by subject mass).

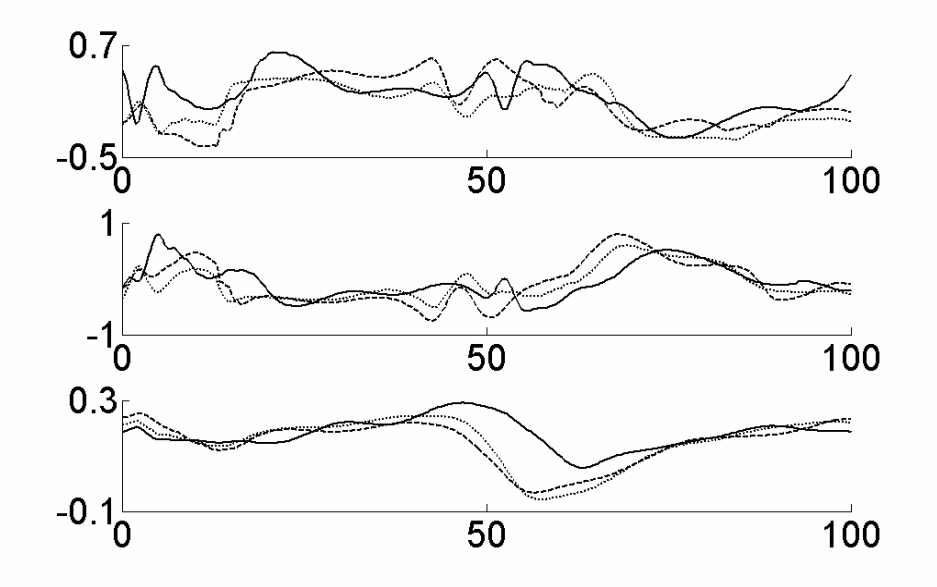

A

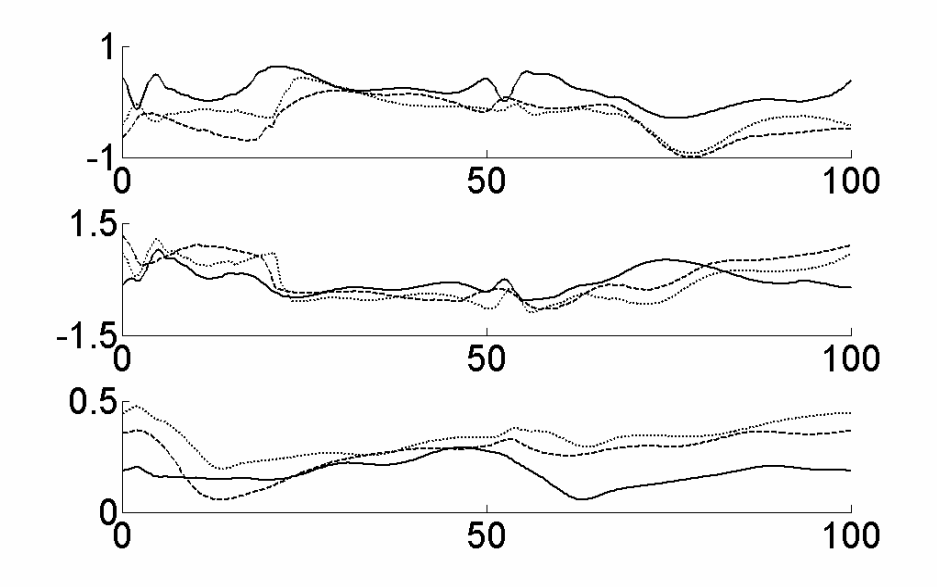

B

Figure 5.47: Pelvis moments for the different tread speeds experimental condition. The top plot (A) shows the adaptation trial joint moments and the bottom plot (B) shows the after-effect trial joint moments. Each subplot shows results for the X, Y and Z rotations (top to bottom). For each trial, the plot shows the null trial performance as a solid line, the average result for the first five strides as a dashed line and the average of the last five strides as a dotted line. The horizontal axes give gait cycle percentage and the vertical axes are the moments in Nm/kg (normalized by subject mass).

of an internal model.

At the start of the right swing phase during the adaptation trial, there are significant changes in the Y- and Z-moments of the pelvis. The Y-moment shows a large increase in moment starting from the left heel strike and into the early right leg swing phase. The Z-moment shows a large decrease heading into the left heel strike and for the early right swing phase. A larger Y-moment on the pelvis generally leads towards a faster forward progression of the right hip. This moment is needed since the right leg is moving at a higher stride rate during the adaptation trial and the right hip and leg need to move faster during the upcoming swing phase. A more negative moment about the pelvis Z-axis is generally associated with tilting the pelvis forward. This is most likely required to maintain the balance of the torso and to support the transition from the fast tread to the slow tread. Both the Y- and Z-moment changes have associated after-effects visible in the results for the next trial.

Overall, the changes seen during the different tread speed experiment were among the most significant out of all the experiments. This is due to the fact that such a task is the most unlike regular everyday walking and therefore it affords the most potential for learning and for the more significant deviations from the null trial behaviour.

5.3 Experiment #3

5.3.1 Kinematics Analysis

Patient #1

In order to a compare the performance of the patients with that of the healthy non-impaired subjects from Experiment #1, the same data analysis was performed. Figures 5.48-49 show the average joint angle trajectories for the right and left legs of the first patient respectively. The orientation of the

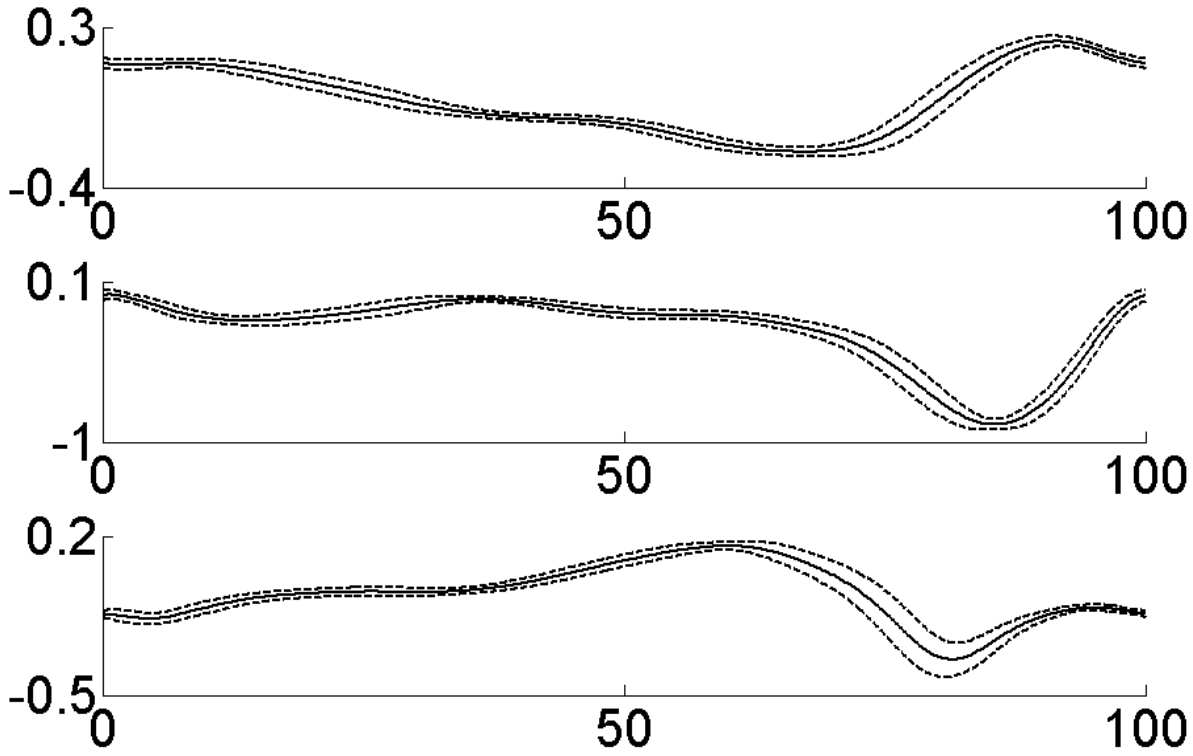

Figure 5.48: Patient #1 right leg joint angle trajectories. Top - Hip joint angle. Middle – Knee joint angle. Bottom – Ankle joint angle The dark solid line is for the mean and the dashed line represents the standard deviation. The horizontal time axis represents gait cycle percentage and all angles are in radians.

patient's HAT segment and the location of the pelvis COM are shown in Figure 5.50. Finally, the Euler angles describing the patient's pelvis orientation are presented in Figure 5.51. Additionally, the gait performance metrics analyzed for the previous experiments were determined for this patient and are given in Table 5.2.

While processing the experimental data for the first patient, it was discovered that there was an error during the data collection that resulted in the force data not being properly synchronized with the kinematic data. As a result, the GRF data for this subject cannot be presented. Additionally, this means that the inverse dynamics analysis was not performed for this patient. Additionally, GRF data was not

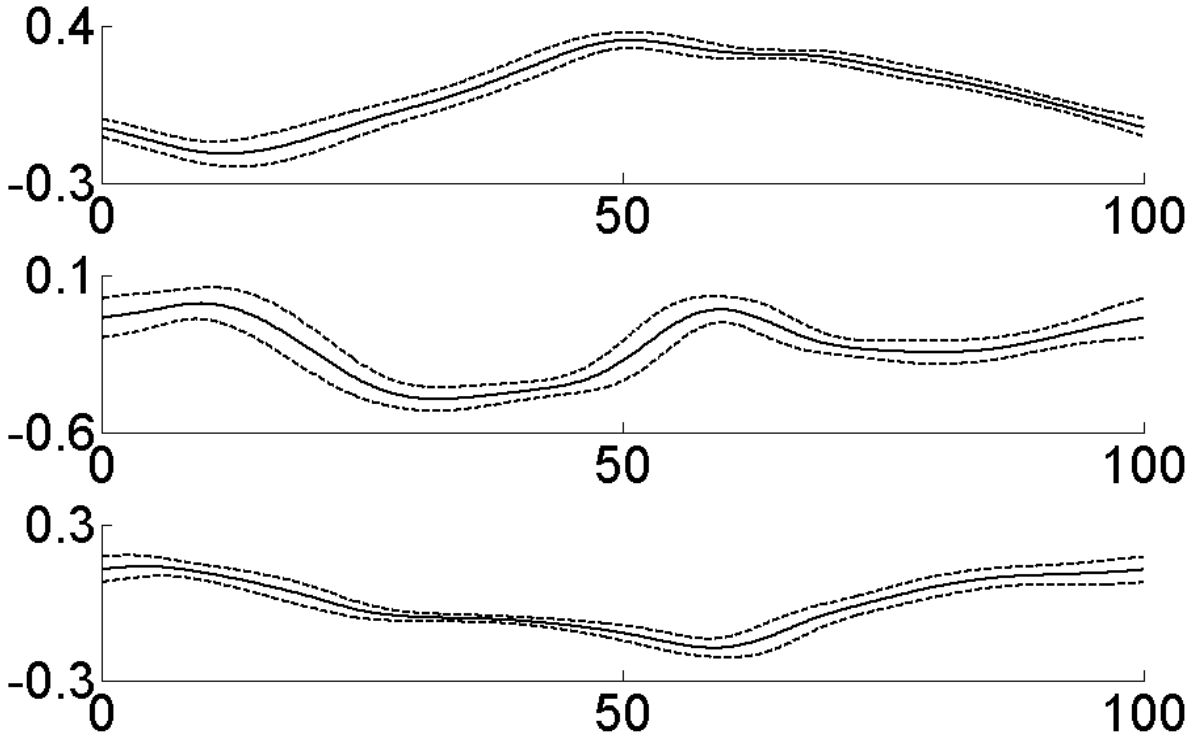

Figure 5.49: Patient #1 left leg joint angle trajectories. Top - Hip joint angle. Middle – Knee joint angle. Bottom – Ankle joint angle The dark solid line is for the mean and the dashed line represents the standard deviation. The horizontal time axis represents gait cycle percentage and all angles are in radians.

used to determine the heel strike and toe off times for this patient. Instead, these values were found using the segment orientation data for the feet of the subject. In particular, the foot orientation reaches a maximum near the heel strike times and a minimum near the toe-off times. These values are an approximation to the actual heel strike and toe-off times as the actual ground contact timing cannot be extracted using force data.

The right leg joint angle data from Figure 5.48 show a stance phase that is significantly longer than that of healthy subjects. This is further supported by the stance percentage reported in Table 5.2. Also, the stance phase time for the left leg is longer than that of healthy patients as well, though significantly shorter than the non-impaired stance percentage. This most likely is due to the slow speed

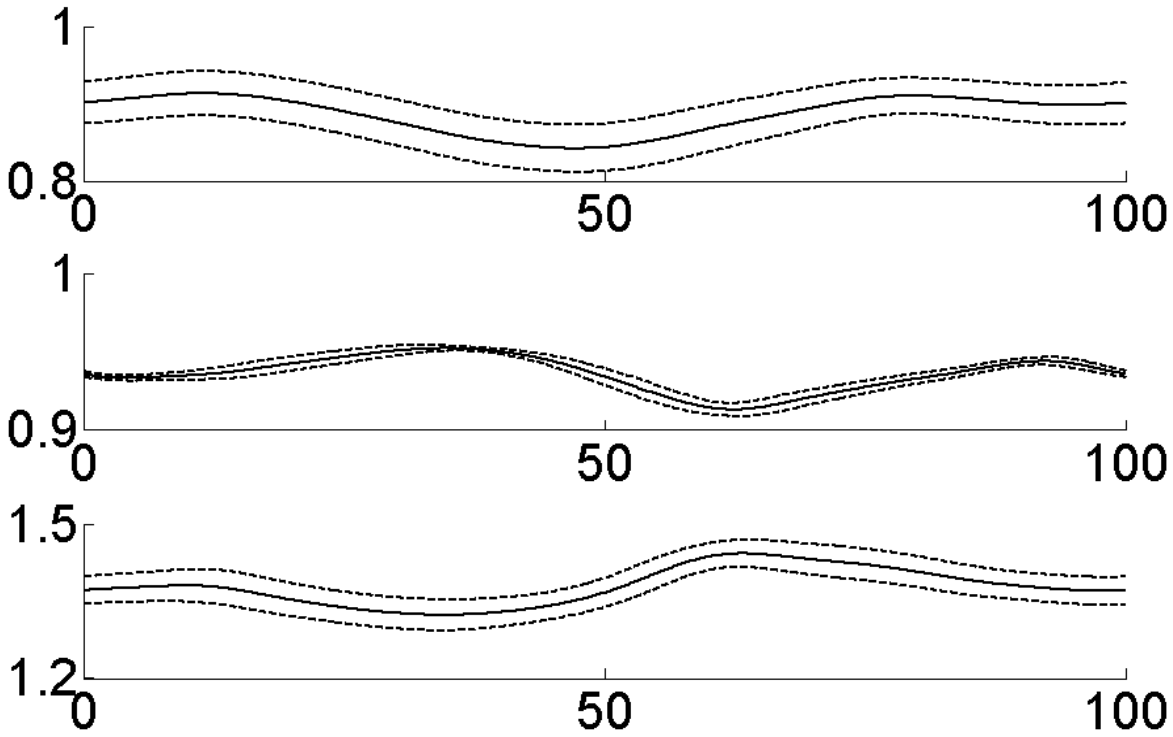

Figure 5.50: Patient #1 HAT segment angle and COM location of the pelvis. Top - Anterior-posterior pelvis COM location. Middle – Pelvis COM height. Bottom – Torso orientation about the X-axis measured from the Y-axis. The dark solid line is for the mean and the dashed line represents the standard deviation. The horizontal time axis represents gait cycle percentage. The COM location values are in meters and the torso angle is in radians.

at which the patient is walking. Also, longer stance phases on both sides implies that the patient was spending extra time in the double support phase and maintaining ground contact with both feet. By doing so, the subject is able to have improved balance control. The longer stance phase is also evident in the differences between the healthy and patient right leg joint angle trajectories. The primary change is that the first half of the patient's trajectories appear to be stretched versions of the healthy subjects' patterns.

The higher pelvis COM seen in Figure 5.50 during the right leg stance phase, when compared to the peak in the second half of the gait cycle, suggests that a vaulting gait compensation may be present

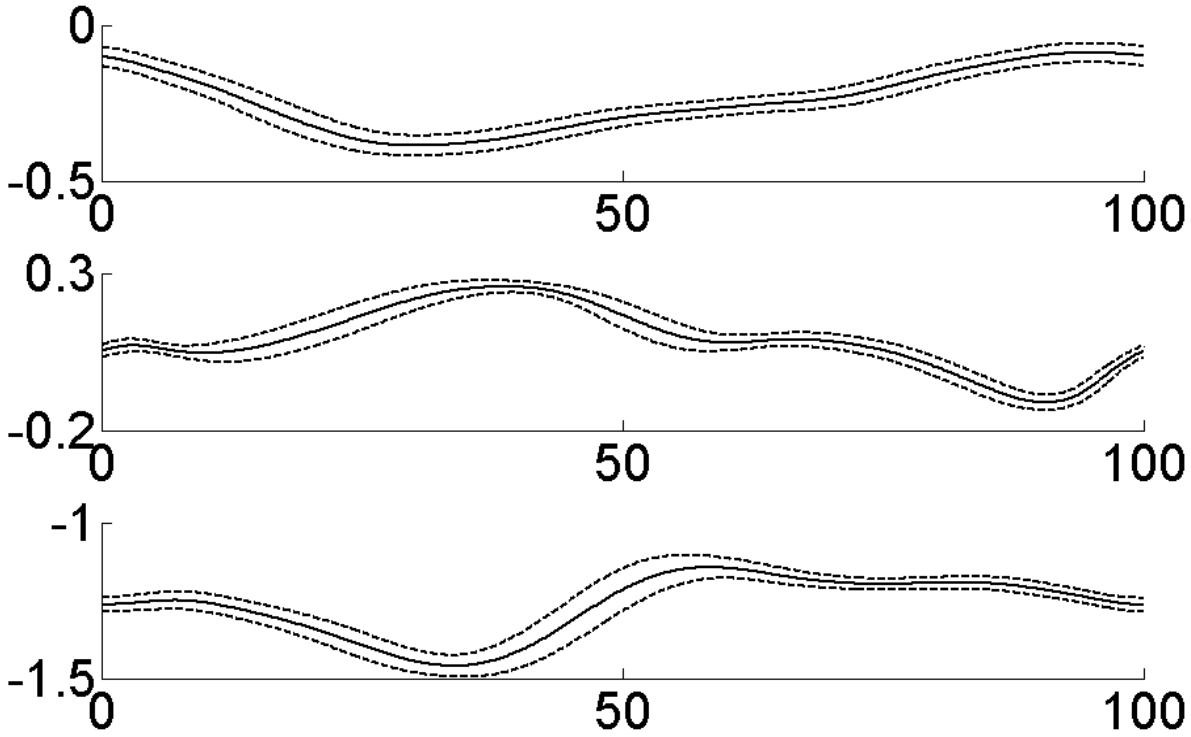

Figure 5.51: Patient #1 pelvis orientation Euler angles. Top - X-axis Euler angle. Middle – Y-axis Euler angle. Bottom – Z-axis Euler angle. The dark solid line is for the mean and the dashed line represents the standard deviation. The horizontal time axis represents gait cycle percentage and all angles are in radians.

For this patient. By having a higher pelvis in general, there is more potential for toe clearance during the left leg swing phase.

Normative gait data corresponding to the anthropometric measurements of this patient at the self-selected walking speed (0.35 m/s) was not available for an accurate statistical comparison with the patient data in this work. However, a general comparison of the results in Table 5.2 with the results in Table 5.1 show increases in stride time and stance percentage compared to the healthy controls. There is also a decrease in stride length and in peak knee flexion. All of these changes correlate with the typical expected results of changes in the speed of walking. This also the case for the general decrease seen in the peak toe clearance level for this patient. When compared with the locked plantarflexion adaptation

Table 5.2: Average (± std dev) performance metric values for Patient #1.

Trial	Right Leg	Left Leg
Stride Time	1.90±.092	1.90±.122
Stance %	81.7±1.61	71.6±2.76
Stride Length	.66±.051	.67±.048
Knee Flexion	.90±.028	.47±.046
Hip Extension	.25±.018	.18±.048
Hip Flexion	.25±.023	.35±.027
Ankle Toe Off	-.36±.071	-.06±.015
Ankle Heel Strike	-.14±.016	-.18±.024
Toe Clearance	.039±.004	.026±.003
Hip Height Stance	.92±.002	.93±.004
Hip Height Swing	.93±.003	.94±.003

performance metric plots in Figures 5.13-16, the stance percentage increase and the peak toe clearance decrease are the only metrics that match that adaptation stage. When compared with the dorsiflexion locked AFO adaptation changes in performance metrics in Figures 5.17-20, the stride length and peak toe clearance decreases match the patient data.

When the patient's hip height during stance and swing data are compared with the same performance metrics during the plantarflexion and dorsiflexion locked AFO experiments, the plantarflexion experiment more closely matches the results for the patient. Both the patient and adaptation subjects show higher hip heights on the impaired side for both the stance and swing phases. These results tend to suggest that the plantarflexion experiment more closely matches the performance for this patient.

Patient #2

Figures 5.52-55 show the kinematic data for the second patient. This data corresponds to the same kinematic data collected for the other patient and for the healthy subjects from Experiment #1. For

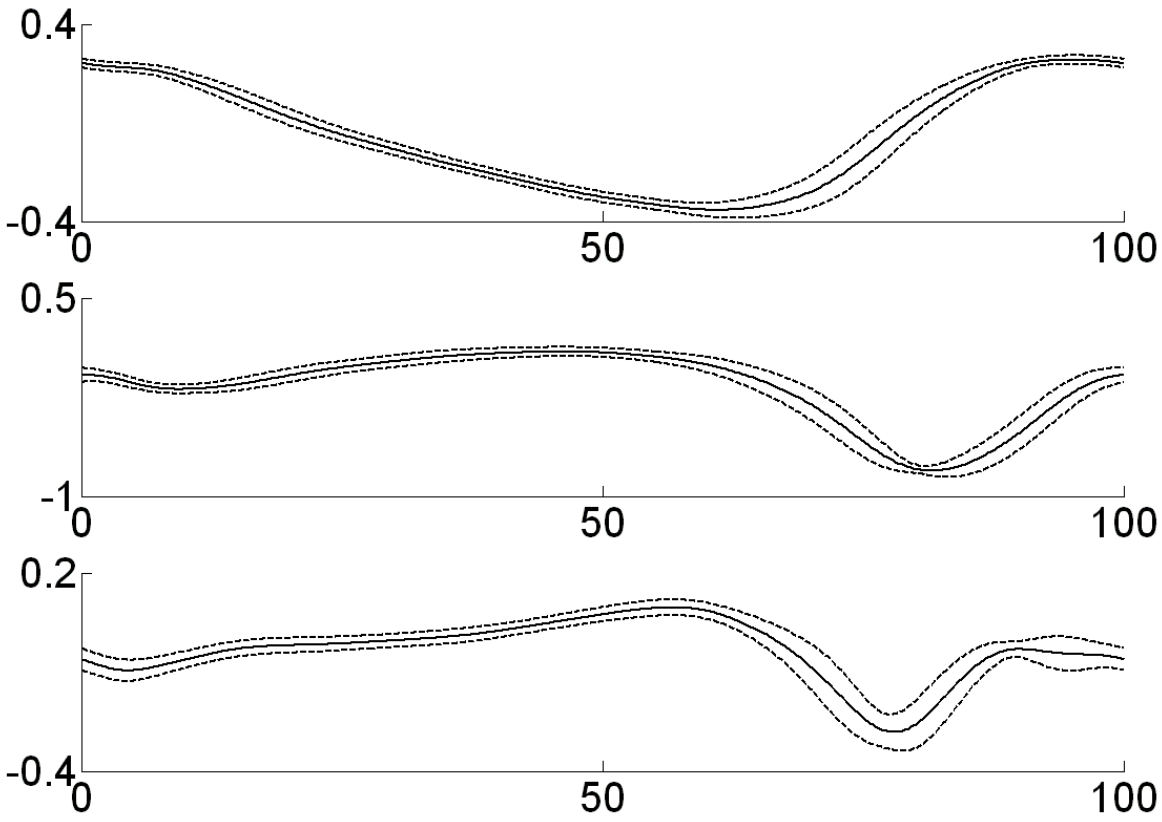

Figure 5.52: Patient #2 right leg joint angle trajectories. Top - Hip joint angle. Middle – Knee joint angle. Bottom – Ankle joint angle The dark solid line is for the mean and the dashed line represents the standard deviation. The horizontal time axis represents gait cycle percentage and all angles are in radians.

this patient the left leg is the impaired leg exhibiting drop foot symptoms. The hip angle results from Figure 5.52 show that the subject has a delayed hip extension peak for the right leg when compared with the trajectories presented in Figure 5.1. This corresponds to a delayed toe off time and a shortened swing phase. Since the patient exhibits weakness in the impaired leg, the faster swing phase on the non-impaired side allows for a shortened stance phase on the weaker impaired leg. This change in the stance/swing ratio is the most prominent feature of the joint angle trajectories on the non-impaired leg.

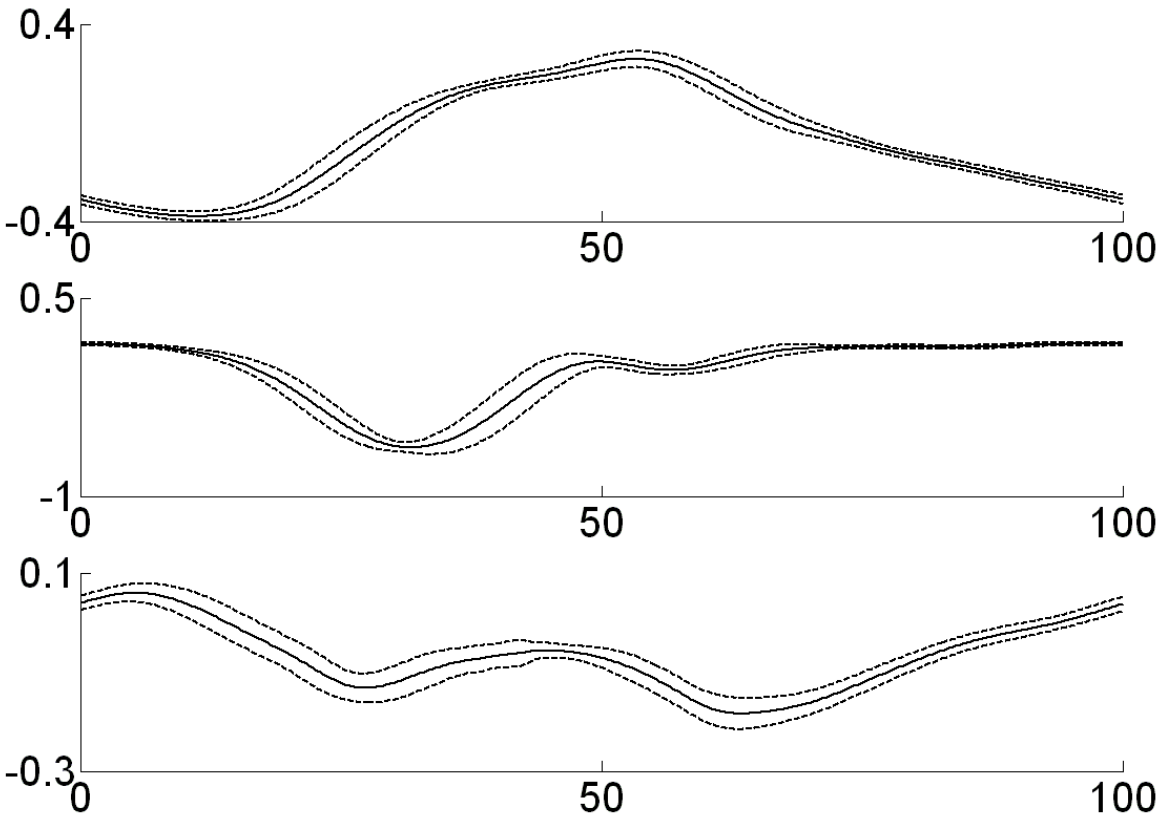

Figure 5.53: Patient #2 left leg joint angle trajectories. Top - Hip joint angle. Middle – Knee joint angle. Bottom – Ankle joint angle The dark solid line is for the mean and the dashed line represents the standard deviation. The horizontal time axis represents gait cycle percentage and all angles are in radians.

Additionally, the gait performance metrics analyzed for the previous experiments were determined for this patient and are given in Table 5.3. The shorter stride length, longer stride time and larger stance percentage compared to the healthy subjects are inline with subjects walking at slower speeds in general. Additionally, the longer stance percentage for the non-impaired leg is consistent with the patient spending a larger portion of their time supporting their weight with their non-impaired leg. The patient also exhibits lower toe clearance levels on the drop foot impaired leg, which is consistent with the nature of the impairment as is to be expected. The lower knee flexion exhibited on the impaired leg supports the general medical history of the patient and the clear evidence of vaulting exhibit in their

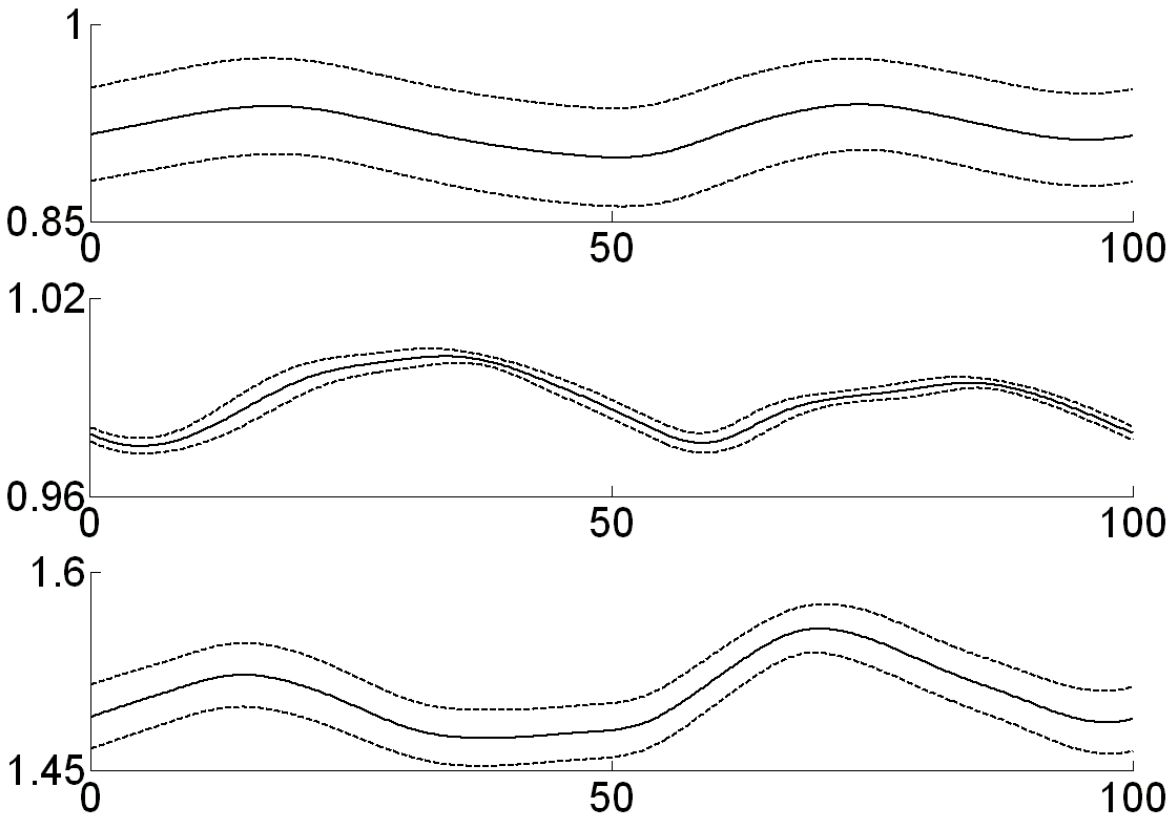

Figure 5.54: Patient #2 HAT segment angle and COM location of the pelvis. Top - Anterior-posterior pelvis COM location. Middle – Pelvis COM height. Bottom – Torso orientation about the X-axis measured from the Y-axis. The dark solid line is for the mean and the dashed line represents the standard deviation. The horizontal time axis represents gait cycle percentage. The COM location values are in meters and the torso angle is in radians.

gait. Less knee flexion implies possible weakness in the knee flexor muscles on the impaired side and such a weakness would promote compensation movements that could support a straighter knee.

Overall these kinematic results show similar patterns as those of the first patient. This is particularly evident when the performance metrics from Table 5.3 are compared with the adaptation experiment results and the results in Table 5.2. This similarity is to be expected since both patients exhibit similar ankle impairments. Overall, for both patients, the comparison with healthy subject and adaptation performance metrics support the use of vaulting gait compensation as no apparent changes

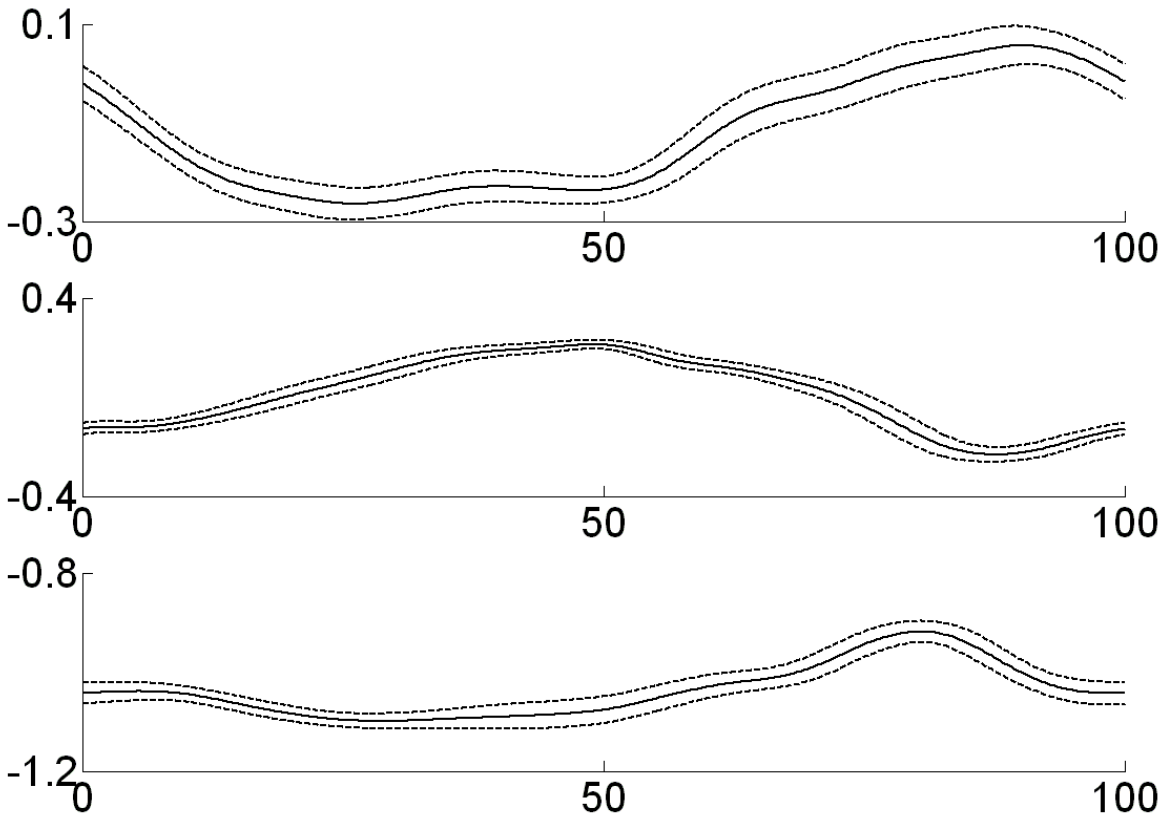

Figure 5.55: Patient #2 pelvis orientation Euler angles. Top - X-axis Euler angle. Middle – Y-axis Euler angle. Bottom – Z-axis Euler angle. The dark solid line is for the mean and the dashed line represents the standard deviation. The horizontal time axis represents gait cycle percentage and all angles are in radians.

resulting from steppage gait were seen with the patients.

For Patient #2, Figure 5.56 shows the GRF values for the right leg and Figure 5.57 presents the GRF plots for the left leg. The GRF data for the right leg (the non-affected limb) show a prolonged stance phase in the range of 75% of the gait cycle. Also, the right foot GRF does not feature the typical dual-peak force profile for healthy subjects. Instead, the force profile plateaus due to the slower transfer of weight over to the left foot and due to the slower walking speed of the patient (0.58 m/s). This is in agreement with the lower force valley during stance at slower speeds seen in the Experiment #1.

The peak force values appear to have similar ranges to those for the healthy subjects in Experiment #1. The initial spike in the right foot force profile is significantly higher for the patient than for the healthy subjects. This is most likely related to the limping gait imposed by the impairment causing a faster transition to right heel strike to shorten the left leg stance time. The shorter stance phase for the left leg is apparent in the GRF data in Figure 5.57.

The major distinction between the healthy and impaired gait is evident in the late stance phase force profile for the left leg. The lack of a positive force at this point demonstrates the patient's impaired ability to generate push-off force during toe-off. This is caused by the inability to generate significant torques about the ankle and the early lifting of the left foot to prematurely terminate the stance phase.

Table 5.3: Average (± std dev) performance metric values for Patient #2.

Trial	Right Leg	Left Leg
Stride Time	1.67±.060	1.67±.060
Stance %	77.8±2.04	68.7±2.74
Stride Length	0.97±.047	0.97±.036
Knee Flexion	0.83±.029	0.65±.042
Hip Extension	0.36±.025	0.38±.02
Hip Flexion	0.26±.017	0.27±.03
Ankle Toe Off	-0.31±.054	-0.14±.037
Ankle Heel Strike	-0.062±.033	-0.13±.031
Toe Clearance	.027±.005	.012±.009
Hip Height Stance	.976±.002	.964±.002
Hip Height Swing	.985±.003	.975±.002

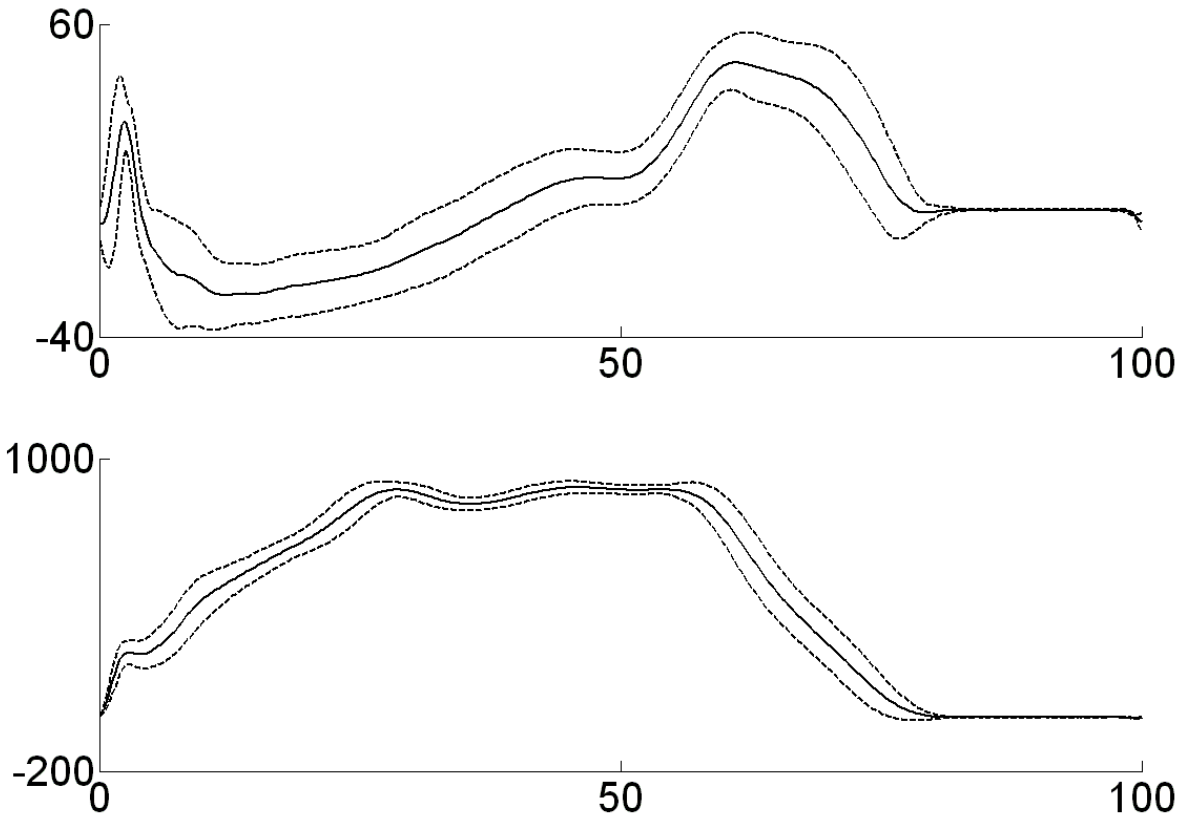

Figure 5.56: Average GRF values acting on the right foot of Patient #2. Top – Anterior posterior force. Bottom – Vertical force. The dark solid line is for the natural walking speed, the dashed line for the slow speed and the dotted line for the fast speed. The horizontal axis is the gait cycle percentage and the force values are in Newtons.

5.3.2 Inverse Dynamics Analysis

As the result of the GRF synchronization problem for Patient #1, the inverse dynamics analysis was performed for Patient #2 only. Figures 5.58-60 show the right leg, left leg and pelvis moment results respectively. Each plot shows the average +/- the standard deviation of the joints moments. The moment values have been normalized with respect to subject mass.

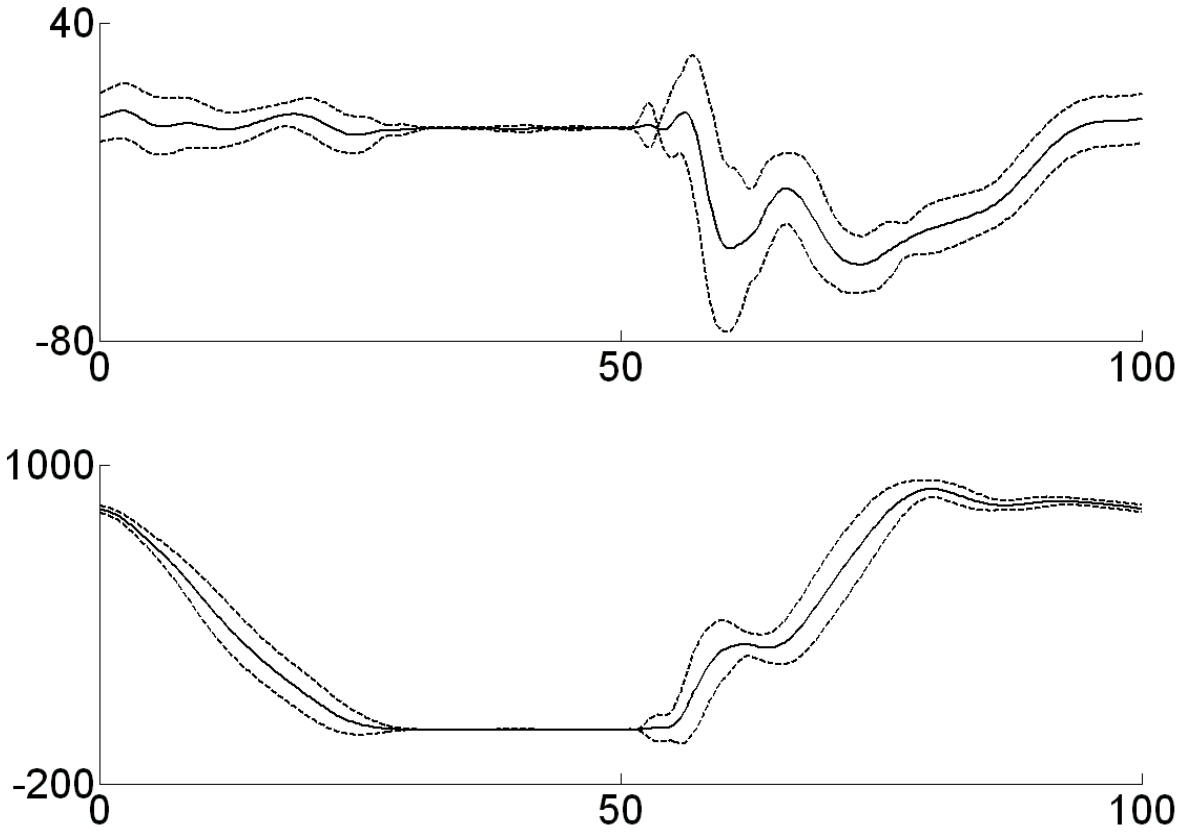

Figure 5.57: Average GRF values acting on the left foot of Patient #2. Top – Anterior posterior force. Bottom – Vertical force. The dark solid line is for the natural walking speed, the dashed line for the slow speed and the dotted line for the fast speed. The horizontal axis is the gait cycle percentage and the force values are in Newtons.

The right leg moments in Figure 5.58 exhibit the expected prolonged stance phase when compared with the natural walking speed of the healthy subjects in Experiment #1. This prolonged stance phase is the primary difference with the healthy subjects, though there is an apparent faster transition from the peak hip moment. This transition may be due to the faster swing phase transition.

The moments for the impaired left leg are significantly different from those of the healthy subjects from Experiment #1. Of particular note is the lower amount of knee extension following left heel strike. Also, throughout the right stance phase, the X-axis pelvis moment has significantly more

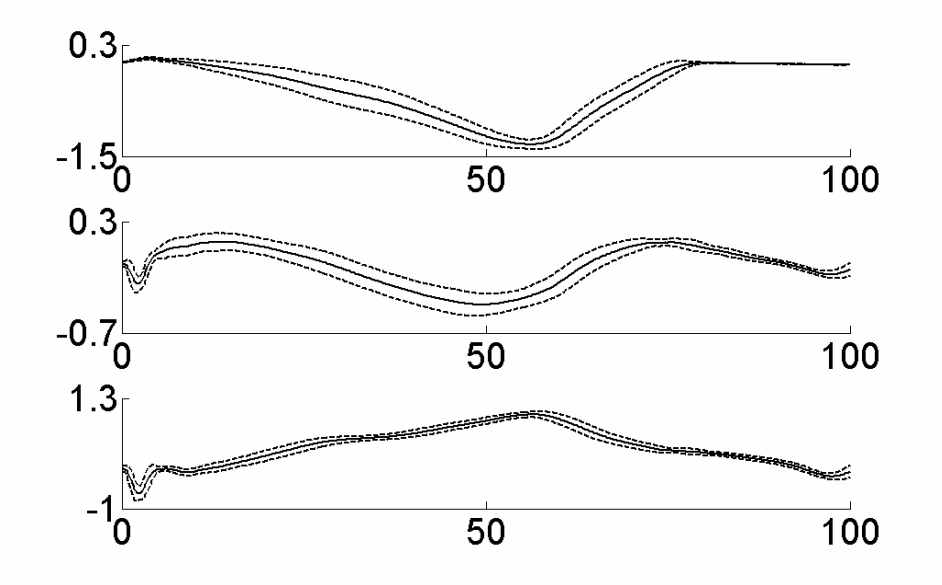

Figure 5.58: Right leg joint moments for Patient #2. Each subplot shows results for the ankle, knee and hip (top to bottom). For each trial, the plot shows the average as a solid line and the standard deviation shown by the dashed lines. The horizontal axes give gait cycle percentage and the vertical axes are the moments in Nm/kg (normalized by subject mass).

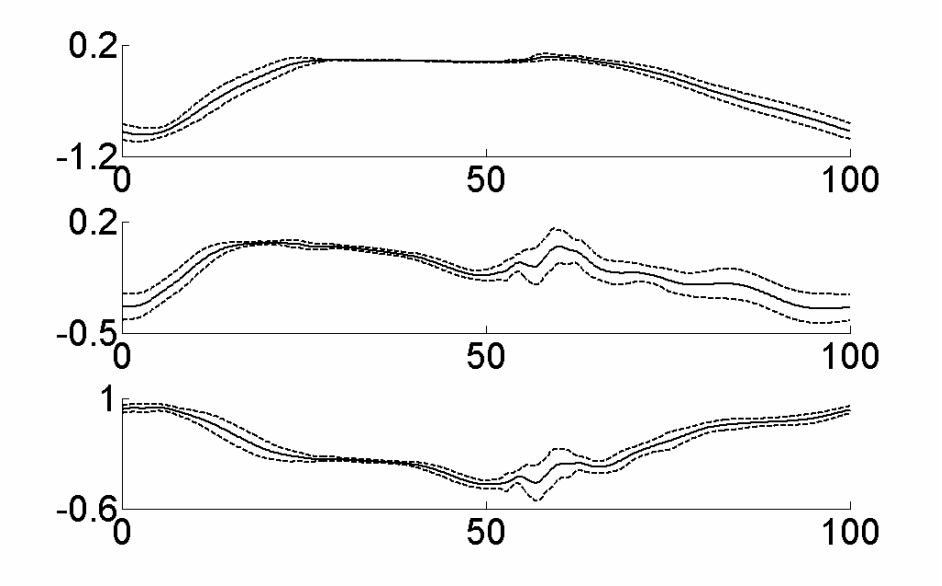

Figure 5.59: Left leg joint moments for Patient #2. Each subplot shows results for the ankle, knee and hip (top to bottom). For each trial, the plot shows the average as a solid line and the standard deviation shown by the dashed lines. The horizontal axes give gait cycle percentage and the vertical axes are the moments in Nm/kg (normalized by subject mass).

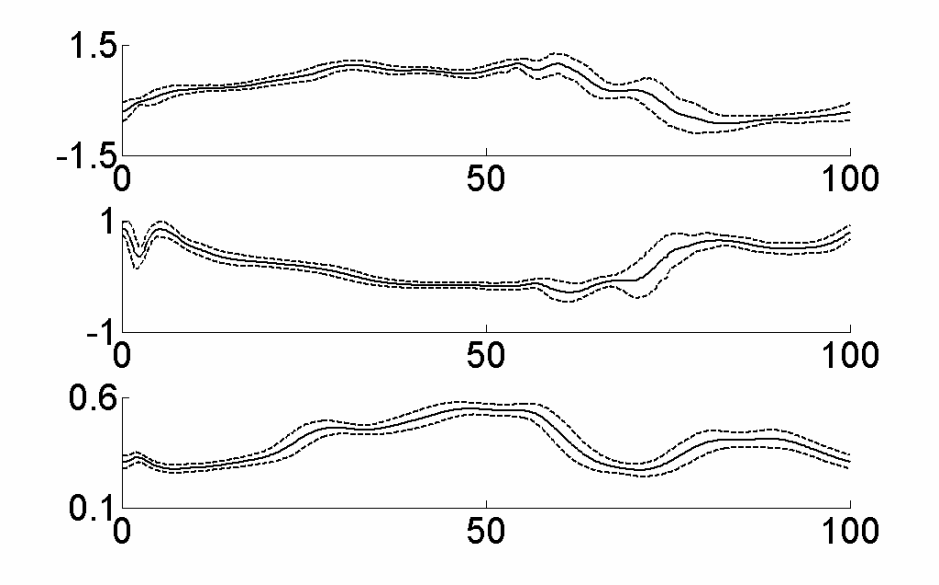

Figure 5.60: Pelvis moments for the Patient #2. Each subplot shows results for the X, Y and Z axis moments (top to bottom). For each trial, the plot shows the average as a solid line and the standard deviation shown by the dashed lines. The horizontal axes give gait cycle percentage and the vertical axes are the moments in Nm/kg (normalized by subject mass).

positive moments. These moments correspond to pelvis tilt lifting the left hip upwards to provide more opportunity for toe clearance. This positive moment to lift the hip on the impaired side matches the X-axis moment behaviour during the plantarflexion adaptation experiment. In the plantarflexion experiment the negative X-moment raised the hip on the simulated impairment side to allow more toe clearance.

Chapter 6: Discussion

6.1 Experiment #1

The kinematic results for the first experiment generally matched the expected kinematic results for changes in walking speed. The only significant deviation from the expected results is that the stride length decreased as walking speed increased. This is most likely due to the uncertainty people experience walking on a treadmill. Generally, when people are uncertain about their gait, they exhibit shorter strides, and even if subjects are given time to become accustomed to walking on a dual belt treadmill, there may still be some uncertainty in their gait. This uncertainty would increase as the speed of the treadmill increased and thus the decrease in stride length.

The stance phase inverse dynamic results agreed with the expected results in that higher moments were seen throughout the stance phase to support higher GRF values and to generate additional moments to progress the body of the stance leg faster and generate greater push-off forces. The inverse dynamics analysis however, did not show the expected swing phase changes due to a change in walking speed. Since the moments during the swing phase are significantly smaller than those during the swing phase may limit the applicability of the analysis to the swing phase. It may require additional analysis to determine if any relationships can be determined.

6.2 Experiment #2

The kinematic results seen during experiment # 2 generally agree with the expected results. As discussed in the Results chapter. For most of the inverse dynamics analysis, as for the first experiment, much of the expected swing phase results were not readily apparent in the results. As expected there was clear kinematic evidence supporting the theory of internal model formation. Subjects exhibited initial deviations from null trial performance at the start of the adaptation trial that returned to normal by

the end of the trial. Then at the start of the after-effect trial there were performance errors resulting from after-effects of the learned internal model. These after-effects tended to diminish within 20-25 strides which correlates well with previous research in the literature.

In some instance, the gradual adaptation expected during the adaptation trial was not seen and a steady state performance was seen throughout the entire trial. However, during the after-effect trial, there were after-effect errors exhibited. This supports the idea of the subjects predicting the effects of the task modification before starting the trial. This was to be expected to some degree with the task modifications employed in this work. Typical motor adaptation studies employ unpredictable forces (both in size and timing) that prevent subjects from knowing what modifications to expect. However, the subjects in this experiment were able to see the actual modification before the adaptation trial began.

Also, the nature of the AFO itself may have contributed to some of the observed analysis limitations. The AFO was not rigidly attached tot he subjects, as it was attached with Velcro straps that had some flexibility. Also, the AFO was molded from one subject and would not have fit all subjects exactly. These issues may have caused the subject's feet (and heel in particular) to move inside of the AFO. This may potentially hide joint moments generated by the subject since there foot may be moving while the reflective markers attached to the AFO appear to not be moving. Also, as mentioned previously, the use of gait modifications that were readily apparent to the subjects makes the study of their adaptation process potentially limited as well. Ideally, if one could study the same contracture simulations in a way that does allow the subject to know what will happen in advance should theoretically provide improved adaptation results.

Overall, the most significant inverse dynamics changes were seen during the locked plantarflexion experiment and the different tread speed experiment. The plantarflexion experiment inverse dynamics results clearly demonstrated pelvis moment changes as the result of adaptation to the

locked AFO. The pelvis moments lifted the hip on the affected side and propelled the hip forward faster to prepare for the next heel strike. These changes were expected and represent typical vaulting adaptations seen in patient populations.

6.3 Experiment #3

The kinematic results seen for the patients generally matched the expected kinematics for an impaired individual with drop foot walking at a slower tread speed. There was evidence of vaulting for both patients which supports the diagnosis given in his brief medical history. The kinematic results also support the drop foot impairment diagnosis because the adaptation experiment most similar to the kinematic performance metric results of the patients was having the AFO locked in a plantarflexed position.

The inverse dynamics analysis of Patient #2 demonstrated vaulting pelvis moments to raise the hip of the affected limb to allow for toe clearance as a compensation for the drop foot impairment. This behvaiour matched both the expected behaviour and that of the healthy subjects during the locked plantarflexion experiment. As with the kinematic results, the correlation with this experiment is of particular interest, since it was intended to simulate drop foot, particularly during the swing phase.

Chapter 7: Conclusions and Recommendations

7.1 Conclusions

The general results have achieved the goals set-out with the specific aims for this research. The study of healthy subjects walking at different speeds and under various gait impairment simulations (AFO contractures and asymmetric gait with two tread speeds) demonstrated kinematic evidence supporting the internal model view of motor adaptation as seen previously in the literature. The results were successful in characterizing the performance changes resulting from git adaptation. This included evidence for vaulting and steppage gait as compensations for simulated drop foot using an AFO locked in a plantarflexed position.

The inverse dynamic model that was developed was able to produce joint moment results that supported the typical leg joint moments seen for natural walking in Experiment #1. The use of this model to study the joint moment changes resulting from gait adaptation was successfully mostly for stance phase adaptations. Since stance phase moments are generally larger than those during swing phase, their relative changes due to adaptation were more easily discernible. The only swing phase adaptations that were clearly evident were the pelvis moments involved in the lifting of the impaired leg's hip during vaulting. The inverse dynamics analysis of the swing phase was not able to identify steppage gait patterns like the kinematic analysis.

The goal of comparing impaired patient gait adaptations with the adaptation experiments showed positive results for the vaulting exhibited by Patient #2. The pelvis moment vaulting patterns seen during the plantarflexed ankle experiment matched those seen in the patient's inverse dynamics analysis. While the matches adaptations were not exactly the same, they were in the same required directions and of comparable magnitudes. In fact, one would not expect to see the exact same adaptations, since the simulated impairment does not exactly match that of the subject and the healthy subjects are not exactly

the same height and weight as the patient. However, the result does show some initial promise with the idea that motor adaptation models may be useful for modeling impairments and rehabilitation in a simulated environment.

The experimental limitations apparent in this work include the AFO not being able to supply a completely rigid lock for the ankle and the ability of the subjects to predict the natures of the gait task modification. Both of these issues will have potentially affected the ability of the inverse dynamic model to make appropriate assessments of the impairments being simulated, since the motion data would have been in error.

7.2 Recommendations

In future, such research and experiments may be more fruitful if a more rigid AFO can be designed that is able to prevent subject motion with respect to the AFO as well as make it more difficult for the subjects to predict what the exact gait modification is going to be. Therefore, in future the researchers plan to investigate the development of an active AFO powered by servo motors or pneumatics that will be able to modify the ankle stiffness and viscosity or add inhibitory or assistive torques at very specific times during the gait cycle (ie: during push-off). If a rigid connection is achievable, such a device would provide much more flexibility in terms of potential experimental protocols for studying motor adaptation.

The specific data analyzed in this work should be studied further to determine if there are any indications of gait adaptations during the swing phase. This may include different visualization method, including separating the analysis of the stance and swing phase results entirely.

The stride-by-stride changes of the kinematic errors exhibited in the selected performance metrics should be related to the stride-by-stride change in peak torque levels. Such an analysis may lead to incremental rules for adjusting joint torques based on given performance criteria. This is the ultimate

goal in modeling the adaptation process; to develop a model that is able to take broad heuristic performance goals such as peak toe clearance, HAT segment orientation, thigh-to-knee torque ratios and infer the appropriate control changes required to adapt to any task modifications causing errors in these metrics.

Additionally, it may be beneficial to perform joint torque learning and adaptation studies on the upper limb. Such a system is much simpler to model and study and may provide insights into the underlying mechanisms that should be used when modeling adaptation during gait.

Finally, with regards to the data analysis aspects of this research, it is recommended that an improved method for tracking the reflective markers be found. While the Simi system provides a great deal of flexibility when tracking, filtering and analyzing motion data, the current tracking process can be very labour intensive and not conducive to gathering large gait adaptation data sets for inverse dynamics analysis.

References

[AmIT90] F. M. L. Amirouche, S. K. Ider and J. Trimble, “Analytical method for the analysis and simulation of human locomotion,” Journal of Biomechanical Engineering, vol. 112, pp. 379-386, 1990.

[Bert07] Bertec Corporation, Instrumented Treadmill User Manual, Columbus OH, 2007.

[BhSh99] N. Bhushan and R. Shadmehr, “Computational nature of human adaptive control during learning of reaching movements in force fields,” Biological Cybernetics, vol. 81, pp 39-60, 1999.

[BLMB04] T. S. Buchanan, D. G. Lloyd, K. Manal and T. F. Besier, “Neuromusculoskeletal modeling: Estimation of muscle forces and joint moments and movements from measurements of neural command,” Journal of Applied Biomechanics, vol. 20, pp. 367-395, 2004.

[CDGS02] S. E. Criscimagna-Hemminger, O. Donchin, M. S. Gazzaniga, and R. Shadmehr, “Learning dynamics of reaching movements generalizes from dominant to non-dominant arm,” Journal of Neurophysiology, vol. 89, pp. 168-176, 2002.

[ChBa07] J. T. Choi and A. J. Bastian, “Adaptation reveals independent control networks for human walking,” Nature Neuroscience, vol. 10, no. 8, pp. 1055-1062, 2007.

[CLBS00] G. Colombo, M. Joerg, R. Schreier and V. Dietz, “Treadmill training of paraplegic patients using a robotic orthosis,” Journal of Rehabilitation Research Devices, vol. 37, pp. 693-700, 2000.

[CoGM97] M. A. Conditt, F. Gandolfo and F. A. Mussa-Ivaldi, “The motor system does not learn the dynamics of the arm by rote memorization of past experience,” Journal of Neurophysiology, vol. 78, pp. 554-560, 1997.

[DoFS03] O. Donchin, J. T. Francis, and R. Shadmehr, “Quantifying generalization from trial-by-trial behavior of adaptive systems that learn with basis functions: Theory and experiments in human motor control,” Journal of Neuroscience, vol. 23, no. 27, pp. 9032-9045, October 2003.

[DoSh02] O. Donchin and R. Shadmehr, “Linking motor learning to function approximation: Learning in an unlearnable field,” In: Advances in Neural Information Processing Systems (T.G. Dietrich, S. Becker and Z. Ghahramani, eds.), vol. 14, pp. 197-203, Cambridge, MA: MIT, 2002.

[EBSB07] J. L. Emken, R. Benitez, A. Sideris, J. E. Bobrow and D. J. Reinkensmeyer, “Motor adaptation as a greedy optimization of error and effort,” Journal of Neurophysiology, vol. 97, pp. 3997-4006, 2007.

[EmRe03] J. L. Emken and D. J. Reinkensmeyer, “Evidence for an internal model dedicated to locomotor control,” Proceedings of the 25th International IEEE Engineering in Medicine and Biology Conference, Cancun, Mexico, pp. 1503-1506, Sept. 2003.

[EmRe05] J. L. Emken and D. J. Reinkensmeyer, “Robot-enhanced motor learning: Accelerating internal model formation during locomotion by transient dynamic amplification,” IEEE Transactions on Neural Systems and Rehabilitation Engineering, vol. 13, no. 1, pp. 33-39, 2005.

[EnWi95] J. J. Eng and D. A. Winter, “Kinetic analysis of the lower limbs during walking: what information can be gained from a three-dimensional model,” Journal of Biomechanics, vol. 28, no. 6, pp. 753-758, 1995.

[GiWi96] L. A. Gilchrist and D. A. Winter, “A two-part, viscoelastic foot model for use in gait simulations,” Journal of Biomechanics, vol. 29, no. 6, pp. 795-798, 1996.

[GiWi97] L. A. Gilchrist and D. A. Winter, “A multisegment computer simulation of normal human gait,” IEEE Transactions on Rehabilitation Engineering, vol. 5, no. 4, pp. 290-299, 1997.

[HaOb02a] K. Hase and G. Obinata, “Computer simulation study of human locomotion with a three-dimensional entire-body neuro-musculo-skeletal model (II. Biomechanical relationship between walking stability and neuro-musculo-skeletal system),” JSME International Journal Series C, vol. 45, no. 4, pp. 1051-1057, 2002.

[HaOb02b] K. Hase and G. Obuchi, “Computer simulation study of human locomotion with a three-dimensional entire-body neuro-musculo-skeletal model (III. Simulation of pathological walking and its application to rehabilitation engineering),” JSME International Journal Series C, vol. 45, no. 4, pp. 1058-1064, 2002.

[HaYa02] K. Hase and N. Yamazaki, “Computer simulation study of human locomotion with a three-dimensional entire-body neuro-musculo-skeletal model (I. Acquisition of normal walking),” JSME International Journal Series C, vol. 45, no. 4, pp. 1040-1050, 2002.

[HeJM75] H. Hemami, V. C. Jaswa and R. B. McGhee, “Some alternative formulations of manipulator dynamics for computer simulation studies,” Proceedings of the 13th Allerton Conference on Circuit Theory, Chicago, IL, October 1975.

[HLAA04] T. Hu, Z. Lin, M. F. Abel and P. E. Allaire, “Human gait modeling: Dealing with holonomic constraints,” Proceedings of the 2004 American Control Conference, Boston, MA, June 30 – July 2, pp. 2296-2301, 2004.

[Jaco97] R. Jacobs, “Control model of human stance using fuzzy logic,” Biological Cybernetics, vol. 77, pp. 63-70, 1997.

[JuMa88] M. Ju and J. M. Mansour, “Simulation of the double limb support phase of human gait,” Journal of Biomechanical engineering, vol. 110, pp. 223-229, 1988.

[KaWo98] M. Kawato and D. Wolpert, “Internal models for motor control,” Novartis Foundation Symposium, vol. 218, pp. 291-304, 1998.

[KNLS05] T. Komura, A. Nagano, H. Leung and Y. Shinagawa, “Simulating pathological gait using the enhanced linear inverted pendulum model,” IEEE Transactions on Biomedical Engineering, vol. 52, no. 9, pp. 1502-1512, 2005.

[KuSt99] L. I. Kuncheva and F. Steimann “Fuzzy diagnosis,” Artificial Intelligence in Medicine, vol. 16, pp. 121–128, 1999.

[LaAD06] T. Lam, M. Anderschitz and V. Dietz, “Contribution of feedback and feedforward strategies to locomotor adaptations,” Journal of Neurophysiology, vol. 95, pp. 766-773, 2006.

[LaWY03] T. Lam, C. Wolstenholme and J. F. Yang, “How do infants adapt to loading of the limb during the swing phase of stepping?,” Journal of Neurophysiology, vol. 89, pp. 1920-1928, 2003.

[Mack02] M. Mackay-Lyons, “Central pattern generation of locomotion: A review of the evidence,” Physical Therapy, vol. 82, no. 1, pp. 69-83, 2002.

[MaMS07] C. MacDonald, Z. Moussavi and T. Sarkodie-Gyan, “Formation of an internal model of environment dynamics during upper limb reaching movements: a fuzzy approach,” 29th IEEE Engineering in Medicine and Biology Conference, Lyon, France, August 23-26, 2007.

[MaSa09] C. MacDonald and T. Sarkodie-Gyan, “Gait phase detection using lower limb joint angles: a fuzzy relational matrix approach,” IEEE Transactions on Neural Systems and Rehabilitation Engineering (submitted), May 2009.

[Muss99] F. A. Mussa-Ivaldi, “Modular features of motor control and learning,” Current Opinion in Neurobiology, vol. 9, pp. 713-717, 1999.

[NgCh97] S. K. Ng and H. J. Chizeck, “Fuzzy model identification for classification of gait events in paraplegics,” IEEE Transactions on Fuzzy Systems, vol. 5, no. 4, pp. 536-544, 1997.

[NoPr06] J. W. Noble and S. D. Prentice, “Adaptation to unilateral change in lower limb mechanical properties during human walking,” Experimental Brain Research, vol. 169, pp. 482-495, 2006.

[OnWi80] S. Onyshko and D. A. Winter, “A mathematical model for the dynamics of human locomotion,” Journal of Biomechanics, vol. 13, pp. 361-368, 1980.

[PaBe89a] M. G. Pandy and N. Berme, “Quantitative assessment of gait determinants during single stance via a three-dimensional model. Part 1. Normal gait,” Journal of Biomechanics, vol. 22, pp. 717-724, 1989.

[PaBe89b] M. G. Pandy and N. Berme, “Quantitative assessment of gait determinants during single stance via a three-dimensional model. Part 2. Pathological gait,” Journal of Biomechanics, vol. 22, pp. 725-733, 1989.

[PaLY03] M. Y. Pang, T. Lam and J. F. Yang, “Infants adapt their stepping to repeated trip-inducing stimuli,” Journal of Neurophysiology, vol. 90, pp. 2731-2740, 2003.

[Popo00] D. B. Popovic, “Control of movements,” in Handbook of Biomedical Engineering, vol. II, J. Bronzino (editor), CRC Press, Boca Raton, FL, Chapter 165:1-20, 2000.

[Popo03] D. B. Popovic, “Control of walking in disabled humans,” Journal of Automatic Control, vol. 13 (supplement), pp. 5-32, 2003.

[PSOL99] D. Popovic, R. B. Stein, N. Oguztorelli and M. Lebiedowska, “Optimal control of walking with functional electrical stimulation: A computer simulation study,” IEEE Transactions on Rehabilitation Engineering, vol. 7, no. 1, pp. 69-79, 1999.

[ReHK06] L. Ren, D. Howard and L. Kenney, “Computational models to synthesize human walking,” Journal of Bionic Engineering, vol. 3, pp. 127-138, 2006.

[ReJH07] L. Ren, R. K. Jones and D. Howard, “Predictive modelling of human walking over a complete gait cycle,” Journal of Biomechanics, vol. 40, pp. 1567-1574, 2007.

[ScDM01] R. A. Scheidt, J. B. Dingwell and F. A. Mussa-Ivaldi, “Learning to move amid uncertainty,” Journal of Neurophysiology, vol. 86, pp. 971-985, 2001.

[ShMo00] R. Shadmehr and Z. M. K. Moussavi, “Spatial generalization from learning dynamics of reaching movements,” Journal of Neuroscience, vol. 20, no. 20, pp. 7807-7815, October 2000.

[ShMu94] R. Shadmehr and F. A. Mussa-Ivaldi, “Adaptive representation of dynamics during learning of a motor task,” Journal of Neuroscience, vol. 14, pp. 3208-3224, 1994.

[Simi07] Simi Motion Reallity Systems, Inverse Dynamics Manual, Munich, Germany, 2007.

[Taga95a] G. Taga, “A model of the neuro-musculo-skeletal system for human locomotion I. Emergence of basic gait,” Biological Cybernetics, vol. 73, pp. 97-111, 1995.

[Taga95b] G. Taga, “A model of the neuro-musculo-skeletal system for human locomotion II. Real-time adaptability under various constraints,” Biological Cybernetics, vol. 73, pp. 113-121, 1995.

[TaZP95] S. Tashman, F. E. Zajac and I. Perkash, “Modeling and simulation of paraplegic ambulation in a reciprocating gait orthosis,” ASME Journal of Biomechanical Engineering, vol. 117, pp. 300-308, 1995.

[ThAn06] D. G. Thelan and F. C. Anderson, “Using computed muscle control to generate forward dynamic simulations of human walking from experimental data,” Journal of Biomechanics, vol. 29, pp. 1107-1115, 2006.

[ThSh00] K. A. Thoroughman and R. Shadmehr, “Learning of action through adaptive combination of motor primitives,” Nature, vol. 407, pp. 742-747, 2000.

[TSMY00] Y. Tagawa, N. Shiba, S. Matsuo and T. Yamashita, “Analysis of human abnormal walking using a multi-body model: Joint models for abnormal walking and walking aids to reduce compensatory action,” Journal of Biomechanics, vol. 33, pp. 1405-1414, 2000.

[WiMD91] D. A. Winter, B. J. Mcfadyen and J. P. Dickey, “Adaptability of the CNS in human walking,” in Adaptability of human gait, A. E. Patla (Editor), Elsevier Science Publishers, North-Holland, pp. 127-144, 1991.

[Wint05] D. A. Winter, Biomechanics and Motor Control of Human Movement, Third Ed., John Wiley & Sons, Hoboken, NJ, 2005.

[Yard07] A. Yardimci, “Fuzzy logic based gait classification for hemiplegic patients,” 7th International Symposium on Intelligent Data Analysis, Ljubljana, Slovenia, pp. 344-354, September, 2007.

[YaWW90] J. F. Yang, D. A. Winter and R. P. Wells, “Postural dynamics of walking in humans,” Biological Cybernetics, vol. 62, pp. 321-330, 1990.

[YaZa90] G. T. Yamaguchi and F. E. Zajac, “Restoring unassisted gait to paraplegics via functional neuromuscular stimulation: A computer simulation study,” IEEE Transactions on Biomedical Engineering, vol. 37, no. 9, pp. 886-902, 1990.

[YeLa98] J. Yen and R. Langari, Fuzzy Logic: Intelligence Control and Information, Prentice Hall, Upper Saddle River, NJ 1998.

[Zade65] L. A. Zadeh, “Fuzzy Sets,” Information and Control, vol. 8, pp. 338-353, 1965.

[ZaNK02] F. E. Zajac, R. R. Neptune and S. A. Kautz, “Biomechanics and muscle coordination of human walking part I: Introduction to concepts, power transfer, dynamics and simulations,” Gait and Posture, vol. 16, pp. 215-232, 2002.

[ZaNK03] F. E. Zajac, R. R. Neptune and S. A. Kautz, “Biomechanics and muscle coordination of human walking part II: Lessons from dynamical simulations and clinical implications,” Gait and Posture, vol. 17, pp. 1-17, 2003.

[Zhou00] C. Zhou, “Neuro-fuzzy gait synthesis with reinforcement learning for a biped walking robot,” Soft Computing: A Fusion of Foundations, Methodologies and Applications, vol. 4, no. 4, pp. 238-250, 2000.

Appendix A: Experiment #1 IRB Protocol and Informed Consent

Research Proposal

I. Title: **Human Motion Analysis & Neurorehabilitation**

II. Investigators (co-investigators): **Dr. Thompson Sarkodie-Gyan**

III. Hypothesis, Research Questions, or Goals of the Project

The purpose of this study is to identify individual gait patterns during walking and/or running in humans by comparing kinetic and kinematic data including ground reaction forces, center of pressure, muscle activity and angular positions, velocities and accelerations of joints. These data will be used to develop a 'gait database' for motion analysis research.

IV. Background and Significance:

Locomotor disabilities are most commonly caused by neurological diseases or insult to the nervous system. Stroke survivors, for example, show marked decreases in their ability to ambulate 6 months post-insult, with 20% of them unable to walk without physical assistance and half of them walking at less than 50% of normal casual speed. These changes in mobility translate into a significant reduction in the patients' quality of life, and increase the burden of therapists and the health care system in treating these patients. Efforts to improve walking ability and efficiency have been undertaken, using rehabilitative strategies such as PWBTT to establish or re-initiate normal gait patterns in human subjects following injury [5-13]. The design of our Smart gait Rehabilitation System (SGRS) is based on data obtained through this type of training.

Recovery of locomotor activity following spinal cord injury has been extensively studied in animal models. Rats and cats that have undergone complete low-thoracic spinal cord transection can be trained to walk on a treadmill, and have been shown to accomplish full weight-bearing stepping at normal speeds [14, 15]. Other data suggest, however, that this type of training induces a motor task-specific kind of learning. For example, Hodgson et al. showed that spinalized cats trained to step were less able to stand and bear weight without the motion of walking, whereas animals trained to stand were deficient in their ability to walk on a moving treadmill [6, 17]. The re-establishment of ambulation following treadmill training may be due to the activation of central pattern generator (CPG) neurons in the spinal cord, in which locomotor-associated motor neuron pools are activated in response to sensory input coming from the limbs [18]. An important aspect of this behavior is that it occurs in the absence of supraspinal input. Crucial to the success of this training, therefore, is the coordination of sensory input to the spinal cord. The ability to step in both human and animal subjects is highly influenced by the pattern of loading placed on the legs and by the kinematics of the gait cycle [19].

Animal studies have led to the development of measures to assist human patients following spinal cord injury (SCI). Wernig et al. [9, 10] demonstrated a significant increase in the ability to ambulate independently or semi-independently following intensive PWBTT in people with incomplete spinal cord transections. Moreover, the positive effects of this intervention persisted for more than 6 years following training. In patients with complete SCI, Dietz et al. showed improved gait patterns as a result of treadmill training, possibly due to the normalization of muscle activation patterns [20]. In support of this idea, Harkema et al. recorded electromyographic (EMG) data in lower limb muscles during stepping in complete SCI patients, and showed that their ambulatory patterns were, in fact, regulated by sensory input to the lumbosacral spinal cord [21]. Results from both human and animal experiments, therefore, provide evidence that spinal cord CPGs can control locomotion, and that their activity is largely a function of

proprioceptive and other sensory inputs from the limbs. Step-related cues can thus alter CPG activity somewhat independently of higher central nervous system activation. Currently in progress is a multi-center, randomized clinical trial sponsored by the NIH/NICHD, investigating the response of patients with incomplete SCI to treadmill training (Dobkin et al at UCLA).

In addition to SCI, patients with brain injury or disease also have been shown to respond positively to PWBTT. One problematic variable in patients learning to walk after a neurological insult is that of maintaining balance during locomotion. The trunk stability provided by PWBTT allows for gait training, through the performance of repetitive and complicated motor activities, without the interference of vestibular reflexes. For example, adult hemiplegic stroke patients who failed to respond to traditional physical therapy interventions showed a 123% improvement in swing symmetry, with a 24% improvement in stance symmetry, after PWBTT [5]. These results were obtained in 25 training sessions carried out over 5 weeks, with the amount of body weight support provided decreasing from 31% to 0% (full weight-bearing) in 7 out of 9 patients. Further comparisons between subjects walking under different levels of body weight support versus normal overground ambulation showed that partial weight support provided the most efficacious circumstance for reducing spasticity, limiting co-contraction of antagonistic muscle groups, and producing appropriate gait patterns [6]. In another controlled study of partial compared to no body weight support in 100 patients, increased performance, as evidenced by positive outcomes in balance, speed, endurance and recovery was seen in the partially supported group following a 6-week treadmill training intervention [8]. Other investigations have resulted in rehabilitative success following PWBTT in stroke [38] and Parkinson's [39] patients.

Young people with neurological disorders also benefit from this type of training. In very young (15-28 months) children suffering from cerebral palsy, PWBTT increased locomotor skills according to both clinical measures and video gait analysis [12]. Similarly, cerebral palsy-afflicted children with minimal walking ability undergoing 3 months of PWBTT at a treatment rate of 3 times per week improved significantly in tests of general mobility, gross locomotor function and transfers [13]. Lastly, a case study by McNevin [11] on a 17-year-old female subject with spastic cerebral palsy showed a decrease in exercise-associated pulse rate and blood pressure, with a concurrent increase in ambulatory speed, as a result of treadmill training with about 30% body weight support.

Taken together, these studies convincingly demonstrate the ability of PWBTT to improve locomotor function in patients with central nervous system damage. This has not been the case, however, in all training interventions of this type. For example, two trials [22, 23] failed to produce improvements in overground ambulatory speeds in subjects exposed to treadmill training, but this may have been due to confounds in the experimental design (e.g., slow treadmill speeds during training, poor description of body weight support manipulations, and lack of data regarding the kinetics, kinematics and temporal symmetries during training). No training method has been published, in fact, that has been shown to be reproducible.

Frequently, fitness equipment has been adapted for use in therapy. Fitness machines like cross-country ski trainers, the Power Walker from Kettler, and the FM340 Skier from BioTrans are used for practising and training "gait-like" movements. These machines only provide a flat sliding motion of the foot and offer a poor representation of the human gait. The Miha Crosswalker (Miha GmbH), the Body Trainer (Reebok), and the Cross Trainer (Life Fitness) add a lifting of the foot (heel higher than the toe) during the swing phase of the gait, providing a "better" gait simulation, based on a 50/50 stance/swing gait cycle.

Going beyond the use of exercise equipment for gait therapy, the first PWBTT machines were simple in concept and design. They relied on the gait therapist to deliver the desired training gait to the patient, while they walked on the treadmill. This was accomplished through a "hands-on" method where the therapist held the patient's leg(s) and moved the limb(s) through the desired motion. Again, the patient's body weight was supported in a harness. Limitations of this approach are:

- it is highly labor intensive;

- the therapist must first learn and become proficient with the procedure and the motion to be given during treatment;
- repeatability and consistency in the gait motion delivered from session-to-session and patient-to-patient is difficult to maintain;
- multiple therapists are frequently needed for each patient in order to maintain proper positioning of the hips and upper / lower legs and joints;
- it is physically demanding on the therapist which limits the duration of each session, and demands a "recovery period" for the therapist(s).

To remedy the problems associated with using therapists to provide the desired gait patterns, some investigators, Uhlenbrock, Sarkodie-Gyan et al [24] and Hesse, Sarkodie-Gyan et al [25] developed gait trainers in which the individual's legs were positioned on foot plates that moved backward and forwards. Tests with non-ambulatory adults post-stroke adults were conducted using this device.

Current commercial robotic assistive devices automatically drive the limbs passively through preset gait cycles. The devices do not take into account the kinematics and torques that a subject can generate, or incorporate the subject's growing ability to ambulate. Actively guiding passive limbs during step training is not an effective strategy to enhance motor learning of a complex motor skill such as walking.

The restoration of healthy locomotion (gait) after stroke, traumatic brain injury, and spinal cord injury, is a major task in neurological rehabilitation. Motor-learning and control research clearly favors task-specific repetitive training [4]. The complexity of the interactions of the various components of human gait has been researched and documented extensively, and to date it is the experienced clinician who continues to perform functional gait assessment and training in the absence of virtually any technological assistance.

Hemiplegic stroke, paraparesis from spinal cord injuries, and other upper motor neuron syndromes such as multiple sclerosis and cerebral palsy cause serious neurological impairments and mobility-related disability. Approximately 700,000 Americans suffer a stroke, 10,000 suffer traumatic spinal cord injury, and over 250,000 are disabled by multiple sclerosis. Approximately 1 in 500 children [1] suffers from cerebral palsy, one of the most common chronic childhood disorders that often impair mobility [2]. With the aging of the U.S. population, the prevalence of people disabled by stroke is likely to rise over the next 10-20 years. Therefore, research efforts are needed to improve the effectiveness of rehabilitative treatments for sensorimotor disabilities, and especially for ambulation, balance, and maintenance of physical fitness across these neurologic diagnoses. With the 25-50% reduction in inpatient rehabilitation length of stay following stroke and spinal cord injury in the past 10 years and the decline in outpatient care days covered by insurers, efficacious and cost-effective interventions that positively impact the recovery of balance and walking have become critical [3].

Whereas the preponderance of data from clinical trials suggests that partial weight bearing treadmill training (PWBTT) increases the likelihood of independent overground walking and improvements in walking speed and walking distance in patients with acute and chronic stroke and spinal cord injury, the technique has clear limitations.

The physical demands on therapists to manually assist the trunk and legs of subjects at treadmill speeds greater than 0.8 mph is substantial, and the ability of therapists to optimize sensory inputs associated with the step cycle, such as kinematics and temporal symmetries during certain aspects of the stance and swing cycles, is constrained by all the various tasks they must simultaneously perform and monitor as they sit by the subject's legs. In order to relieve the therapist from having to perform numerous tasks simultaneously during a treatment session, robotic assistive devices have become a focus of clinical research.

We propose the development of a new method to deliver therapy to patients with gait disabilities unlike previous attempts such as partial weight bearing treadmill training (PWBTT). The Smart Gait Rehabilitation System (SGRS) will offer capabilities unavailable using current gait therapy devices and

methods. Step-training that incorporates sensory feedback, provides feedback about kinematics and torques, and proceeds at walking speeds typical of overground ambulation is more likely to drive basic mechanisms of motor learning and representational plasticity for the lower extremities [4]. Potential health benefits resulting from these capabilities include more effective and individualized therapy programs; the opportunity to lessen one of the most common disabilities in patients who suffer neurological diseases; reduce the time and labor needed to deliver therapy; and enhance gait-related diagnostic and research tools. To accomplish this, we will develop a mechanical device based on the concept of task-oriented Partial Weight Bearing Treadmill Training (PWBTT) along with an innovative knowledge-based control system that includes an intelligent sensing, a data acquisition, processing and effectuation scheme. The end result will be a therapy system that offers the patient, the doctor, and the therapist a new set of tools to test in clinical trials to improve gait therapy. The proposed device will also be well suited for use in gait diagnostic and clinical research efforts. For example, perturbations during the step cycle can be incorporated into the control scheme to test postural adjustments and evaluate mechanisms of motor control. Development of the feedback system may also lend itself to other devices for overground walking and for improving functional use of a paretic upper extremity.

We anticipate that the SGRS will assess efficacy and outcomes of medical rehabilitation therapies and practices, and also promote the patient's behavioral adaptation to functional losses. The device may be used in training research scientists in the field of medical rehabilitation, and offer more insight into further improvements in the development of assistive devices. The proposed development effort is structured to further develop a prototype, assess its safety in a trial phase, and set the ground work to assess its utility. The proposed development effort is structured to validate the claims including but not limited to:

- The SGRS will be able to offer both passive gait training and locomotor training with optimal feedback about kinematics and forces.
- The system will be safe for use in able-bodied adult subjects and in disabled adults who have a hemiparesis or paraparesis, across typical body sizes and leg lengths.
- The data acquisition and presentation capabilities of the SGRS will provide a more thorough understanding of gait data directly related to a patient's locomotor therapy during treadmill training.
- Data from able-bodied persons collected during SGRS testing will be similar to data gained from overground gait analysis.
- Data related to improved gait parameters during SGRS training of disabled subjects will be reflected in parallel improvements in overground walking as training progresses.
- The data gathering capabilities of the SGRS will improve the quality of data about pathological gait deviations during treadmill walking at normal casual walking speeds and provide objective data of outcome measures of change in individuals.

Hence, the SGRS will help address the main objectives of medical rehabilitation of the National Center for Medical Rehabilitation Research (NCMRR).

V. Research Method, Design, and Proposed Statistical Analysis:

Data collection will take place at the Human Motion Analysis & Neurorehabilitation Laboratory, located at the Electrical & Computer Engineering Department at UTEP. Healthy male and female subjects will be recruited from UTEP and the nearby community for the study. Each subject will complete an informed consent form after the testing procedures have been explained to them (see attachments). If the subject is under 18, a parental signature will be obtained on the informed consent form. Anthropometric measurements including height, weight, segmental length, width, depth and circumference will be obtained.

A. Kinematic Data, Ground Reaction Forces and Moment using SIMI and instrumented treadmill respectively

Reflective markers will be placed on the subject's joint centers to obtain kinematic data using the SIMI three-dimensional motion capture system. Each subject will be asked to perform practice walks a nd/or runs on an instrumented treadmill with built-in force plates for each foot. After the practice on the treadmill, each subject will walk and/or run on the treadmill for 5-10 minutes. The walking / running patterns will be videotaped for the purpose of qualitative and kinematic comparison. The estimated data collection time including preparation and warm-up will be about two hours per subject.

B. Kinematic Data using Electrical Sensors

The kinematic data can also be collected using Multi-axis sensors (Accelerometers – linear acceleration, Goniometers – angular position, and Gyroscopes – angular velocity) directly. These multi-axis sensors will be placed on the foot, shank, and thigh of each subject to measure the limb segment kinematics. The kinematic data collected from SIMI can be used to calibrate those sensors.

C. Muscle Activity (surface Electromyography – sEMG)

Electromyography (EMG) involves recording the electrical activity of muscles during walking and/or running. Surface EMG electrodes will be placed on multiple muscles of low-body of the subjects.

D. Data Processing

Three-dimensional ground reaction forces measured using the instrumented treadmill will be analyzed. The center of pressure will be calculated. Joint angles, velocities and accelerations will be computed using the SIMI motion analysis system, and can be used to calibrate the data derived from electrical sensors. Walking and /or running gaits for each individual will be analyzed using computer software (e.g. MatLab, Labview, and LifeMOD) for different proposes, i.e. feature extraction, intelligent diagnosis, rehabilitation strategies, knowledge-based database.

VI. Human Subject Interactions

A. Identify the sources of potential participants, derived materials, or data.

Both male and female subjects will be recruited. They may be students, staff or other personnel around the UTEP area. Subjects may be women, minorities and / or under the age of 21. The experiments will begin in May 2008 and end in December 2008.

B. Privacy and Confidentiality of participants

The data collected will be confidental. No names will be used as identifiers for the data or appear in presentations or publications. Some of the subjects may be asked to shave the part of their body hair prior to the experiment, since it will affect the markers and sensors atteching to the body surface. Subjects will have the right to deny participation at any time.

C. Describe the procedure for obtaining informed consent.

IRB approval and informed consent will be received prior to data collection. All UTEP research regulations will be observed. If the subject is under the age of 18, parental agreement and signaturewill be obtained in the informed consent prior to the testing. The proposed informed consent form is attached.

D. Confidentiality of the research data.

All data and video tapes will be locked in the researchers' office at UTEP and kept indefinitely. Only the researchers will have access to the data and the video tapes.

VII. Potential risks

Subjects may have delayed onset muscle soreness (DOMS) 24-48 hours after data collection. This soreness is likely to peak at 48-72 hours after the exercise bout and ease afterwards. This will not have any long-term effect on muscle function. Subjects will be informed about this potential muscle soreness. Subjects will be instructed to do a warm-up to reduce the risk of injuries and a cool-down to enhance recovery.

VIII. Potential benefits

The findings of this study will provide you with information about your walking and running gaits at constant speed with bare feet. These data will be used to develop a 'gait database' for future reference and research. Each participant will be provide some snacks and drink during the break of the experiment.

Literature Cited:

[1] Eicher PS, Batshaw ML: Cerebral Palsy. Pediatric Clinics of North America1993; 40(3):537-51.

[2] Kuban KC: Cerebral Palsy. New England Journal of Med. 1994; 330(3):188-95.

[3] B.H. Dobkin: The Clinical Science of Neurologic Rehabilitation. Oxford University Press, New York, 2003.

[4] Dobkin, B. H: Overview of treadmill locomotor training with partial body weight support: A neurophysiology sound approach whose time has come for randomized clinical trials. Neurorehabil and Neural Repair 13: 157-165, 1999.

[5] Hesse S, Bertelt C, Schaffrin A, et al: Restoration of gait in nonambulatory hemiparetic patients by treadmill training with partial body-weight support. Arch Phy Med Rehabil, 1994; 75:1087-1093.

[6] Hesse S, Konrad M, Uhlenbrock D, et al: Treadmill walking with partial body weight support versus floor walking in hemiparetic subjects. Arch Phys Med Rehabil1999; 80:421-427.

[7] Sullivan KJ, Dobkin BH, Tavakol M, et al: Post-stroke cortical plasticity induced by step training. Society for Neuroscience Proceedings 2001; 27.

[8] Visintin M, Barbeau H, Korner-Bitensky N, et al: A new approach to retain gait in stroke patients through body weight support and treadmill stimulation. Stroke, 1998; 28:1122-1128.

[9] Wernig A, Muller S, Nanassy A, et al: Laufband therapy based on rules of spinal locomotion is effective in spinal cord injured persons. Eur J Neurosci 1995; 7:823-829.

[10] Wernig A, Nanassy A, Muller S: Laufband (treadmill) therapy in incomplete paraplegia and tetraplegia. J Neurotrauma 1999; 16:719-726.

[11] McNevin NH, Coraci L, Schafer J: Gait in adolescent cerebral palsy: the effect of partial unweighting. Arch Phys Med Rehabil 2000; 81 :525-528.

[12] Richards CL, Malouin F, Dumas F, et al: Early and intensive treadmill locomotor training for young children with cerebral palsy: a feasibility study. Pediatr Phys Ther 1997; 9:258-265.

[13] Schindl MR, Forstner C, Kern H, et al: Treadmill training with partial body weight support in nonambulatory patients with cerebral palsy. Arch Phys Med Rehabil 2000; 81 :3001-3006.

[14] Barbeau H, & Rossignol S: Recovery of locomotion after chronic spinalization in the adult cat. Brain Res 1987; 412:84-95.

[15] Lovely RG, Gregor RJ, Roy RR, et al: Effects of training on the recovery of full weight-bearing stepping in the adult spinal cat. Exp Neuro11986; 92:421-435.

[16] Hodgson JR, Roy, RR, deLeon R, et al: Can the mammalian lumbar spinal cord learn a motor task? Med Sci Sports Exerc, 1994; 26:1491-1497.

[17] Lovely RG, Gregor RJ, Roy RR, et al: Weight-bearing hindlimb stepping in treadmill-exercised adult cats. Brain Res 1990; 514:206-218.

[18] Muir GO, Steeves JD: Sensorimotor stimulation to improve locomotor recovery after spinal cord injury. Trends Neurosci 1997; 20:72-77.

[19] Duysens, Dietz; Duysens J, Pearson, K: From cat to man: basic aspects of locomotion relevant to motor rehabilitation of SCI. NeuroRehabilitation 1998; 10:107-118.

[20] Dietz V, Colombo G, Jensen L, et al: Locomotor capacity of spinal cord in paraplegic patients. Ann Neurol 1995; 37:555-556.

[21] Harkema SJ, Hurley SL, Patel UK, et al: Human lumbosacral spinal cord interprets loading during stepping. J Neurophysiol1997; 77:797-811.

[22] Kosak M, Reding, M: Comparison of partial body weight-supported treadmill gait training versus aggressive bracing assisted walking post stroke, Neurorehabil Neural Repair 2000; 14: 13-19.

[23] Nilson, L, Carlsson, J, Danielsson, A, et al: Walking training of patients with hemiparesis at an early stage after stroke: a comparison of walking training on a treadmill with body weight support and walking training on the ground. Clinical Rehab 2002; 15: 515-527.

[24] Uhlenbrock, D., Sarkodie-Gyan, T., Reiter, F., Konrad, M., Hesse, S., (1997), "Development of a servo-controlled gait trainer for the rehabilitation of non-ambulatory patients," Biomed Tech, Vol. 7-8, 42, pp. 196-202.

[25] Hesse, S, Uhlenbrock, D, Sarkodie-Gyan, T, (1999) "Gait pattern of severely disabled hemiparetic subjects on a new controlled gait trainer as compared to assisted treadmill walking with partial body weight support, " Journal Clinical Rehabil, 13, pp. 401-410.

[26] Rowe, P.J., Nicol, A.C., Kelly, I.G., Flexible goniometer computer system for assessment of hip function, Clinical Biomechanics 1989, 4: 68-72.

[27] Troke, M., Moore, A.P., Ckeek, E., Reliability of the OSI CA 6000 spine motion analyzer with a new skin fixation system when used on the thoracic spine. Manual Therapy, 1998, 3: (1) 27-33.

[28] Cosgrove, A.P., Graham, H.K., Mollan, R.A.B., Gait analysis in children with cerebral palsy using electrogoniometers, Presentation, British Orthopaedic Research Meeting, 1991.

[29] Myles, C., Rowe, P.J., Salter, P., Nicol, A., An electrogoniometer system used to investigate the ability of the elderly to ascend and descend stairs, Physiotherapy 1995, 81 (10): 640.

[30] Hazelwood, M.E., Rowe, P.J., Salter, P.M., The use of electrogoniometers as a measurement tool for passive movement and gait analysis, Physiotherapy, 1995, 81 (10): 639.

[31] Sullivan, K., Knowlton, B., Dobkin, B.: Step training with body weight-support: Effect of treadmill speed and practice paradigms on post-stroke locomotor recovery, Arch Phys Med Rehab, 2002, 83: 683-691.

[32] Clinical Guidelines on the Identification, Evaluation, and Treatment of Overweight and Obsesity in Adults. National Institutes of Health, National Heart, Lung and Blood Institute, June, 1998.

[33] Winter, D.A., Biomechanics and motor control of human movement (2nd Ed.), 1990, New York, John Wiley and Sons.

[34] D. Uhlenbrock: "Construction and evaluation of a servo-controlled gait trainer for early gait rehabilitation in non-ambulatory stroke patients" M.S. Thesis University of Teesside, UK, April 1997.

[35] Dietmar Uhlenbrock; "An advanced biomedical gait training machine for the rehabilitation of non-ambulatory stroke patients based on computer-aided human motion analysis," Ph.D. Thesis, University of Teesside, UK, April 1999.

[36] Sarkodie-Gyan, T., Jamshidi, M., Sensor-fusion based intelligent robot planning algorithm, Proc. IMEKO conf. On Knowledge based Measurement-Application, Research and Education, Germany, 1990, pp.295-302.

[37] Sarkodie-Gyan, T., Jamshidi, M., Dev. of a prototype robot task planning algorithm using sensor fusion, Proc. 3rd Int. Symp. In robotics and manufacturing, Canada, 1990, ASME press, pp. 155-160.

[38] da Cunha, I.T. Jr., Lim, P.A., Qureshy, H., Henson, H., Monga, T., & Protas, E.J., Gait outcomes after acute stroke rehabilitation with supported treadmill ambulation training: a randomized controlled pilot study. Ach Phs Med & Reha, 2002, 83, 1258-65.

[39] Miyal, I., Fujimoto, Y., Yamamoto, H., Ueda, Y., Saito, T., Nozaki, S., & Kang, J., Long-term effect of body weight-supported treadmill training in Parkinson's disease: A randomized controlled trial, Arch Phys Med & Rehab, 2002, 83, 1370-1373.

[40] Dawson, M., Sarkodie-Gyan, T., Provincialli, L., Hesse, S., Gait initiation, development of a measurement system for use in the clinical environment, Biomed. Technik, 1996, 41, pp. 213-217.

[41] Stefan Hesse, Dietmar Uhlenbrock et al, A mechanized gait trainer for restoration of gait, Journal of Rehabilitation Research and Dev., 2000, Vol. 37, No.6

[42] D. Uhlenbrock, S. Hesse, T. Sarkodie-Gyan: Development of an advanced mechanized gait-trainer, controlling movement of the center of mass, for restoration of gait in non-ambulatory subjects, Journal of Biomed. Technik, 1999, Band 44, Heft 7-8, pp. 194-201.

[43] Jensen, K.J: Diagnostics of Human Locomotion, M.S. Thesis, New Mexico Institute of Mining and Technology, Department of Mechanical Engineering, Mechatronics Program, 2005

[44] Amyyotrophic Lateral Sclerosos Fact Sheet. National Institute of Neurological Disorder and Stroke, 9/28/2004, http://www.ninds.nih.gov/health_and_medical/pubs/als.htm?format=printable

[45] Sarkodie-Gyan, T. 2nd Annual Bioengineering Technology Seminar, ASME Continuing Education Institute, 2004: Course Director

[46] Sarkodie-Gyan, T. Biomedicine Miniaturization, April 5-8, 2005, Irvine, California; ASME Continuing Education Institute, 2005: Course Director.

[47] Vaughan, C.L., Davis, B.L., O'Connor, J.C. (1992) "Dynamics of Human Gait", 2nd Ed., Kiboho Publishers, Cape Town, South Africa.

[48] Lung-Wen T, Robot Analysis: The Mechanics of Serial and Parallel Manipulators. New York, NY: John Wiley, 1999.

[49] Niku S.B., Introduction to Robotics: Analysis, Systems, and Applications. Upper Saddle River, NJ: Prentice Hall, 2001.

[50] Sarkodie-Gyan, T. (2005) "Neurorehabilitation Devices: Engineering Design, Measurement, and Control", McGraw-Hill Companies, Inc. New York, Chicago, London, Madrid, Mexico City, Milan, New Delhi, Seol, Singapore, Sydne, Toronto; ISBN: 007-144830-6.

[51] Amirouche, F.M., Ider, S.K., Trimble, J. (1990) "Analytical Method for the Analysis and Simulation of Human Locomotion", Journal of Biomechanical Engineering, Nov. 1990, vol. 112, pp. 379-386.

[52] Ramakrishnan, H.K., Kadaba, M.P. (1991) "On the Estimation of Joint Kinematics during Gait", J. Biomechanics, vol. 24, No. 10, pp. 969-977.

53] Cappozzo, A. (1991) "The mechanics of human walking", in Adaptability of Human Gait., A Patla (Hrsg.), No. 78; North-Holland Elsevier Science Publishers B.V., Amsterdam, pp. 167-186.

[54] Yen, V., Nagurka, M.L. (1987) "Biomechanics of normal and prosthetic gait", ASME Winter Annual Meeting (Boston, Dec. 1987), pp. 17-22.

[55] R. E. Moore, Interval Analysis, Prentice Hall, 1966.

[56] J. Jaffar and M. Maher, Constraint Logic Programming: a Survey, Journal of Logic Programming, vol. 19/20, pp. 503-581, 1994.

[57] H. Collavizza, F. Delobel and M. Rueher, Comparing Partial Consistencies, Reliable Computing, vol. 5, pp. 1-16, 1999.

[58] F. Benhamou, Interval Constraint Logic Programming, in Constraint programming: basics and trends, Springer-Verlag, 1994.

[59] M. Ceberio and F. Modave, Interval-based Multi-Criteria Decision Making, in the proceedings of AI+MATH'04, 2004.

[60] M. Ceberio and F. Modave, An Interval-valued, 2-additive Choquet Integral for Multi-Criteria Decision Making, in the proceedings of IPMU 2004.

[61] S. A. Starks, V. Kreinovich, L. Longpre, M. Ceberio, G. Xiang, R. Araiza, J. Beck, R. Kandathi, A. Nayak and R. Torres, Towards Combining Probabilistic and Interval Uncertainty in Engineering Calculations, in the Proc. of the NSF Workshop on Reliable Eng. Computing, pp. 193-213, 2004.

[62] M. Ceberio, V. Kreinovich, L. Longpre, E. Saad, B. Ludascher, C. Baral and H. T. Nguyen, Affine Arithmetic-Type Techniques for Handling Uncertainty in Expert Systems, with Applications to Geoinformatics and Computer Science, in the Proceedings of the 11th GAMM-IMACS International Symposium on Scientific Computing, Computer Arithmetic, and Validated Numerics, 2004.

[63] Hesse, S., Werner, C., v. Frankenberg, S., Bardeleben, A. (2003) "Treadmill training with partial weight support after stroke," Phs Med Rehabil Clin N Am 2003, 14: 111-123.

[64] Werner, C., v. Frankenberg, S., Treig, T., Konrad, M., Hesse, S. (2002) "Treadmill Training with partial body weight support and an electromechanical gait trainer for restoration of gait in subacute stroke patients," Stroke 2002; 33: 2895-2901

[65] Hesse, S. (2001) "Locomotor therapy in neurorehabilitation," NeuroRehabilitation 2001; 16:1-7.

[66] Hesse, S., Werner, C., Uhlenbrock, D., v. Frankenberg, S., Bardeleben, A., Brandl-Hesse, B. (2001) "An electromechanical gait trainer for restoration of gait in hemiparetic stroke patients: preliminary results," Neurorehabilitation and Neural Repair 2001; 15: 39-50.

[67] Hesse, S., Uhlenbrock, D., Werner, C., Bardeleben, A. (2000) " A mechanized gait trainer for restoring gait in non-ambulatory subjects," Arch Phys Med Rehabil 2000; 81: 1158-1162.

[68] Uhlenbrock, D., Sarkodie-Gyan, T., Reiter, F., Konrad, M., Hesse, D. (1997) "Entwicklung eines Gangtrainers mit geregeltem Servoantrieb zur Rehabilitation gehunfaehiger Patienten," Biomed. Technik 1997; 42: 196-202.

[69] Hesse, S., Sarkodie-Gyan, T., Uhlenbrock, D. (1999) "Development of an advanced mechanized Gait Trainer, controlling movement of the centre of mass, for restoring gait in non-ambulant subjects," Biomed. Technik 1999; 44:194-201.

[70] Hesse, S., Uhlenbrock, D., Sarkodie-Gyan, T. (1999) "Gait pattern of severely disabled hemiparetic subjects on a new controlled gait trainer as compared to assisted treadmill walking with partial body weight support," Clinical Rehabilitation 1999; 13:401-410.
[71] Hesse, S., Uhlenbrock, D. (2000) "A mechanized Gait Trainer for restoration of gait," Journal Rehab Res Dev 2000; 376): 701-708.
[72] Jensen, K., Sarkodie-Gyan "The Paradigm of a Smart Gait Emulator," Proceedings of the 2004 Japan-USA Symposium on Flexible Automation, Denver, CO, July 19-21, 2004.
[73] Jensen, Kirt, Sarkodie-Gyan, "Experimental Investigations on a Gait Emulator for Neurological Rehabilitation," World Automatic Control Congress, Proceedings, WAC Seville, Spain, 2004.
[74] " Spring Element for the Insert at Treadmill Training," German Patent DE 197 25 972 C1
[75] "First Prototype of a Gait Trainer," German Patent DE 197 25 973 C2
[76] "Gait Training Machine," German Patent DE 198 05 164
[77] W. Mitchell Parks (2002) "Smart gait Emulator Project," Interim Report, New Mexico Institute of Mining and Technology, Department of Mechanical Engineering, August 2002.
[78] W. Mitchell Parks, Angela Tipton, Kirt Jensen, Glorianna Grado, Jason Kemp, Michael Jackson (2002) "Smart gait Emulator Design/Construction ," Interim Report, New Mexico Institute of Mining and Technology, Department of Mechanical Engineering, October 2002
[79] Jason Paschis, Justin Stolworthy, James Stauder, Nick Jacka, Erin Gulley (2003) "Smart Gait Emulator," Final Report, New Mexico Institute of Mining and Technology, Department of Mechanical Engineering, December 2003.
[80] Nick Jacka, James Stauder, Justin Stolworthy (2004) "Smart gait Emulator," Final Report, New Mexico Institute of Mining and Technology, Department of Mechanical Engineering, May 10, 2004.
[81] Justin Stolworthy, James Stauder, Nick Jacka, Josh Kern (2005) "Smart Gait Emulator," Final Report, New Mexico Institute of Mining and Technology, Department of Mechanical Engineering, Spring 2005.

University of Texas at El Paso (UTEP) Institutional Review Board

Informed Consent Form for Research Involving Human Subjects

Protocol Title: Human Motion Analysis and Neurorehabilitation

Principal Investigator: Thompson Sarkodie-Gyan, Ph.D.

UTEP : Department of Electrical and Computer Engineering

Introduction

You are being asked to take part voluntarily in the research project described below. Please take your time making a decision and feel free to discuss it with your friends and family. Before agreeing to take part in this research study, it is important that you read the consent form that describes the study. Please ask the study researcher or the study staff to explain any words or information that you do not clearly understand.

Why is this study being done?

You have been asked to take part in a research study to identify individual gait patterns during walking and running.

Approximately, 100 study subjects will be enrolling in this study at UTEP. You are being asked to be in the study because you are a male or a female over the age of 18. If you decide to enroll in this study, your involvement will last about one week.

What is involved in the study?

If you choose to participate in this study, you will report to the Human Motion Analysis and Neurorehabilitation Laboratory, Room E313B, in the Engineering Building. You will need to wear proper workout attire. We will also measure your height, weight, segmental length, width, depth and circumference. A warm-up consisting of stretching and light jogging will be performed.

You will be asked to walk and/or run on an instrumented treadmill at constant speed with bare foot. The force platform built in the treadmill will measure the forces exerted on you during walking and running. Reflective markers will be placed on your joint centers to facilitate analysis of your gait patterns. Trials will be videotaped for the purpose of the movement analysis and comparison.

You will also be asked to place three different multi-axis sensors (accelerometers, goniometers, and gyroscopes) on the surface of the lower limb, and will repeat the same experiment as above to collect the kinematic data.

At the same time, you will be asked to wear electromyographic (EMG) electrodes, to measure the dynamic activities of the muscles during walking and/or running.

You may be asked to shave the hairs of the part your body prior to the experiment, since it will affect the markers and sensors attachment to the body surface.

The estimated data collection time including preparation and warm-up will be approximately two hours.

What are the risks and discomforts of the study?

The potential risks that may occur with participating in this research include those associated with exercise testing. The potential risks associated with running include muscle fatigue and muscle strain. There is also a risk of local muscle and/or joint soreness following any exercise. The soreness is likely to peak at 2-3 days after the exercise bout and ease afterwards. A warm-up period will decrease the likelihood of injury and soreness. A research team member will advise you on cool-down stretching exercises to minimize muscle soreness. You are free to stop the exercise procedure at any time.

What will happen if I am injured in this study?

The University of Texas at El Paso and its affiliates do not offer to pay for or cover the cost of medical treatment for research related illness or injury. No funds have been set aside to pay or reimburse you in the event of such injury or illness. You will not give up any of your legal rights by signing this consent form. You should report any such injury to (Dr. Thompson Sarkodie-Gyan, Phone Number: 915-747-7011) and to Lola Norton of the Institutional Review Board (IRB) at UTEP at (915-747-8841) or lola@utep.edu.

Are there benefits to taking part in this study?

There will be no direct benefits to you for taking part in this study.

The findings of this study will provide you with information about your walking and running gaits at constant speed with bare feet. These data will be used to develop a 'gait database' for future reference and research. Each participant will be provide some snacks and drink during the break of the experiment.

This research may help us to understand the variations in gait with respect to gender and body mass index.

What other options are there?

As a volunteer in this study, you have the option not to take part in the study or to withdraw from the study at any time. If you do not take part in the study, there will be no penalty whatsoever.

Who is paying for this study?

Internal Funding:

Funding for this study is provided by UTEP Department of Electrical and Computer Engineering, and the UTEP NSF Advance.

External funding:

UTEP and Dr. Thompson Sarkodie-Gyan are receiving funding from the NSF Advance and from the ECE department to conduct this study.

What are my costs?

There are no direct costs. You will be responsible for travel to and from the research site and any other incidental expenses.

Will I be paid to participate in this study?

Participation is voluntary. You will not be paid for taking part in this research study.

What if I want to withdraw, or am asked to withdraw from this study?

Taking part in this study is voluntary. You have the right to choose not to take part in this study. If you do not take part in the study, there will be no penalty.

If you choose to take part, you have the right to stop at any time. However, we encourage you to talk to a member of the research group so that they know why you are leaving the study. If there are any new findings during the study that may affect whether you want to continue to take part, you will be told about them.

The researcher may decide to stop your participation without your permission, if he or she thinks that being in the study may cause you harm.

Who do I call if I have questions or problems?

You may ask any questions you have now. If you have questions later, you may call insert Dr. Thompson sarkodie-Gyan; Phone Number 915-747-7011, Email: tsg@ece.utep.edu.

If you have questions or concerns about your participation as a research subject, please contact Lola Norton of the Institutional Review Board (IRB) at UTEP at (915-747-8841) or by email at lola@utep.edu.

What about confidentiality?

1. Your part in this study is confidential. None of the information will identify you by name. Only you and individuals directly involved in this research will have access to your results. All data collected in this study will be coded by subject number rather than by name and will be kept in a locked file in Room E313B for 5 years. Only the researchers and/or the research assistants will have access to the data. The results will be used for scholarly publications or presentations but you will not be identified.

2. Every effort will be made to keep your information confidential. Your personal information may be disclosed if required by law. Organizations that may inspect and/or copy your research records for quality assurance and data analysis include, but are not necessarily limited to:

The sponsor or an agent for the sponsor

Department of Health and Human Services

UTEP Institutional Review Board

Because of the need to release information to these parties, absolute confidentiality cannot be guaranteed. The results of this research study may be presented at meetings or in publications; however, your identity will not be disclosed in those presentations.

Mandatory reporting

If information is revealed about child abuse or neglect, or potentially dangerous future behavior to others, the law requires that this information be reported to the proper authorities.

Authorization Statement

I have read each page of this paper about the study (or it was read to me). I know that being in this study is voluntary and I choose to be in this study. I know I can stop being in this study without penalty. I will get a copy of this consent form now and can get information on results of the study later if I wish.

Participant Name: _____ Date: _____

Participant Signature: _____ Time: _____

Participant Signature: _____

Consent form explained/witnessed by: _____

Signature

Printed name: _____

Date: Time:

Appendix B: Experiment #2 IRB Protocol and Informed Consent

Research Proposal

I. Title

Human motor adaptation to changes in gait task dynamics

II. Investigators (co-investigators)

Chad MacDonald, M.Sc.
Thompson Sarkodie-Gyan, Ph.D.

III. Hypothesis, Research Questions, or Goals of the Project

The purpose of this research is to experimentally determine how subjects will adapt to changes in task dynamics during walking. In particular, modifications to the dynamics of the subject's body and modifications to the dynamics of the environment will be studied.

The hypothesis is that subjects will adapt to the task modifications and that this adaptation will result in improved performance. Additionally, it is hypothesized that this adaptation will have correlates in the subject's electromyographic signals (EMG) that are related to the subject's adaptation strategy.

IV. Background and Significance:

The human motor system is very adaptable and robust when it comes to experiencing new environments. One task that has been of particular interest is that of upper limb reaching movements. Researchers have used a robotic manipulandum [1] [2] to exert varying types of perturbing forces to a subject's movement to try and understand the characteristics of the motor system. Shadmehr and Mussa-Ivaldi, demonstrated that when adapting to a novel dynamic environment, the human central nervous system, CNS, generates an internal model, IM, of the environment [3]. This model is then used to generate a series of feed-forward predictive commands to actively compensate for the forces experienced. Since then, much other work has been performed to understand different features of this internal model. For example, [4] and [5] studied how learning generalizes from one environment to another.

While this adaptation has been studied in detail for upper-limb reaching movements, there has been less focus on adaptation during gait. Specific aspects of gait adaptation have been studied previously. In [6] the adaptation of subjects subjected to an externally applied force field was studied. Specifically, this study focused on how adaptation affected step height. In [7] adaptation to modified leg dynamics was studied. In [8], adaptation to different treadmill speeds for each leg was analyzed to study adaptation to changes in environmental task dynamics. However, in this previous work, a detailed model of the adaptation process has not been created. The goal of this work is to collect experimental data that can be used to develop such a model.

[1] I.C. Faye, *An impedance controlled manipulandum for human movement studies* (S.M. Thesis, MIT, Department of Mechanical Engineering, Cambridge, MA, 1986).

[2] C. MacDonald, S. Balakrishnan and Z. Moussavi, "Development of a low-cost robotic manipulator and its application to human motor control studies," *Proc. IASTED Conference on Control and Applications*, May 2006.

[3] R. Shadmehr & F.A. Mussa-Ivaldi, Adaptive representation of dynamics during learning of a motor task, *Journal of Neuroscience, 14*(5), 1994, 3208-3224.

[4] R. Shadmehr & Z.M.K. Moussavi, Spatial generalization from learning dynamics of reaching movements, *Journal of Neuroscience,*(20),2000, 7807-7815.

[5] K.A. Thoroughman and R. Shadmehr, "Learning of action through adaptive combination of motor primitives," *Nature*, vol. 407, pp. 742-747, October 2000.

[6] J.L. Emken and D.J. Reinkensmeyer, "Robot-enhanced motor learning: Accelerating internal model formation during locomotion by transient dynamics amplification," *IEEE Transactions on Neural Systems and Rehabilitation Engineering*, vol. 13, no. 1, pp. 33-39, March 2005.

[7] J.W. Noble and S.D. Prentice, "Adaptation to unilateral change in lower limb mechanical properties during human walking," *Experimental Brain Research*, vol. 169, pp. 482-495, 2006.

[8] J.T. Choi and A.J. Bastian, "Adaptation reveals independent control networks for human walking," *Nature Neuroscience*, vol. 10, no. 8, pp. 1055-1062, August 2007.\

V. Research Method, Design, and Proposed Statistical Analysis:

Research Methodology and Design:

The research methodology was designed to determine the nature of human motor adaptation during walking. In particular, the experimental conditions were selected to study adaptation to changes in the ankle range of motion. Specifically, an Ankle Foot Orthosis (AFO) will be applied to limit the range of motion of the subject's right foot. Also, in order to study the effect of changes in gait timing, other subjects will be asked to walk on a dual-belt treadmill with both treads going at different speeds.

The null condition, disturbed condition, after-effect condition protocol emulates previously used protocols for motor adaptation studies. The null condition records the performance of the subject with no task modification. The disturbed condition records how the subjects perform with a modified task. The performance is tracked to determine any changes resulting from the subject adaptation. The after-effect condition records the subject's performance after the disturbance is removed. The performance is analyzed to determine any after-effects of the adaptation process.

Research Protocol:

The specific research protocol used is outlined in Section *VI.D.* below.

Data Analysis:

The kinematic data will be collected using an eight-camera motion capture system (Simi Reality Motion Systems, Munich, Germany). Each camera records two-dimensional video of reflective markers attached to specific anatomical locations of the subject. From these recordings the three-dimensional position, velocity and acceleration of the markers can be determined. The ground

reaction forces will be recorded using an instrumented treadmill (Bertec Corporation, Columbus, OH). This treadmill provides three-dimensional force and moment data. The EMG data will be recorded using a 16-channel wireless EMG system (Delsys Inc., Boston, MA).

The recorded data will be used to determine kinematic, ground reaction force and EMG correlates of motor adaptation. The kinematic and ground reaction force data will display any performance changes resulting from the disturbance and the adaptation process. The EMG data will be analyzed to determine how muscle activity changes during the adaptation process. The performance during the null, disturbed and after-effect conditions will be compared to determine the significance of any differences between the trial performances. The average performance across all subjects will be analyzed to determine the consistency of the adaptation process.

The kinematic and ground reaction force data will be used as input data for the design of a model to simulate human walking. The adaptation process will be modeled using fuzzy logic and the simulated adaptation/gait model will be compared to the experimental results. Half of the experimental data will be used to design the models and the other half of the data will be used to verify the model performance.

The data may also be analyzed using the LifeMOD simulation software (LifeModeler Inc, San Clemente, CA) to verify the models mentioned above. This software provides detailed biomechanical simulations given kinematic data as input.

VI. Human Subject Interactions

A. Sources of potential participants,

This study will seek to recruit 30-40 participants. Potential participants will be students from UTEP aged from 18 to 30. Subjects will be limited to those with no known motor or balance impairments. Subjects will all have a similar shoe size to allow for the use of a single AFO. Efforts will be made to select subjects with similar height and weight. Also, due to size restrictions for the AFO, subjects will be limited to males with a shoe size from 9 to 10.

B. Procedures for the recruitment of the participants.

Subjects matching the above requirements will be recruited directly by the principal investigator. Volunteers may be solicited from the UTEP community by the co-investigators listed above. Potential subjects will be asked if they would like to participate in a human walking study and whether they have no movement or balance impairments. Any subject answering in the affirmative to these questions will participate in the study.

C. Procedure for obtaining informed consent.

Subjects will be given the opportunity to review the informed consent form (see attached) and to ask any questions they may have. Subjects will indicate their consent to participate in the study by signing the same informed consent form.

D. <u>Research Protocol</u>.

***Location and Informed Consent*:**

Data collection will take place at the Human Motion Analysis & Neurorehabilitation Laboratory, located at the Electrical & Computer Engineering Department at UTEP. Each subject will complete an informed consent form after the testing procedures have been explained (see attached).

Subject Preparation:

Subjects will be asked to change into the spandex sports clothing provided. Males will be asked to wear shorts only and females will wear shorts along with a top. Subjects will change in E313B during which time the experimenters will wait outside of the lab to give the subject privacy. After changing clothes, the subjects will be given the opportunity to do some light jogging and light stretching to reduce any potential for muscle strains during the experiment.

The subjects will then have their anthropometric data measured and recorded. This will include height, weight and segment measurements (length, width and circumference).

This will be followed by the attachment of the EMG electrodes to the muscles of the lower limbs. The EMG procedure involves shaving the hair where the electrode must be placed and cleaning the surface using alcohol. Once the electrodes have been attached, the quality of the EMG signals will be verified and adjustments made as needed.

This will be followed by placing reflective markers on the participant's body using a standard configuration (see attached). Each reflective marker will be attached using double-sided tape to specific anatomical locations.

Experiment:

The subjects will then be given an explanation of the specific experiment protocol with emphasis on safety. They will be advised to use the safety bars in the event that they feel they are going to fall during the experiment.

For each of the experimental trials, the reflective markers will be used in conjunction with an eight-camera motion capture system to collect the participant's three-dimensional kinematic data. The treadmill used in this experiment is instrumented to record the three-dimensional ground reaction force data (forces and moments) for the trial.

The experiment is divided into eight stages as outlined below:

Speed Determination (AFO subjects only): The natural walking speed of the subject is determined by having the subjects self-select the speed at which they usually walk.

Treadmill Learning: The subjects will get used to walking on the treadmill by walking at 15% greater than their self-selected natural walking speed (AFO subjects) or 1 m/s (non-AFO subjects) for three minutes. No data will be collected during this trial.

Static Trial: The subject will be recorded standing on the treadmill with their arms out at shoulder level and their feet shoulder width apart.

Null Condition: The subjects will be recorded for one minute walking at the same speed as the Treadmill Learning stage.

AFO Learning (AFO subjects only): The treadmill learning stage will be repeated with subject wearing the AFO. The AFO will not be set to limit the subject range of motion.

AFO Static Trial (AFO subjects only): The Static Trial will be repeated with the AFO, since it will change the relationships between the reflective markers on the right foot.

AFO Null Condition (AFO subjects only): The Null Condition stage will be repeated with the subject wearing the AFO. Again, the AFO will not be set to limit the range of motion of the subject.

Disturbed Condition: This stage follows the Null Condition stage. The subject will be subjected to a gait task modification and recorded walking for three minutes. Each modification will be used for 2-4 subjects. The gait task modification will be selected from the list below. Subjects in the AFO trials will not be told beforehand which type of modification is being applied.

> Different Tread Speeds – The left tread will be moving at 0.65 m/s and the right tread will be moving at 1.35 m/s.
>
> AFO Limiting Plantarflexion – The AFO will be set to limit the amount of downward flexion. The plantarflexion will be limited to 0°, 10° or 20°.
>
> AFO Limiting Dorsiflexion – The AFO will be set to prevent the foot from flexing upward. The dorsiflexion will be limited to 0° or 10°.
>
> Rigid AFO – The AFO will be set to a given angle and the ankle will not be permitted to flex in either direction. Several ankle locations will be used throughout the range of motion (Neutral, Dorsiflexed 10°, Plantarflexed 10°, Plantarflexed 20°).

After-Effect Condition: This stage follows immediately after the Disturbed Condition stage. The modification will be removed and the subject will be recorded walking undisturbed for three minutes.

Wrap-Up:

After the perturbed trials, the reflective markers will be removed from the subject and they will be given the opportunity to perform some light stretching (particularly of the calf muscles) to prevent potential muscle soreness. The experimenters will give the subject an opportunity to ask any additional questions they have regarding the nature of the experiment and what the data will be used for. This question period is mostly provided as an educational opportunity for subjects who may be interested in the field of biomechanics and motion analysis. The experimenters will then leave the room allowing the subject to change out of the sports clothes provided.

E. <u>Privacy and confidentiality of participants</u>

To protect the privacy of the subject, during the experiment only the two experimenters will be present in the lab.

All of the data collected will be stored with no reference to the subject name to protect the confidentiality of the participant. The subject will be assigned a unique identifier that will appear with the data. The only association of a subject with a specific identifier will be the signed informed consent, which will be stored in a locked cabinet in the office of Dr. Thompson Sarkodie-Gyan. The subject's name will not appear in any presentations or publications resulting from this research.

F. Confidentiality of the research data.

All data collected in this study will be coded by subject number rather than by name and will be stored on a server in Room E313B of the Engineering Building for an indefinite period of time. Only the researchers and/or the research assistants will have access to the data on this server.

The video recorded during this study will be stored along with the extracted data. The videos will not be destroyed in order to allow for future potential analyses. This may include the visual verification of the extracted motion data or the extraction of additional motion variables. As with the extracted data, the subject's name will not appear on the recorded video.

G. Research resources

The research will take place in the Laboratory for Human Motion Analysis and Rehabilitation in E313B Engineering. This research space contains the instrumented treadmill and eight-camera motion capture system required for this study. Each experiment will last for 2-3 hours. The research space is dedicated for the recording and analysis of experimental data and will be available for the required time periods. The experiments will be performed by the principal investigator along with the assistance of 3-5 research assistants. For any given experiment, there will be two researchers present with the subject.

VII. Potential risks

The potential risks that may occur with participating in this research include those associated with exercise testing. The potential risks associated with any human motion studies include muscle fatigue and muscle strain. There is also a risk of local muscle and/or joint soreness following any exercise. In particular, the calf muscle and ankle joint may experience soreness. This soreness is likely to peak at 2-3 days after the exercise bout and ease afterwords. A warm-up period will decrease the likelihood of any such injury and soreness.

The walking task modifications and treadmill speeds have been selected such that the risk of falling is reduced, however, since this research focuses on perturbed walking, there is a risk of falling during the modified trials. The treadmill system has safety bars for the subject to hold in the event of a loss of balance.

VIII. Potential benefits

There will be no direct benefits or compensation for the participants. There is a potential educational benefit for any participants who are interested in how motion analysis works.

The potential benefits to society include a further understanding of human motor control and adaptation. This understanding will include the development of a model of human walking and adaptation that will be a useful tool for simulating rehabilitation scenarios. This improved understanding also has potential application in the fields of prosthetics and robotics.

IX. Sites or agencies involved in the research project

N/A

X. Review by another IRB

N/A

University of Texas at El Paso (UTEP) Institutional Review Board
Informed Consent Form for Research Involving Human Subjects

Protocol Title: Human motor adaptation to changes in gait task dynamics

Principal Investigator: Chad MacDonald, M.Sc., Thompson Sarkodie-Gyan, Ph.D.

UTEP: Department of Electrical and Computer Engineering

Introduction

You are being asked to take part voluntarily in the research project described below. Please take your time making a decision and feel free to discuss it with your friends and family. Before agreeing to take part in this research study, it is important that you read the consent form that describes the study. Please ask the study researcher or the study staff to explain any words or information that you do not clearly understand.

Why is this study being done?

You have been asked to take part in a research experiment to study motor adaptation during walking. Approximately, 20 to 40 study subjects will be enrolling in this study at UTEP. You are being asked to be in the study because you are a male between the ages of 18 and 30 with no known movement or balance impairments. If you decide to enroll in this study, your involvement will last 2 to 3 hours.

What is involved in the study?

If you agree to take part in this study, the research team will ask you to change into appropriate work-out attire (spandex sports shorts) A warm up consisting of light jogging and stretching will be performed. Your height, weight and segmental length, width, depth and circumference will be measured. Reflective markers will be placed on your body to facilitate analysis of your motion data. The analysis involves videotaping the trials and studying the locations of the markers in the recorded video. You will have EMG electrodes placed on your legs. The EMG recording requires shaving the hair from the mounting locations on the leg..

The walking trials will be performed on a treadmill system. You will be given an opportunity to get used to walking on the treadmill. After this, you will be asked to walk for three trials (one minute, three minutes, three minutes). These trials will follow immediately after each other with no rest period between them. The first and third trials will be regular unmodified walking. For the second trial, you will be asked to walk under the modification indicated below:

___ The treads will be run at two different speeds.

___ An ankle foot orthosis will be mounted on your foot to affect the range of motion of the ankle.

What are the risks and discomforts of the study?

The potential risks that may occur with participating in this research include those associated with exercise testing. The potential risks associated with any human motion studies include muscle fatigue and muscle strain. There is also a risk of local muscle and/or joint soreness following any exercise. In particular, the calf muscle and ankle joint may experience soreness. This soreness is likely to peak at 2-3 days after the exercise bout and ease afterwards. The warm-up and stretching periods will decrease the likelihood of injury and soreness. You are free to stop the exercise procedure at any time.

The walking task modifications and treadmill speeds have been selected such that the risk of falling is reduced, however, since this research focuses on perturbed walking, there is a risk of falling during the modified trials. The treadmill system has safety bars for you to hold in the event of a loss of balance and the treadmill is equipped with an emergency safety stop.

What will happen if I am injured in this study?

The University of Texas at El Paso and its affiliates do not offer to pay for or cover the cost of medical treatment for research related illness or injury. No funds have been set aside to pay or reimburse you in the event of such injury or illness. You will not give up any of your legal rights by signing this consent form. You should report any such injury to Chad MacDonald at (915) 747-7081 and the Institutional Review Board Office at (915) 747-8841 or irb.orsp@utep.edu.

There will be no direct benefits to you for taking part in this study. This research will help us to understand how the central nervous system adapts to changes in walking task dynamics. The data will be used to develop models of gait and adaptation to help study both healthy and impaired gait.

What other options are there?

You have the option not to take part in this study. There will be no penalties involved if you choose not to take part in this study.

Who is paying for this study?

Funding for this study is provided by the UTEP Department of Electrical Engineering and by the UTEP Graduate School.

What are my costs?

There are no direct costs. You will be responsible for travel to and from the research site and any other incidental expenses.

Will I be paid to participate in this study?

You will not be paid for taking part in this research study.

What if I want to withdraw, or am asked to withdraw from this study?

Taking part in this study is voluntary. You have the right to choose not to take part in this study. If you do not take part in the study, there will be no penalty. If you choose to take part, you have the right to stop at any time. However, we encourage you to talk to a member of the research group so that they know why you are leaving the study. If there are any new findings during the study that may affect whether you want to continue to take part, you will be told about them. The researcher may decide to stop your participation without your permission, if he or she thinks that being in the study may cause you harm.

Who do I call if I have questions or problems?

You may ask any questions you have now. If you have questions later, you may contact Dr. Thompson Sarkodie-Gyan at (915) 747-7011 or by email at tsg@ece.utep.edu. You may also contact Chad MacDonald at (915) 747-7081 or by email at cemacdonald@miners.utep.edu.

If you have questions or concerns about your participation as a research subject, please contact the Institutional Review Board Office at (915) 747-8841 or irb.orsp@utep.edu.

.

What about confidentiality?

Your part in this study is confidential. None of the information will identify you by name. Only you and individuals directly involved in this research will have access to your results. The results may be used for scholarly publications and/or presentations but you will not be identified. All data collected in this study will be coded by subject number rather than by name and will be kept on a secure server in Room E313B Engineering for an indefinite period of time. The indefinite time period is required to allow for future potential analyses that may be required. Only the researchers and/or the research assistants will have access to the data.

Every effort will be made to keep your information confidential. Your personal information may be disclosed if required by law. Organizations that may inspect and/or copy your research records for quality assurance and data analysis include, but are not necessarily limited to:

- The sponsor or an agent for the sponsor
- Department of Health and Human Services
- UTEP Institutional Review Board

Because of the need to release information to these parties, absolute confidentiality cannot be guaranteed. The results of this research study may be presented at meetings or in publications; however, your identity will not be disclosed in those presentations.

Authorization Statement

I have read each page of this paper about the study (or it was read to me). I know that being in this study is voluntary and I choose to be in this study. I know I can stop being in this study without penalty. I will get a copy of this consent form now and can get information on results of the study later if I wish.

Subject ID: _____

Participant Name: _____

Participant Signature: _____

Date: _____ Time:_____

Consent form explained/witnessed by:

Printed name: _____

Signature: _____

Date: _____ Time:_____

Appendix C: Experiment #3 IRB Protocol and Informed Consent

Research Protocol

I. Title: Development of an Assessment for Functional Recovery after Neurological Disorders and Peripheral Nerve Transfers

II. Investigators (co-investigators): Dr. Thompson Sarkodie-Gyan

III. Hypothesis, Research Questions, or Goals of the Project

This study is the extension of the previous approved one, "**Human Motion Analysis & Neurorehabilitation**" whose approved deadline extends to June 2009. The purpose of the previous study was to develop a 'gait database or knowledge-base' among healthy able-bodied subjects. The purpose of this extension study is to design a novel cerebral evaluation methodology for peripheral nerve transfer system for substitution surgery transfer and also to identify other neurological impairments with gait abnormalities secondary to upper motor neuron injury. This intelligent system is proposed to facilitate the objective diagnosis and treatment based on the laboratory measurement of kinematics, kinetics, somatosensory evoked potentials, nerve conduction, and electromyographic (EMG) data collection.

IV. Background and Significance

Chronic diseases, such as arrhythmias, stroke, multiple sclerosis, congestive heart failure, cancer, arthritis, chronic respiratory diseases and diabetes, are leading causes of morbidity and mortality in the world, representing 60% of all deaths. Hemiplegic post-stroke, paraparesis from spinal cord injury, and other secondary upper motor neuron syndromes frequently cause serious mobility-related disabilities. Stroke survivors, for example, show marked decreases in their ability to ambulate 6 months post-insult, with 20% of them unable to walk without physical assistance and half of them walking at less than 50% of normal casual speed. These changes in mobility translate into a significant reduction in the patients' quality of life, and increase the burden of therapists and the health care system in treating these patients. Efforts to improve walking ability and efficiency have been undertaken, using rehabilitative strategies such as PWBTT to establish or re-initiate normal gait patterns in human subjects following injury.

Functional recovery of locomotor activity following spinal cord injury has been extensively studied in animal models. Rats and cats that have undergone complete low-thoracic spinal cord transaction can be trained to walk on a treadmill, and have been shown to accomplish full weight-bearing stepping at normal speeds [14, 15]. The re-establishment of ambulation following treadmill training may be due to the activation of central pattern generator (CPG) neurons in spinal cord, in which locomotor-associated motor neuron pools are activated in response to sensory input coming from the limbs [18]. The ability to step in both human and animal subjects is highly influenced by the pattern of loading placed on the legs and by the kinematics of the gait cycle [19].

The concept of neural plasticity includes not only synaptogenesis and dendritic branching, but also neurogenesis, a relatively novel aspect of structural regeneration. Neurogenesis occurs in the adult mammalian central nervous system (CNS) following the migration and differentiation of the neural stem cells. The majority of these cells reside in one of two germinal zones: the subventricular zone (SVZ) in the wall of the lateral ventricles and the subgranular zone (SGZ) of the hippocampus [48]. It has been reported that voluntary exercise increases SGZ cell proliferation and neurogenesis [80]. The authors from [81] used some specific antibodies markers such as 5-bromo-2'-deoxyuridine (BrdU), double cortin (Dcx), neuronal nuclei (NeuN), and glial fibrillary acidic protein (GFAP) to find evidence of cell proliferation and neurogenesis. These antibodies are currently the most widely used techniques for studying adult nerogenesis in situ despite some limitations. These data importantly suggest an association between physical exercise and neurogenesis. However, clinically applied physical therapy for chronic gait disorders is an enforced, scheduled, non-voluntary form of exercise that is fundamentally different from the proposed experimental voluntary exercise protocols.

The restoration of healthy locomotion (gait) after stroke, traumatic brain injury, and spinal cord injury, is a major task in neurological rehabilitation. Motor-learning and control research clearly favors task-specific repetitive training [4]. The complexity of the interactions of the various components of human gait has been researched and documented extensively, and to date it is the experienced clinician who continues to perform functional gait assessment. Computerized assessments that involve sophisticated kinematic and kinetic analyses have not been applied widely in clinical assessments of gait disorders. Instead, a set of functional gait-related tests (such as usual and maximal gait speed, 6-Minute walk test, long-distance corridor walk, gait abnormality rating scale –GARS, timed up and go test, and performance-oriented mobility assessment - POMA) have been widely used as semi-quantitative assessments.. Compared to computerized assessments, these are easy to perform, do not require expensive equipments and long testing time. However, those semi-quantitative assessments could not accurately detect the optimal rehabilitation and evaluation of treatment effects.

A major limitation of the computerized assessment is lack of the knowledge to perform and analyze the acquired data from those instrumented equipment. A novel intelligent instrumented gait analysis system is proposed to facilitate the objective diagnosis and treatment based on the laboratory measurement of kinematics, kinetics, nerve conduction device, and electromyographic (EMG) data. It will assist physicians and therapists to gain adequate knowledge of the patient and disease characteristics that determine functional outcome. This research will increase knowledge of basic mechanisms of motor learning and representational plasticity for the lower extremities and for the maximal recovery for digital nerve transfers. Potential health benefits resulting from these capabilities include more effective and individualized therapy programs; the opportunity to lessen one of the most common disabilities in patients who suffer neurological diseases; a reduction in the time and labor needed to deliver therapy; and an enhancement of gait-related diagnostic and research tools.

V. Research Method, Design, and Proposed Computerized Analysis
Participants

Participants

Both male and female patients with gait abnormality secondary to upper motor neuron injury, and subjects with injuries following nerve transfers will be recruited as subjects from within the

community. Each subject will complete an informed consent form after the testing procedures have been explained to them.

Clinical Specialists Support

Clinical doctors, nurses, neurologists, or physical therapists from Texas Tech University Medical School will accompany their respective subjects throughout the data collection. A harness is readily available to support the patient's weight.

Kinematic Data, Ground Reaction Forces and Moment using SIMI and instrumented treadmill respectively

Reflective markers will be placed on the subject's joint centers to obtain kinematic data using the SIMI three-dimensional motion capture system. Each subject will be asked to practice walking both overground and on an instrumented treadmill with built-in force plates for each foot. After the practice on the treadmill, each subject will walk on the treadmill for up to 3 minutes. The walking patterns will be videotaped for the purpose of qualitative and kinematic comparison. The estimated data collection time including preparation and warm-up will be about two hours per subject.

Kinematic Data using Multi-axis Sensors

The kinematic data may also be collected using Multi-axis sensors (Accelerometers – linear acceleration, Goniometers – angular position, and Gyroscopes – angular velocity) directly. These multi-axis sensors will be placed on the head, trunk, foot, shank, and thigh of each subject to measure the upper and lower body segment kinematics. The kinematic data collected from SIMI can be used to calibrate those sensors since they will be collected simultaneously. Cortical, sciatic nerve action and lumbar potentials will be recorded as somatosensory evoked potentials.

Muscle Activity Measurement (surface Electromyography – sEMG)

Electromyography (EMG) involves recording the electrical activity of muscles during walking and/or running. Surface EMG electrodes will be placed on multiple muscles of low-body of the subjects.
Needle EMG and EEG devices will be used on the subjects for data collection. The medical doctors in this project will be responsible for the needle EMG including and also for the activation of certain nerves for somatosensory evoked potentials.

Data Processing

Three-dimensional ground reaction forces measured using the instrumented treadmill will be analyzed. The center of pressure will be calculated. Joint angles, velocities and accelerations will be computed using the SIMI motion analysis system, and can be used to calibrate the data derived from electrical sensors. 3-D data for each individual will be analyzed using computer software (e.g. MatLab, Labview, and LifeMOD) for feature extraction, intelligent diagnosis, rehabilitation strategies of gait disorders.

VI. Human Subject Interactions

- **Identify the sources of potential participants, derived materials, or data**

Both male and female patients with gait abnormality secondary to upper motor neuron injury and subjects with nerve transfers will be recruited as subjects from within the community. Subjects may be women and/or minorities. The anthropometric data such as subject's height, weight, segment length/circumference/depth will be measured. The experiments are expected to begin in May 2009 and end in June 2010.

- **Procedures for the recruitment of the participants**

Patients will be recruited from local community. Patients will be excluded if they had severe cognitive impairment (unable to follow simple directions), nursing home residents, or refused to participate. To characterize more functional and neurophysiologic status of the subject population, factors that might contribute to gait disorders, as described below, and factors that have been associated with those impairments will be also included in the evaluation:

- Subject's age, gender, level of formal education as well as health status, mental status, self-rated quality of life, functional status, muscle strength, balance, and gait.
- Marker of health status includes: Body Mass Index (BMI), number of prescription medications.
- Physical activity levels will be estimated prior to be recruited as subjects.

- **Describe the procedure for obtaining informed consent**

IRB approval and informed consent will be received prior to data collection. All UTEP research regulations will be observed. If the subject is under the age of 18, parental agreement and signature will be obtained in the informed consent prior to the testing. The proposed informed consent form is attached.

- **Privacy and Confidentiality of participant**

The data collected will be confidential. No names will be used as identifiers for the data or appear in presentations or publications. Some of the subjects may be asked to shave the part of their body hair prior to the experiment, since it will affect the markers and sensors atteching to the body surface. Subjects will have the right to deny participation at any time.

- **Confidentiality of the research data**

All data and video tapes will be locked in the researchers' office at UTEP and kept indefinitely. Only the researchers will have access to the data and the video tapes.

- **Potential risks**

Subjects may have delayed onset muscle soreness (DOMS) 24-48 hours after data collection. This soreness is likely to peak at 48-72 hours after the exercise bout and ease afterwards. This will not have

any long-term effect on muscle function. Subjects will be informed about this potential muscle soreness. Subjects will be instructed to do a warm-up to reduce the risk of injuries and a cool-down to enhance recovery.

VIII. Potential benefits

The findings of this study will provide information about patient's gaits at his/her causal walking speed. By comparing with our able-bodied knowledge-base, these data will be used to develop an 'automatic diagnostic tool' for each gait disorder.

References:

[1] Eicher PS, Batshaw ML: Cerebral Palsy. Pediatric Clinics of North America1993; 40(3):537-51.

[2] Kuban KC: Cerebral Palsy. New England Journal of Med. 1994; 330(3):188-95.

[3] B.H. Dobkin: The Clinical Science of Neurologic Rehabilitation. Oxford University Press, New York, 2003.

[4] Dobkin, B. H: Overview of treadmill locomotor training with partial body weight support: A neurophysiology sound approach whose time has come for randomized clinical trials. Neurorehabil and Neural Repair 13: 157-165, 1999.

[5] Hesse S, Bertelt C, Schaffrin A, et al: Restoration of gait in nonambulatory hemiparetic patients by treadmill training with partial body-weight support. Arch Phy Med Rehabil, 1994; 75:1087-1093.

[6] Hesse S, Konrad M, Uhlenbrock D, et al: Treadmill walking with partial body weight support versus floor walking in hemiparetic subjects. Arch Phys Med Rehabil1999; 80:421-427.

[7] Sullivan KJ, Dobkin BH, Tavakol M, et al: Post-stroke cortical plasticity induced by step training. Society for Neuroscience Proceedings 2001; 27.

[8] Visintin M, Barbeau H, Korner-Bitensky N, et al: A new approach to retain gait in stroke patients through body weight support and treadmill stimulation. Stroke, 1998; 28:1122-1128.

[9] Wernig A, Muller S, Nanassy A, et al: Laufband therapy based on rules of spinal locomotion is effective in spinal cord injured persons. Eur J Neurosci 1995; 7:823-829.

[10] Wernig A, Nanassy A, Muller S: Laufband (treadmill) therapy in incomplete paraplegia and tetraplegia. J Neurotrauma 1999; 16:719-726.

[11] McNevin NH, Coraci L, Schafer J: Gait in adolescent cerebral palsy: the effect of partial unweighting. Arch Phys Med Rehabil 2000; 81 :525-528.

[12] Richards CL, Malouin F, Dumas F, et al: Early and intensive treadmill locomotor training for young children with cerebral palsy: a feasibility study. Pediatr Phys Ther 1997; 9:258-265.

[13] Schindl MR, Forstner C, Kern H, et al: Treadmill training with partial body weight support in nonambulatory patients with cerebral palsy. Arch Phys Med Rehabil 2000; 81 :3001-3006.

[14] Barbeau H, & Rossignol S: Recovery of locomotion after chronic spinalization in the adult cat. Brain Res 1987; 412:84-95.

[15] Lovely RG, Gregor RJ, Roy RR, et al: Effects of training on the recovery of full weight-bearing stepping in the adult spinal cat. Exp Neuro11986; 92:421-435.

[16] Hodgson JR, Roy, RR, deLeon R, et al: Can the mammalian lumbar spinal cord learn a motor task? Med Sci Sports Exerc, 1994; 26:1491-1497.

[17] Lovely RG, Gregor RJ, Roy RR, et al: Weight-bearing hindlimb stepping in treadmill-exercised adult cats. Brain Res 1990; 514:206-218.

[18] Muir GO, Steeves JD: Sensorimotor stimulation to improve locomotor recovery after spinal cord injury. Trends Neurosci 1997; 20:72-77.

[19] Duysens, Dietz; Duysens J, Pearson, K: From cat to man: basic aspects of locomotion relevant to motor rehabilitation of SCI. NeuroRehabilitation 1998; 10:107-118.

[20] Dietz V, Colombo G, Jensen L, et al: Locomotor capacity of spinal cord in paraplegic patients. Ann Neurol 1995; 37:555-556.

[21] Harkema SJ, Hurley SL, Patel UK, et al: Human lumbosacral spinal cord interprets loading during stepping. J Neurophysiol1997; 77:797-811.

[22] Kosak M, Reding, M: Comparison of partial body weight-supported treadmill gait training versus aggressive bracing assisted walking post stroke, Neurorehabil Neural Repair 2000; 14: 13-19.

[23] Nilson, L, Carlsson, J, Danielsson, A, et al: Walking training of patients with hemiparesis at an early stage after stroke: a comparison of walking training on a treadmill with body weight support and walking training on the ground. Clinical Rehab 2002; 15: 515-527.

[24] Uhlenbrock, D., Sarkodie-Gyan, T., Reiter, F., Konrad, M., Hesse, S., (1997), "Development of a servo-controlled gait trainer for the rehabilitation of non-ambulatory patients," Biomed Tech, Vol. 7-8, 42, pp. 196-202.

[25] Hesse, S, Uhlenbrock, D, Sarkodie-Gyan, T, (1999) "Gait pattern of severely disabled hemiparetic subjects on a new controlled gait trainer as compared to assisted treadmill walking with partial body weight support, " Journal Clinical Rehabil, 13, pp. 401-410.

[26] Rowe, P.J., Nicol, A.C., Kelly, I.G., Flexible goniometer computer system for assessment of hip function, Clinical Biomechanics 1989, 4: 68-72.

[27] Troke, M., Moore, A.P., Ckeek, E., Reliability of the OSI CA 6000 spine motion analyzer with a new skin fixation system when used on the thoracic spine. Manual Therapy, 1998, 3: (1) 27-33.

[28] Cosgrove, A.P., Graham, H.K., Mollan, R.A.B., Gait analysis in children with cerebral palsy using electrogoniometers, Presentation, British Orthopaedic Research Meeting, 1991.

[29] Myles, C., Rowe, P.J., Salter, P., Nicol, A., An electrogoniometer system used to investigate the ability of the elderly to ascend and descend stairs, Physiotherapy 1995, 81 (10): 640.

[30] Hazelwood, M.E., Rowe, P.J., Salter, P.M., The use of electrogoniometers as a measurement tool for passive movement and gait analysis, Physiotherapy, 1995, 81 (10): 639.

[31] Sullivan, K., Knowlton, B., Dobkin, B.: Step training with body weight-support: Effect of treadmill speed and practice paradigms on post-stroke locomotor recovery, Arch Phys Med Rehab, 2002, 83: 683-691.

[32] Clinical Guidelines on the Identification, Evaluation, and Treatment of Overweight and Obsesity in Adults. National Institutes of Health, National Heart, Lung and Blood Institute, June, 1998.

[33] Winter, D.A., Biomechanics and motor control of human movement (2nd Ed.), 1990, New York, John Wiley and Sons.

[34] D. Uhlenbrock: "Construction and evaluation of a servo-controlled gait trainer for early gait rehabilitation in non-ambulatory stroke patients" M.S. Thesis University of Teesside, UK, April 1997.

[35] Dietmar Uhlenbrock; "An advanced biomedical gait training machine for the rehabilitation of non-ambulatory stroke patients based on computer-aided human motion analysis," Ph.D. Thesis, University of Teesside, UK, April 1999.

[36] Sarkodie-Gyan, T., Jamshidi, M., Sensor-fusion based intelligent robot planning algorithm, Proc. IMEKO conf. On Knowledge based Measurement-Application, Research and Education, Germany, 1990, pp.295-302.

[37] Sarkodie-Gyan, T., Jamshidi, M., Dev. of a prototype robot task planning algorithm using sensor fusion, Proc. 3rd Int. Symp. In robotics and manufacturing, Canada, 1990, ASME press, pp. 155-160.

[38] da Cunha, I.T. Jr., Lim, P.A., Qureshy, H., Henson, H., Monga, T., & Protas, E.J., Gait outcomes after acute stroke rehabilitation with supported treadmill ambulation training: a randomized controlled pilot study. Ach Phs Med & Reha, 2002, 83, 1258-65.

[39] Miyal, I., Fujimoto, Y., Yamamoto, H., Ueda, Y., Saito, T., Nozaki, S., & Kang, J., Long-term effect of body weight-supported treadmill training in Parkinson's disease: A randomized controlled trial, Arch Phys Med & Rehab, 2002, 83, 1370-1373.

[40] Dawson, M., Sarkodie-Gyan, T., Provincialli, L., Hesse, S., Gait initiation, development of a measurement system for use in the clinical environment, Biomed. Technik, 1996, 41, pp. 213-217.

[41] Stefan Hesse, Dietmar Uhlenbrock et al, A mechanized gait trainer for restoration of gait, Journal of Rehabilitation Research and Dev., 2000, Vol. 37, No.6

[42] D. Uhlenbrock, S. Hesse, T. Sarkodie-Gyan: Development of an advanced mechanized gait-trainer, controlling movement of the center of mass, for restoration of gait in non-ambulatory subjects, Journal of Biomed. Technik, 1999, Band 44, Heft 7-8, pp. 194-201.

[43] Jensen, K.J: Diagnostics of Human Locomotion, M.S. Thesis, New Mexico Institute of Mining and Technology, Department of Mechanical Engineering, Mechatronics Program, 2005

[44] Amyyotrophic Lateral Sclerosos Fact Sheet. National Institute of Neurological Disorder and Stroke, 9/28/2004, http://www.ninds.nih.gov/health_and_medical/pubs/als.htm?format=printable

[45] Sarkodie-Gyan, T. 2nd Annual Bioengineering Technology Seminar, ASME Continuing Education Institute, 2004: Course Director

[46] Sarkodie-Gyan, T. Biomedicine Miniaturization, April 5-8, 2005, Irvine, California; ASME Continuing Education Institute, 2005: Course Director.

[47] Vaughan, C.L., Davis, B.L., O'Connor, J.C. (1992) "Dynamics of Human Gait", 2nd Ed., Kiboho Publishers, Cape Town, South Africa.

[48] Lung-Wen T, Robot Analysis: The Mechanics of Serial and Parallel Manipulators. New York, NY: John Wiley, 1999.

[49] Niku S.B., Introduction to Robotics: Analysis, Systems, and Applications. Upper Saddle River, NJ: Prentice Hall, 2001.

[50] Sarkodie-Gyan, T. (2005) "Neurorehabilitation Devices: Engineering Design, Measurement, and Control", McGraw-Hill Companies, Inc. New York, Chicago, London, Madrid, Mexico City, Milan, New Delhi, Seol, Singapore, Sydne, Toronto; ISBN: 007-144830-6.

[51] Amirouche, F.M., Ider, S.K., Trimble, J. (1990) "Analytical Method for the Analysis and Simulation of Human Locomotion", Journal of Biomechanical Engineering, Nov. 1990, vol. 112, pp. 379-386.

[52] Ramakrishnan, H.K., Kadaba, M.P. (1991) "On the Estimation of Joint Kinematics during Gait", J. Biomechanics, vol. 24, No. 10, pp. 969-977.

[53] Cappozzo, A. (1991) "The mechanics of human walking", in Adaptability of Human Gait., A Patla (Hrsg.), No. 78; North-Holland Elsevier Science Publishers B.V., Amsterdam, pp. 167-186.

[54] Yen, V., Nagurka, M.L. (1987) "Biomechanics of normal and prosthetic gait", ASME Winter Annual Meeting (Boston, Dec. 1987), pp. 17-22.

[55] R. E. Moore, Interval Analysis, Prentice Hall, 1966.

[56] J. Jaffar and M. Maher, Constraint Logic Programming: a Survey, Journal of Logic Programming, vol. 19/20, pp. 503-581, 1994.

[57] H. Collavizza, F. Delobel and M. Rueher, Comparing Partial Consistencies, Reliable Computing, vol. 5, pp. 1-16, 1999.

[58] F. Benhamou, Interval Constraint Logic Programming, in Constraint programming: basics and trends, Springer-Verlag, 1994.

[59] M. Ceberio and F. Modave, Interval-based Multi-Criteria Decision Making, in the proceedings of AI+MATH'04, 2004.

[60] M. Ceberio and F. Modave, An Interval-valued, 2-additive Choquet Integral for Multi-Criteria Decision Making, in the proceedings of IPMU 2004.

[61] S. A. Starcks, V. Kreinovich, L. Longpre, M. Ceberio, G. Xiang, R. Araiza, J. Beck, R. Kandathi, A. Nayak and R. Torres, Towards Combining Probabilistic and Interval Uncertainty in Engineering Calculations, in the Proc. of the NSF Workshop on Reliable Eng. Computing, pp. 193-213, 2004.

[62] M. Ceberio, V. Kreinovich, L. Longpre, E. Saad, B. Ludascher, C. Baral and H. T. Nguyen, Affine Arithmetic-Type Techniques for Handling Uncertainty in Expert Systems, with Applications to Geoinformatics and Computer Science, in the Proceedings of the 11th GAMM-IMACS International Symposium on Scientific Computing, Computer Arithmetic, and Validated Numerics, 2004.

[63] Hesse, S., Werner, C., v. Frankenberg, S., Bardeleben, A. (2003) "Treadmill training with partial weight support after stroke," Phs Med Rehabil Clin N Am 2003, 14: 111-123.

[64] Werner, C., v. Frankenberg, S., Treig, T., Konrad, M., Hesse, S. (2002) "Treadmill Training with partial body weight support and an electromechanical gait trainer for restoration of gait in subacute stroke patients," Stroke 2002; 33: 2895-2901

[65] Hesse, S. (2001) "Locomotor therapy in neurorehabilitation," NeuroRehabilitation 2001; 16:1-7.

[66] Hesse, S., Werner, C., Uhlenbrock, D., v. Frankenberg, S., Bardeleben, A., Brandl-Hesse, B. (2001) “An electromechanical gait trainer for restoration of gait in hemiparetic stroke patients: preliminary results,” Neurorehabilitation and Neural Repair 2001; 15: 39-50.
[67] Hesse, S., Uhlenbrock, D., Werner, C., Bardeleben, A. (2000) “ A mechanized gait trainer for restoring gait in non-ambulatory subjects,” Arch Phys Med Rehabil 2000; 81: 1158-1162.
[68] Uhlenbrock, D., Sarkodie-Gyan, T., Reiter, F., Konrad, M., Hesse, D. (1997) “Entwicklung eines Gangtrainers mit geregeltem Servoantrieb zur Rehabilitation gehunfaehiger Patienten,” Biomed. Technik 1997; 42: 196-202.
[69] Hesse, S., Sarkodie-Gyan, T., Uhlenbrock, D. (1999) “Development of an advanced mechanized Gait Trainer, controlling movement of the centre of mass, for restoring gait in non-ambulant subjects,” Biomed. Technik 1999; 44:194-201.
[70] Hesse, S., Uhlenbrock, D., Sarkodie-Gyan, T. (1999) “Gait pattern of severely disabled hemiparetic subjects on a new controlled gait trainer as compared to assisted treadmill walking with partial body weight support,” Clinical Rehabilitation 1999; 13:401-410.
[71] Hesse, S., Uhlenbrock, D. (2000) “A mechanized Gait Trainer for restoration of gait,” Journal Rehab Res Dev 2000; 376): 701-708.
[72] Jensen, K., Sarkodie-Gyan “The Paradigm of a Smart Gait Emulator,” Proceedings of the 2004 Japan-USA Symposium on Flexible Automation, Denver, CO, July 19-21, 2004.
[73] Jensen, Kirt, Sarkodie-Gyan, “Experimental Investigations on a Gait Emulator for Neurological Rehabilitation,” World Automatic Control Congress, Proceedings, WAC Seville, Spain, 2004.
[74] “ Spring Element for the Insert at Treadmill Training,” German Patent DE 197 25 972 C1
[75] “First Prototype of a Gait Trainer,” German Patent DE 197 25 973 C2
[76] “Gait Training Machine,” German Patent DE 198 05 164
[77] W. Mitchell Parks (2002) “Smart gait Emulator Project,” Interim Report, New Mexico Institute of Mining and Technology, Department of Mechanical Engineering, August 2002.
[78] W. Mitchell Parks, Angela Tipton, Kirt Jensen, Glorianna Grado, Jason Kemp, Michael Jackson (2002) “Smart gait Emulator Design/Construction ,” Interim Report, New Mexico Institute of Mining and Technology, Department of Mechanical Engineering, October 2002
[79] Jason Paschis, Justin Stolworthy, James Stauder, Nick Jacka, Erin Gulley (2003) “Smart Gait Emulator,” Final Report, New Mexico Institute of Mining and Technology, Department of Mechanical Engineering, December 2003.
[80] Nick Jacka, James Stauder, Justin Stolworthy (2004) “Smart gait Emulator,” Final Report, New Mexico Institute of Mining and Technology, Department of Mechanical Engineering, May 10, 2004.
[81] Justin Stolworthy, James Stauder, Nick Jacka, Josh Kern (2005) “Smart Gait Emulator,” Final Report, New Mexico Institute of Mining and Technology, Department of Mechanical Engineering, Spring 2005.

University of Texas at El Paso (UTEP) Institutional Review Board
Informed Consent Form for Research Involving Human Subjects

Protocol Title: Development of an Assessment for Functional Recovery after Neurological Disorders and Peripheral Nerve Transfers
Principal Investigator: Thompson Sarkodie-Gyan, Ph.D.
UTEP : Department of Electrical and Computer Engineering

Introduction

You are being asked to take part voluntarily in the research project described below. Please take your time making a decision and feel free to discuss it with your friends and family. Before agreeing to take part in this research study, it is important that you read the consent form that describes the study. Please ask the study researcher or the study staff to explain any words or information that you do not clearly understand.

Why is this study being done?

You have been asked to take part in a research study to identify individual gait patterns during walking and running. Approximately, 100 study subjects will be enrolling in this study at UTEP. You are being asked to be in the study because you are a male or a female over the age of 18. If you decide to enroll in this study, your involvement will last about one week.

What is involved in the study?

If you choose to participate in this study, you will report to the Human Motion Analysis and Neurorehabilitation Laboratory, Room E313B, in the Engineering Building. You will need to wear proper workout attire. We will also measure your height, weight, segmental length, width, depth and circumference. A warm-up consisting of stretching and light jogging will be performed.

You will be asked to walk and/or run on an instrumented treadmill at constant speed with bare foot. The force platform built in the treadmill will measure the forces exerted on you during walking and running. Reflective markers will be placed on your joint centers to facilitate analysis of your gait patterns. Trials will be videotaped for the purpose of the movement analysis and comparison.

You will also be asked to place three different multi-axis sensors (accelerometers, goniometers, and gyroscopes) on the surface of the lower limb, and will repeat the same experiment as above to collect the kinematic data.

At the same time, you will be asked to wear electromyographic (EMG) electrodes, to measure the dynamic activities of the muscles during walking and/or running. You may be asked to shave the hairs of the part your body prior to the experiment, since it will affect the markers and sensors attachment to the body surface.

The estimated data collection time including preparation and warm-up will be approximately two hours.

What are the risks and discomforts of the study?

The potential risks that may occur with participating in this research include those associated with exercise testing. The potential risks associated with running include muscle fatigue and muscle strain. There is also a risk of local muscle and/or joint soreness following any exercise. The soreness is likely to peak at 2-3 days after the exercise bout and ease afterwards. A warm-up period will decrease the likelihood of injury and soreness. A research team member will advise you on cool-down stretching exercises to minimize muscle soreness. You are free to stop the exercise procedure at any time.

What will happen if I am injured in this study?

The University of Texas at El Paso and its affiliates do not offer to pay for or cover the cost of medical treatment for research related illness or injury. No funds have been set aside to pay or reimburse you in the event of such injury or illness. You will not give up any of your legal rights by signing this consent form. You should report any such injury to (Dr. Thompson Sarkodie-Gyan, Phone Number: 915-747-7011) and to the Institutional Review Board (IRB) at UTEP at (915-747-8841) or irb.orsp@utep.edu.

Are there benefits to taking part in this study?

There will be no direct benefits to you for taking part in this study.

The findings of this study will provide you with information about your walking and running gaits at constant speed with bare feet. These data will be used to develop a 'gait database' for future reference and research. Each participant will be provide some snacks and drink during the break of the experiment.

This research may help us to understand the variations in gait with respect to gender and body mass index.

What other options are there?

As a volunteer in this study, you have the option not to take part in the study or to withdraw from the study at any time. If you do not take part in the study, there will be no penalty whatsoever.

Who is paying for this study?

Internal Funding:

Funding for this study is provided by UTEP Department of Electrical and Computer Engineering, and the UTEP NSF Advance.

External funding:

UTEP and Dr. Thompson Sarkodie-Gyan are receiving funding from the NSF Advance and from the ECE department to conduct this study.

What are my costs?

There are no direct costs. You will be responsible for travel to and from the research site and any other incidental expenses.

Will I be paid to participate in this study?

Participation is voluntary.

You will not be paid for taking part in this research study.

What if I want to withdraw, or am asked to withdraw from this study?

Taking part in this study is voluntary. You have the right to choose not to take part in this study. If you do not take part in the study, there will be no penalty.

If you choose to take part, you have the right to stop at any time. However, we encourage you to talk to a member of the research group so that they know why you are leaving the study. If there are any new findings during the study that may affect whether you want to continue to take part, you will be told about them.

The researcher may decide to stop your participation without your permission, if he or she thinks that being in the study may cause you harm.

Who do I call if I have questions or problems?

You may ask any questions you have now. If you have questions later, you may call insert Dr. Thompson sarkodie-Gyan; Phone Number 915-747-7011, Email: tsg@ece.utep.edu.
If you have questions or concerns about your participation as a research subject, please contact the Institutional Review Board (IRB) at UTEP at (915-747-8841) or by email at irb.orsp@utep.edu.

What about confidentiality?

1. Your part in this study is confidential. None of the information will identify you by name.
Only you and individuals directly involved in this research will have access to your results. All data collected in this study will be coded by subject number rather than by name and will be kept in a locked file in Room E313B for 5 years. Only the researchers and/or the research assistants will have access to the data. The results will be used for scholarly publications or presentations but you will not be identified.

2. Every effort will be made to keep your information confidential. Your personal information may be disclosed if required by law. Organizations that may inspect and/or copy your research records for quality assurance and data analysis include, but are not necessarily limited to:

The sponsor or an agent for the sponsor

Department of Health and Human Services

UTEP Institutional Review Board

Because of the need to release information to these parties, absolute confidentiality cannot be guaranteed. The results of this research study may be presented at meetings or in publications; however, your identity will not be disclosed in those presentations.

Mandatory reporting

If information is revealed about child abuse or neglect, or potentially dangerous future behavior to others, the law requires that this information be reported to the proper authorities.

Authorization Statement

I have read each page of this paper about the study (or it was read to me). I know that being in this study is voluntary and I choose to be in this study. I know I can stop being in this study without penalty. I will get a copy of this consent form now and can get information on results of the study later if I wish.

Participant Name: Date:

Participant Signature: Time:

Participant Signature:

Consent form explained/witnessed by:

Signature
Printed name:

Date: Time:

Vita

Born and raised in northern Manitoba in Canada, Chad MacDonald earned his Bachelor of Science in Computer Engineering from the University of Manitoba in 2003. He received his Master of Science degree in Electrical and Computer Engineering in 2006 also from the University of Manitoba. In 2005 he joined the doctoral program at the University of Texas at El Paso.

While pursuing his undergraduate degree, Dr. MacDonald worked as a Control Engineering summer student with Manitoba Hydro on Gillam, MB. He also completed a 16 month internship as a software developer with Nortel Networks in Ottawa, ON as part of his undergraduate degree program.

While pursuing his doctoral degree, Dr. MacDonald worked as a Research Assistant and Teaching Assistant for the department of Electrical and Computer Engineering. Most recently he has worked as an Assistant Instructor in the Electrical and Computer Engineering department and as the technical coordinator for the Laboratory for Human Motion Analysis and Neurorehabilitation.

Dr. MacDonald has presented his research at conferences and meetings including the 2006 IASTED Control and Applications Conference, the 2007 IEEE International Conference on Rehabilitation Robotics, the 2007 IEEE Engineering in Medicine and Biology Conference, the 2007 Annual Meeting of the Biomedical Engineering Society and the 2008 Southern Biomedical Engineering Conference. Dr. MacDonald has submitted his research for publication in the IEEE Transactions on Neural Systems and Rehabilitation Engineering and to the Gait and Posture journal.

Permanent address: 121 Tukwakin St
Gillam, MB, Canada, R0B 0L0

This dissertation was typed by Chad MacDonald.